UNIVERSIDADE DE BRASÍLIA - UnB
INSTITUTO DE GEOCIÊNCIAS - IG

REGIME TERMAL E TECTÔNICA TIPO THIN-SKIN NA ZONA EXTERNA DA FAIXA BRASÍLIA

DISSERTAÇÃO DE MESTRADO N° 364

DÉBORA RABELO MATOS

Orientador:
Prof. Dr. Elton Luiz Dantas

Brasília, maio de 2016.

UNIVERSIDADE DE BRASÍLIA - UnB
INSTITUTO DE GEOCIÊNCIAS - IG

REGIME TERMAL E TECTÔNICA TIPO THIN-SKIN NA ZONA EXTERNA DA FAIXA BRASÍLIA

DISSERTAÇÃO DE MESTRADO N° 364

DÉBORA RABELO MATOS

Banca Examinadora:

Prof. Dr. Elton Luiz Dantas (Universidade de Brasília)

Prof. Dr. Carlos Emanoel de Souza Cruz (Universidade de Brasília)

Dra. Loiane Gomes de Moraes Rocha (Serviço Geológico do Brasil)

Ficha catalográfica elaborada automaticamente,
com os dados fornecidos pelo(a) autor(a)

Rabelo Matos, Débora
RD287f FLUXO DE CALOR E TECTÔNICA TIPO THIN-SKIN NA ZONA EXTERNA DA FAIXA BRASÍLIA / Débora Rabelo Matos; orientador Elton Luiz Dantas. -- Brasília, 2016.
109 p.

Dissertação (Mestrado - Mestrado em Geologia) -- Universidade de Brasília, 2016.

1. Geologia Regional. 2. Geologia Estrutural. 3. Geofísica. 4. Aeromagnetometria. 5. Fluxo de Calor. I. Dantas, Elton Luiz, orient. II. Título.

DEDICATÓRIA

Às coisas boas da vida!

AGRADECIMENTOS

Gostaria de agradecer imensamente aos meus pais (Francisco e Maria) por terem aceitado meu desprendimento nesses quase 3 anos de mestrado, sem hora pra chegar em casa, indo a UnB sábado, domingo, feriado e em todas as férias, mas principalmente pelo amor, pelo conforto quando eu já não tinha mais forças e ânimo para seguir em frente.

Agradeço a minha irmã Lulu e a meu querido namorado Rafael pelo apoio e por terem aguentado momentos estressantes na divisão do tempo entre academia, trabalho e lazer. Além disso, as minhas primas e a todos que torcem por mim.

Ao meu orientador pela grande disponibilidade e por alguns fins de semanas dedicados a correções sem fim. E também às minhas co-orientadoras Vidotti e Tati, por todos os tropeços e sopinhas de abóbora. Ao CNPq pelo processo 550259-2011-2 que custeou os gastos de toda essa pesquisa.

A CPRM, em nome dos meus chefes e colegas de trabalho, por todas as horas, dias e momentos que me proporcionou em ir a UnB rapidinho resolver alguma coisa ou até mesmo por conselhos e dicas acadêmicas e profissionais imprescindíveis ao bom andamento da pesquisa.

Por fim, gostaria de reconhecer imensamente a ajuda de Deus que sempre esteve comigo nos momentos mais difíceis desse mestrado sempre me dando forças para continuar, seguir em frente e fazer o meu melhor.

RESUMO

Estudamos o arcabouço tectônico da porção central da Sequência Paracatu-Vazante, localizada Zona Externa da Faixa Brasília, Orógeno Neoproterozoico de tectônica dominantemente tipo *thin skin*, a fim de se entender a relação entre os Grupos Canastra, Vazante e Bambuí, bem como os diferentes tipos de mineralização, ambientes tectônicos e explorar os métodos de fluxo de calor, *matched filter* e deconvolução de Euler. Para o cálculo do fluxo de calor, utilizaram-se dados aerogamaespectrométricos de alta resolução (espaçamento das linhas de vôo de 250 m) e foram geradas médias da estimativa de produção de calor. A contribuição dos seus fluxos de calor variam de 38 mW/m² para o Grupo Canastra e 48 mW/m² para o Grupo Vazante. Dentro dessas unidades foram encontrados valores distintos de produção para as diversas litologias: siltitos (1,9 – 4,5 μW/m³), carbonatos (2,1 - 3,9 μW/m³), folhelhos negros (2,2 – 4,5 μW/m³) e arenitos (1,9 – 5,3 μW/m³). A discrepância entre os resultados obtidos para essas duas unidades indicam ambientes deposicionais e épocas de deposição distintas, sendo justapostas apenas no fim do Neoproterozoico, além de suas formações sedimentares de diferentes espessuras, podendo inferir diferentes posições do embasamento para cada um desses grupos. Localmente, falhas e a percolação de fluidos também são responsáveis pela variação da produção volumétrica de calor nessa região. Além disso, pôde-se filtrar, por meio da produção volumétrica de calor os valores de produção de calor correspondentes aos carbonatos e folhelhos negros, rochas hospedeiras da mineralização de Pb-Zn e Au da região, constituindo assim um importante guia prospectivo. Foi possível o reconhecimento de 4 fases deformacionais distintas e progressivas na região, além da individualização, pela magnetometria e dados estruturais de campo, de 5 domínios estruturais-geofísicos relacionados às diferenças de comportamento estrutural das diferentes unidades litológicas mapeadas, bem como magnitude, mergulho da foliação principal S2 e diferenças no relevo magnético, sendo os limites dos domínios representados por falhas de empurrão de sentido N-S – Coromandel, de sentido NE-SW – Serra das Araras, Serra das Antas, Extremo Norte e Lagamar, zonas de cisalhamento transcorrentes de sentido NE-SW – Paracatu, Vazante, Morro Agudo e Arrenegado, de sentido E-W – Januário, e altos estruturais, que servem de contato entre os Grupos Canastra, Bambuí e Vazante. A partir da aplicação da deconvolução de Euler e do *matched filter* nos dados magnetométricos pode-se estimar a profundidades das grandes estruturas que controlam a região, sendo elas: Falha de Empurrão Coromandel com aproximadamente 1,2 – 9 km, Falha de Empurrão Serra das Araras com aproximadamente 9 km, ZC Morro Agudo com 1,2 km, ZC Januário com 9 km, ZC Vazante 1,2 - 9 km, ZC Paracatu com 1 km, Falha de Empurrão Extremo Norte com 1,2 km e Falha de Empurrão de Lagamar com 1 km. Sendo assim, percebe-se que o contato entre os Grupos Canastra e Vazante é cerca de 9 vezes mais profundo que o contato entre os Grupos Vazante e Bambuí e pode-se dividir as estruturas da região em dois grupos distintos, sendo o primeiro formado pelas estruturas mais a oeste da área, de maior profundidade envolvendo o embasamento, e o segundo formado pelas estruturas mais a leste da área, de menor profundidade afetando somente a cobertura. Sendo assim, propõe-se que para a área de estudos há um afinamento do pacote sedimentar de oeste para leste, o que vai de acordo com interpretações de linhas sísmicas da região.

ABSTRACT

We studied the tectonic framework of the central portion of the Paracatu-Vazante sequence located at the External Zone of the Brasília Belt, Neoproterozoic orogeny, thin skin tectonics dominantly, in order to understand the relationship between the Canastra, Vazante and Bambuí groups and different types of mineralization, tectonic environments and exploit the heat flux, matched filter and Euler deconvolution methods. For calculating the heat flow, we used high resolution aero gamma-ray spectrometry data (survey line spacing of 250 m), were generated the estimate of the average heat production. The contribution of the heat flows range from 38 mW / m² for the Canastra Group and 48 mW / m² for the Vazante Group. Within these units were found different production values for the various lithologies: siltstones (1.9 to 4.5 μW / m³), carbonates (2.1 to 3.9 μW / m³), black shales (2.2 to 4 5 μW / m³) and sandstones (1.9 to 5.3 μW / m³). The discrepancy between the results obtained for these two units indicate different depositional environments and deposition times, besides its sedimentary formations of different thicknesses, that may even imply different positions of the basement for each of these groups. Locally, the faults and percolation fluids are also responsible for the variation of the heat volumetric production in this region. In addition, it was possible to filter through the volumetric heat, the heat production values corresponding to black carbonates and shales, host rocks of Pb-Zn mineralization and Au in the area, thus constituting an important prospective guide. It was possible to recognize 4 distinct and progressive deformational phases in region, as well as individualization, by magnetometry and structural field data, 5 structural-geophysical domains. As the domais are related to differences in structural behavior of different mapped lithological units and magnitude, dip of the S2 main foliation and differences in the magnetic relief, and the limits of the areas represented by thrust faults of N-S direction- Coromandel, NE-SW direction - Serra das Araras, Serra das Antas, Extremo Nort and Lagamar, transcurrent shear zones of NE - SW direction - Paracatu, Vazante, Morro Agudo and Arrenegado, E-W direction - Januário, and structural highs that serve as contact between the Canastra, Bambuí and Vazante groups. From the application of Euler deconvolution and matched filter in magnetiometric data, the depths of the great structures that control the region could be estimated, namely: Coromandel Thrust Fault with approximately 1.2 - 9 km, Serra Araras Thrust Fault approximately 9 km, Serra das Antas Thrust Fault with 9 km, Arrenegado Shear Zone with 1.2 km, Morro Agudo Shear Zone 1.2 km, Januário Shear Zone with 9 km, Vazante Shear Zone with 1.2 to 9 km, Paracatu Shear Zone with 1 km, Extremo Norte Thrust Fault to 1.2 km and Lagamar Thrust Fault with 1 km. Thus, it is clear that the contact between the Canastra and Vazante groups is about 9 times deeper than the contact between the Vazante and Bambuí groups and the structures of the region can be divided into two distinct groups: the first formed the structures over the western area of greater depth involving the basement, and the second formed by the structures further east area, shallower only affecting coverage. Therefore, it is proposed for the study area there is a thinning of western sedimentary east, which is in accordance with interpretations of seismic lines in the region.

Sumário

1. Introdução

Essa dissertação está inserida no projeto *Metalogenia da Zona Externa da Faixa Brasília*, importante orógeno Neoproterozoico (Fuck, 1994, Dardenne, 2000) em que se propõe desenvolver estudos geológicos-estruturais e geofísicos destinados a enaltecer o potencial metalogenético das diversas unidades sedimentares e metassedimentares que compõem a zona externa da Faixa de Dobramentos Brasília.

1.1.Justificativa do tema

As unidades estudadas hospedam importantes minas de classe mundial, com a maior mina de zinco do Brasil, bem como uma das principais minas de ouro, zinco e chumbo do País. Desta forma, consideramos de interesse estratégico uma avaliação dessas unidades tendo por base o avanço do conhecimento geológico a partir de novos dados geológicos, geofísicos e de sensores remotos.

A estrutura de Guarda-Mor está localizada na porção central da Sequência Paracatu-Vazante, sendo muito relevante na inflexão dessa grande faixa. Muitos estudos já foram realizados nessa região, principalmente nos carbonatos (isótopos de C e O) hospedeiros da mineralização de Pb e Zn, e no próprio minério (inclusões fluidas e isótopos de Pb, C, S e O – Dardenne & Freitas-Silva, 1998; Misi et al., 2005; Monteiro, 2002, Monteiro et al., 2006; Cunha et al., 2000 e 2001; Neves, 2011). Há também importantes trabalhos envolvendo a geologia estrutural da região, como o de Pereira (1992), porém, estudos integrados envolvendo técnicas geofísicas, de sensores remotos e geológicas ainda são uma novidade.

Dessa forma, o objetivo deste trabalho é estudar o arcabouço tectônico da porção central da Sequência Vazante-Paracatu por meio de dados de fluxo de calor, estruturais e aeromagnéticos, bem como um melhor entendimento das unidades compreendidas nessa região.

Essa sequência é definida como uma bacia do tipo *foreland* (Coelho et al., 2008; Uhlein et al, 2012), em que sistemas de falhas de empurrão longitudinais invertem a sequência dos Grupos Canastra e Vazante (Campos Neto, 1979; Freitas-Silva, 1991; Pereira, 1992), sendo sua porção central marcada pela inflexão dessa sequência. Por meio de uma linha sísmica que atravessa a área de estudos, Coelho et al. (2008) propõem a existência de dois conjuntos de estruturas que atravessariam a região, com diferentes profundidades, sendo que o primeiro domínio encontra-se restrito às coberturas e o segundo domínio atingiria até o embasamento, definindo faixas de thin e thick-skin.

Os Cinturões de Dobras e Empurrões (CDEs) são considerados um laboratório natural para o estudo da arquitetura das rochas, deformação e evolução tectônica (Macedo & Marshak,

1999; Kwon et al., 2009). A maioria dos CDEs abrange uma grande região e apresenta padrões encurvados vistos em planta (como nos Himalaias e nos Alpes), com traços de empurrão convexos bem marcados em direção a *foreland*. Zonas de transcorrência nesses cinturões podem ser formadas como transportadoras de falhas cisalhantes paralelas, ou rampas laterais ou como transportadoras de falhas de transferência oblíquas ou até como rampas oblíquas. É importante ressaltar que muitas são zonas fracas de longa duração que precederam empurrões e variações laterais controlados na geometria da bacia (Mitra, 1997).

Os domínios *foreland* de orógenos convergentes são formados por cinturões de dobra e empurrão, que compreendem também as camadas sedimentares sobrejacentes ao embasamento cristalino ou de rocha dura. O encurtamento nesses domínios é marcado por um estado de tensão compressional regionalmente dominado que ocorre em diferentes contextos geodinâmicos, tais como cunhas de subducção acrescionárias e cinturões de empurrão colisionais (Dahlen, 1990, Davis et al., 1983 e Suppe, 1987). Nos cinturões de empurrão *foreland*, a deformação da cobertura sedimentar é a porção mais externa do encurtamento crustal profundo que ocorre ao longo dos empurrões internos ao embasamento. A profundidade do cinturão de dobras e empurrão depende da presença de um nível horizontal de descolamento que permita um desacoplamento mecânico entre as unidades superiores e inferiores. Numa primeira aproximação, quando esse descolamento existe e é eficiente a deformação *foreland* é caracterizada por um estilo tectônico *thin-skin* (Affolter & Gratier, 2004). Esse modelo tem sido generalizado para o fronte dos alpes (Philippe et al., 1998). Pelo outro lado, quando o descolamento é ineficiente ou inexistente, a cobertura deformada remanesce acoplada ao seu embasamento, sendo então chamado de estilo tectônico thick-skin – modelo geralmente aplicado para a fase compressional dos Pirineus, onde a cobertura permanece acoplada ao seu embasamento ou no maciço cristalino externo dos Alpes (Espurt et al., 2012; Bellahsen et al., 2012).

1.2.Métodos e base de dados

Os dados magnetométricos e gamaespectrométricos utilizados são provenientes da Área 1 dos levantamentos geofísicos aéreos conduzidos pela CODEMIG (Companhia de Desenvolvimento Econômico do Estado de Minas Gerais) em parceria com o Serviço Geológico do Brasil. As linhas de vôo foram levantadas na direção N30W, com espaçamento de 250 m. A altura nominal do vôo foi de 100 m com uma velocidade média de 200 km/h.

No Brasil, os primeiros relatos do uso de gamaespectrometria remetem à década de 1950 como instrumento de prospecção mineral e à década de 1970 como ferramenta de mapeamento geológico, isso só é possível graças à desintegração de elementos radioativos, principalmente K, Th e U contidos nas rochas e a sua relação com a quantidade de SiO_2, a forma de ocorrência,

dentre outros fatores (Vasconcellos et al., 1994). Por meio dessa técnica e dos estudos de Bücker e Rybach (1996) foi possível obter o mapa de fluxo de calor, que é o registro da história térmica da região, encontrando-se relacionado à contagem total dos elementos radioativos principais, tendo em vista que a produção de calor radiogênico em rochas é normalmente atribuída à sua respectiva densidade e à concentração de K, Th e U (Rybach, 1986).

Processamentos desse tipo, envolvendo gamaespectrometria, tem sido aplicados com alguma frequência em outras regiões do Brasil e do mundo, como por exemplo, o trabalho em conjunto de pesquisadores da Bahia e do centro de pesquisas da Petrobrás (Argollo et al., 2012). Este estudo teve como um dos objetivos a construção de um modelo crustal e fluxo de calor em porções emersas da Bacia Sergipe-Alagoas, e os resultados do fluxo de calor foram bastante úteis no entendimento da espessura dessa parte da bacia e a sua correlação com os campos de petróleo.

O uso da magnetometria é aplicado de maneira direta ao mapeamento de feições magnetométricas, como horizontes estratigráficos e litotipos específicos, que podem ou não estar mineralizados, como no caso os depósitos de Pb e Zn das minas de Vazante e Morro Agudo. As medidas magnetométricas podem fornecer informações sobre lineamentos, contatos geológicos, alinhamentos estruturais, limites de bacias sedimentares e agregar mais informações a um corpo mineralizado, tais como susceptibilidade, profundidade, dimensão e mergulho. Nesse trabalho o método foi de grande auxílio na identificação dessas estruturas. Tendo sido feitos 2 tipos de processamento utilizando a magnetometria, os quais são: interpretação qualitativa magnetométrica e filtragem espectral.

A interpretação magnetométrica envolve fases iniciais em que os parâmetros geométricos são identificados em função do que se espera na sua resposta geológica. Nos dados aeromagnetométricos busca-se identificar 2 (dois) tipos principais de feições: unidades magnetométricas e as descontinuidades lineares, que podem, em um segundo momento, ser interpretados como corpos de litologias diferentes e lineamentos estruturais, como falhas, grandes fraturas, etc.

As unidades magnetométricas compreendem porções de diferentes intensidades magnéticas (susceptibilidades), não necessariamente estão relacionadas a diferentes unidades geológicas. As descontinuidades lineares são, em geral, bem evidentes e costumam representar falhas, fraturas ou até mesmo tendências estruturais de uma certa região. Sua representação é mais subjetiva que a das unidades e o seu formato deverá ser verificado para estabelecer a natureza geológica das feições identificadas.

O filtro combinado ou *matched filter* é uma técnica em que a partir do espectro de potência ponderado para a área de estudos é possível verificar os comprimentos de onda das principais fontes magnéticas. Com isso, são calculadas suas profundidades e assim, aplicando

uma série de filtros, pode-se obter mapas magnetométricos para as diferentes profundidades da crosta, em que apresentam-se as fontes magnéticas (Phillips 1997 e 2001), dessa forma foi possível estimar a profundidade das principais estruturas que controlam a região, relacionando assim os limites dos Grupos Canastra, Vazante e Bambuí.

Como exemplo, na Fossa de Benue, estrutura pertencente ao sistema de rifteamento central da África, que corta toda a Nigéria, foi feita uma interpretação magnetométrica por meio dos novos dados de alta resolução, na qual foi possível a melhor caracterização de suas unidades, dando uma melhor estimativa de extensão em subsuperfície, além de sua possível profundidade (Anudu et al., 2014).

A execução deste Projeto se justifica pela necessidade de melhor entendimento dos ambientes de sedimentação e da evolução dessas sucessões sedimentares durante a Orogênese Brasiliana e dos controles e processos críticos para formação dos depósitos minerais, a fim de estabelecer o potencial da zona externa da Faixa Brasília em hospedar outros depósitos minerais de zinco, chumbo, fosfato e ouro. Os novos dados gerados no quadro desse projeto serão integrados com os resultados obtidos durante os últimos anos na geologia regional e metalogenia dos depósitos associados às sucessões sedimentares da Zona Externa da Faixa Brasília.

2. Contexto Geológico

A área de estudos localiza-se no extremo oeste do Estado de Minas Gerais, próxima às cidades de Guarda-Mor, Paracatu e Vazante. Encontra-se na porção leste da Faixa Brasília, em sua zona externa (Dardenne, 2000) ou meridional (Araújo-Filho, 2000), que está inserida na Província Tocantins.

A Faixa Brasília representa um cinturão de dobras e empurrões que se estende ao longo de aproximadamente 1.100 km (Figura 1), com vergência tectônica e metamórfica em direção ao Cráton São Francisco. Situada na porção central da Faixa Brasília, na altura do paralelo do Distrito Federal (DF), a Sintaxe dos Pirineus condiciona a compartimentação da FDB em dois segmentos, um setentrional de direção NE e outro meridional de direção NW, com superposição de estruturas do segmento norte ao segmento sul, representando a intersecção de dois cinturões de dobra-falha com evolução distinta e diferenças estruturais, tectônicas, metamórficas e estratigráficas marcantes (Araújo Filho, 2000).

A Faixa Brasília apresenta duas compartimentações. Uma separa em Faixa Brasília setentrional e meridional, com limite dado pela sintaxe dos Pirineus (Almeida, 1967). E a outra separa a Faixa em zona cratônica, zona interna e zona externa, sendo a zona interna com grau metamórfico maior em relação à zona externa. (Almeida, 1977, 1981 e Hasui & Almeida, 1970). A compartimentação da Faixa Brasília advém da classificação moderna de cinturões colisionais (Pimentel, 2004), e é dividida em: (i) Maciço de Goiás, terreno siálico alóctone, que contém terrenos granito gnáissicos e greenstone belts e, a sul, complexos máficos – ultramáficos associados; (ii) Arco magmático de Goiás, separados em Mara-Rosa, a norte e Arenópolis a sul; (iii) Zona Interna, que é representado por rochas do Complexo Anápolis-Itauçu metamorfizadas em fácies granulito e rochas metassedimentares do Grupo Araxá, imbricadas no embasamento; (iv) Zona Externa, representada por: Pilha metassedimentar Proterozóica, que inclui os grupos Paranoá, Canastra, Ibiá, Vazante, formados em ambiente de margem continental passiva, além dos Grupos Serra da Mesa e Natividade, equivalentes laterais do Grupo Araí, que foi formado em ambiente de rifte; v) Zona Cratônica, localizada na borda oeste do Cráton São Francisco, que inclui sedimentos do Grupo Bambuí e exposições do embasamento (Almeida et al., 1981; Fuck, 1994; Pimentel, 2000).

A Zona Externa da Faixa Brasília é composta por unidades metassedimentares (Grupos Paranoá, Canastra, Ibiá, Vazante e, localmente, o Bambuí) e porções do seu embasamento. Nela, predominam as fácies sedimentares correspondentes à margem passiva, e o metamorfismo é de fácies xisto verde (Figura 1). Na Figura 2 vemos a geologia da área de estudos.

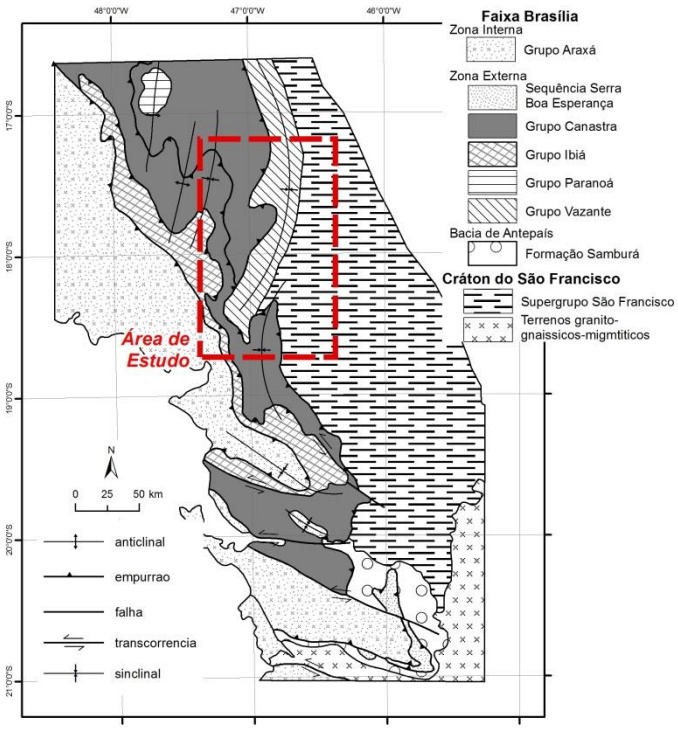

Figura 1- Localização da área de estudos (destaque em tracejado vermelho) em meio à Zona Externa da Faixa Brasília. (Baseado em Tuller et al., 2013; Signorelli et al., 2013a; Signorelli et al., 2013b; Ribeiro & Féboli, 2013; Tuller, 2014; Brito, 2014).

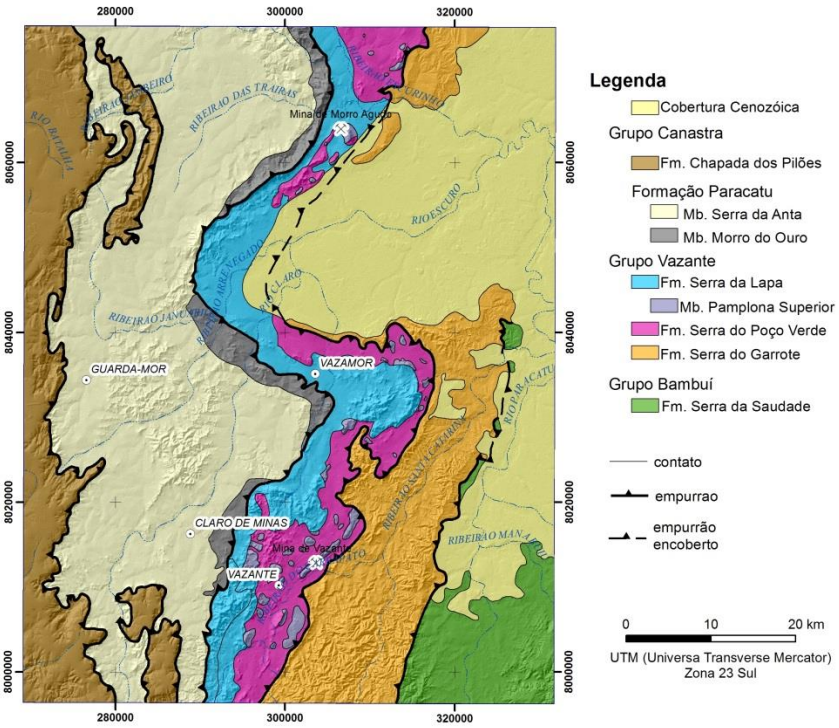

Figura 2 - Detalhe da área de estudos com a geologia (Baseado em Tuller et al., 2013; Signorelli et al., 2013a; Signorelli et al., 2013b; Ribeiro & Féboli, 2013; Tuller, 2014; Brito, 2014) e os empurrões regionais.

2.1.Grupo Vazante

O Grupo Vazante ocupa uma alongada faixa N-S, com comprimento aproximado de 250 km entre as cidades de Unaí e Coromandel e consiste em uma espessa sequência argilo-dolomítica (Dardenne et al., 1997). A idade desse grupo ainda não é bem definida. Suas correlações baseadas em estromatólitos colunares favorecem uma equivalência com o Grupo Paranoá, enquanto os diamictitos da base sugerem uma correlação com o Grupo Bambuí ou Grupo Jequitaí. De acordo com Dardenne (2000) pode ser dividido da base para o topo em 7 (sete) formações: Retiro, Rocinha, Lagamar, Serra do Garrote, Serra do Poço Verde, Morro do Calcário e Formação Serra da Lapa.

A Formação Retiro (Dardenne, 2000) é considerada como a formação basal do Grupo e consiste de bandas métricas de quartzito branco, localmente conglomeráticas, intercaladas com ardósias. Grandes concentrações de fosfato são encontradas na fácies de ardósia e na camada de fosfoarenito, rica em intraclastos e *pellets*. A camada de diamictitos representa um fluxo de detritos depositados em uma profundidade relativa de água por correntes de gravidade (Dardenne et al., 1978).

A Formação Rocinha na sua base consiste de uma sequência rítmica de arenitos e pelitos que grada ascente para a Formação Retiro (Dardenne, 2000). Na sua parte superior consiste de uma espessa sequência de ardósias e metassiltitos. Passam verticalmente para um carbonato e uma ardósia, podendo ocorrer alguns grãos esparsos de pirita, com finas laminações fosfáticas que vagarosamente se transformam em intraclastos e pellets ricos em fosfarenito – Depósito de Rocinha. Na sua parte superior sequências sedimentares rítmicas hospedam o Depósito Fosfático de Lagamar.

A Formação Lagamar de acordo com Dardenne (2000) consiste de uma unidade psamo-pelito-carbonatada e é representada na sua parte basal por camadas alternadas de carbonato, quartzito, metassiltito e ardósia. A unidade conglomerática apresenta uma trama suportada por quartzito, metassiltito e clastos de calcário verde escuro, conhecido como o Membro Arrependido. Essa camada psamítica é sobreposta por brechas dolomíticas intraformacionais com intercalações de brechas lamelares seguidas por um dolomito estromatolítico.

A Formação Serra do Garrote é composta por uma espessa sequência de ardósia, localmente rítmica, carbonosa e contendo pirita, com finas intercalações de quartzito (Madalosso & Vale, 1978; Madalosso, 1980, Dardenne, 1978; Campos Neto, 1984; Dardenne et al., 1997, 1998).

A Formação Serra do Poço Verde corresponde a uma sequência dominantemente dolomítica, inicialmente descrita por Dardenne (1978, 1979) e subsequentemente incorporada à Formação Vazante por Rigobello et al. (1988). É dividida em 4 (quatro) membros da base para o

topo: Morro do Pinheiro Inferior, Morro do Pinheiro Superior, Pamplona Inferior e Pamplona Médio.

A Formação Morro do Calcário (Dardenne, 2000) caracteriza-se por dolomitos interpretados como construções estromatolíticas recifais de profundidade variável entre 100 e 200 m a sul e 650 m a norte. Os flancos dessa sequência contém dolarenito oolítico e oncolítico, além de brechas dolomíticas, interpretadas como brechas intraformacionais. As rochas dessa formação hospedam os depósitos de Morro Agudo, Ambrósia e Fagundes (Monteiro et al., 2006).

A Formação Serra da Lapa (Dardenne, 2000) é representada por filito carbonoso, metassiltito com aspecto carbonático, lentes de dolomito e camadas de quartzito. As lentes de dolomito mostram várias fácies como dolomito laminado com esteiras de cianobactérias, dolomitos com estromatólitos colunares e dolomitos com brechas intraformacionais, interdigitados com a sequência pelítica que cobre regionalmente as formações dominantemente dolomíticas do Morro do Calcário e da Serra do Poço verde.

2.2.Grupo Canastra

O Grupo Canastra ocorre em uma faixa contínua entre o sudoeste de Minas Gerais e o centro e oeste de Goiás. Este grupo foi estudado por Freitas-Silva e Dardenne (1994) e Dias (2011). Na região entre Guarda-Mor e Coromandel, próxima à área de estudos, foi amplamente estudado por Pereira (1992).

De acordo com estes autores, o Grupo Canastra é formado essencialmente por quartzitos, eventualmente micáceos e filitos, por vezes negros e contendo pirita. Estas rochas estão intercaladas, com a predominância de cada uma variando de local para local. Associadas a estas se encontram rochas carbonáticas, carbonáceas e micaxistos. Todas estas sofreram metamorfismo em fácies xisto verde.

É considerado que a espessura média da sequência de filitos e quartzitos varia consideravelmente desde a porção norte, onde sustenta chapadões de grande extensão, até a porção sul, onde parece ter ocorrido encurtamento crustal por força da tectônica compressiva imposta à área (Pereira, 1992). A sequência completa pode atingir cerca de 2000 m de espessura.

Esse conjunto compreende uma sequência iniciada por filitos que apresentam, em direção ao topo, um aumento contínuo da contribuição arenosa, passando a quartzo-filitos, quartzitos micáceos, quarzitos e aos ortoquartzitos que sustentam as escarpas das serras e os chapadões (Pereira, 1992).

Toda essa sequência apresenta uma variação lateral e vertical entre as camadas de filito e quartzito. Essas camadas apresentam, internamente, a mesma gradação em escala menor, evidenciando uma ritmicidade do conjunto.

O ambiente deposicional tido para as rochas do Grupo Canastra é em plataforma marinha, durante um ciclo regressivo, com base na sua característica fundamental de granocrescência ascendente, verificada na gradação dos estratos argilosos da base até estratos arenosos nas porções superiores. As estruturas sedimentares associadas, tais como hummocky, estratificações cruzadas e laminações flaser, também fortalecem essa proposição (Pereira, 1992).

2.3.Grupo Bambuí

O Grupo Bambuí aparece inicialmente em uma pequena porção no sudeste da área de estudos. Ocupa a porção leste da Faixa Brasília e uma ampla área dentro do Cráton São Francisco (Dardenne, 2000). Representa uma associação de fácies bioquímicas e siliciclásticas, na forma de sedimentos plataformais depositados em um extenso mar epicontinental.

Sua espessura é bem variável ao longo da bacia, relacionada a existência de falhas no embasamento (Misi et al., 2005), podendo chegar a até 1000 m no centro da bacia, de acordo com levantamentos sísmicos realizados pela Petrobrás.

Para o Grupo Bambuí foram definidas 6 (seis) formações por Dardenne (1978), são elas: Formação Jequitaí, Formação Sete Lagoas, Formação Serra de Santa Helena, Formação Lagoa do Jacaré, Formação Serra da Saudade e Formação Três Marias.

Ainda há um grande debate quanto à sua idade de deposição. Rodrigues (2008) indica uma idade de 880 Ma para a Formação Jequitaí, correlacionando-a à glaciação global Stuartiana. Para a Formação Sete Lagoas, a mesma autora encontrou uma idade máxima de sedimentação de 610 Ma, indicando assim, uma idade máxima de deposição para toda a sequência do Grupo Bambuí.

2.4.Contexto Geotectônico

A evolução da Faixa Brasília, especialmente da sua zona externa tem sido motivo de discussão por diversos autores durante muito tempo. Em termos mais gerais, temos por Valeriano (1999) a sua evolução iniciada no arqueano (2,6 Ga), com a formação da crosta continental com término no Neoproterozóico-Eopaleozóico (500-450 Ma) após sucessivos eventos de retrabalhamento, distensão, orogenéticos, tafrogenéticos, subduccionais e colisionais, culminando assim no fechamento e na aglutinação do Gondwana.

Modelos de Dardenne (1978, 2000), Fuck (1994), Pimentel (2000) consideram a zona externa da Faixa Brasília como um típico foreland fold and thrust belt, produzido pela inversão de uma margem passiva Neoproterozoica na borda oeste do Craton São Francisco.

Para Uhlein et al. (2012) o estilo de deformação da Faixa Brasília varia com seu nível crustal, assim, no domínio externo da Faixa predomina um estilo thin-skinned (Grupos Canastra, Bambuí e Vazante) enquanto que no domínio interno aparecem zonas de deformação dúcteis mais intensas e largas com metamorfismo em fácies mais altas (estilo thick-skinned – Grupo Araxá e Sequência Anápolis-Ituaçú).

Del Rey et al. (2011) afirmam que para o Domo Brasília as estruturas tectônicas gravam uma deformação polifásica consistindo em um fluxo dúctil D1e D2 e encurtamentos D3. Não obstante, as estruturas D3 caracterizam ambos os encurtamentos nas direções WNW e ESE (D3N), típico do segmento norte da Faixa Brasília e na direção SW-NE (D3S), que é encontrada exclusivamente no segmento sul.

Pereira et al. (1994), estudando a Sequência Paracatu-Vazante, entre Coromandel-MG e Guarda-Mor-MG, defendem que a evolução dessa porção deu-se por 2 (dois) diferentes domínios estruturais: um a sul, de maior deformação, e outro a norte, de menor deformação, sendo os elementos geométricos identificados relacionados a um único evento progressivo de deformação (E1) com dois estágios distintos. O primeiro estágio de deformação (D1) representa uma deformação com intenso componente de cisalhamento simples, de caráter dúctil, ficando atribuído a ele o desenvolvimento de estruturas típicas e zonas de cisalhamento, além da falha de cavalgamento que superpõe os grupos Canastra e Ibiá à unidade Vazante-Paracatu. O seu estágio tardio (D1-tardio) é representado pelo desenvolvimento de uma fase de dobramentos responsável pela geração de diversos estilos de dobras, com vergência geral para leste.

O segundo estágio (D2) caracteriza-se por um componente de cisalhamento puro também compressivo, já em condições dúcteis-rúpteis, produzindo *kink-bands* e *tension gashes*, geralmente em pares conjugados de zonas de cisalhamento com clivagens de crenulação pervasivas, com mergulhos verticalizados e direção N-S e algumas dobras mesoscópicas simétricas em *chevron*, também com plano axial verticalizado e eixo N-S.

Freitas-Silva (1991, 1996) afirma que o Grupo Vazante foi afetado por uma deformação progressiva durante o Ciclo Brasiliano, exibindo um estilo de deformação típico de regiões situadas à frente de fronts de cavalgamentos, dominada por uma componente de cisalhamento puro, com a seguinte sucessão: F1 como o deslizamento intraestratal gerado no início da inversão da Faixa Brasília, F2 como um dobramento flexural com direção NNE-SSW com geração, principalmente nos pelitos, de clivagem plano axial e falhamentos inversos também com direção NNE-SSW subparalelos ao plano axial dos dobramentos. Além das dobras flexurais e falhas inversas, a acomodação da deformação durante a fase F2 foi complementada por falhamentos direcionais, com direções predominantes NE-SW, NW-SE e EW, que podem ser verdadeiros cisalhamentos ou apenas rampas laterais do transporte geral de massa para leste. Com a

atenuação da deformação, foram geradas as estruturas da fase F3, caracterizada pela formação de dobramentos suaves e *kinks* conjugados, com a interferência de seus dobramentos gerando um padrão típico de domo e bacia, que responde pela grande dispersão e pelo duplo caimento de seus eixos.

A Fase F4 é caracterizada por falhamentos normais e fraturamentos generalizados de caráter rúptil em resposta à descompressão da Sequência Paracatu-Vazante, sendo a Falha de Vazante uma das mais importantes falhas dessa fase.

Marcia (2014), estudando a região próxima a Paracatu-MG, sugere a existência de duas fases deformacionais – D1 e D2, sendo D1 caracterizada pela formação de uma clivagem ardosiana e foliação de plano axial das dobras isoclinais P1, além da geração de uma foliação milonítica secundária associada ao sistema de falhas transcorrentes F1. A segunda fase deformacional, D2, está relacionada à formação de uma clivagem de crenulação, clivagem penetrativa de plano axial e dobras quilométricas individualizadas pela imagem de satélite. A Tabela 1 expressa a evolução tectônica em regiões próximas à área de estudo na visão de seis autores: Freitas-Silva (1991), Pereira (1992), Marcia (2014), Silva et al. (2011), Campos-Neto, 1984 e Rostirolla et al. (2002).

Tabela 1- Resumo dos estágios estruturais à qual a região de estudos foi submetida de acordo com Freitas Silva (1991) – Morro do Ouro, Pereira (1992) – Guarda-Mor a Coromandel, Marcia (2014) região de Paracatu, Silva et al (2011) no Domo Brasília, Campos Neto (1984) no oeste de Minas Gerais e Rostirolla et al (2002) na Mina de Vazante.

Eventos	Freitas Silva (1991)	Pereira (1992)	Marcia (2014)	Silva et al (2011)	Campos Neto (1984)	Rostirolla et al (2002)
D1	S_0 transposta e o desenvolvimento de uma recristalização através de diferenciação metamórfica	Domínio 1 - Dobras isoclinais com foliação plano-axial. Na fase tardia dobras assimétricas suaves com vergência para E	S_1 formada por uma clivagem ardosiana, sendo a foliação o plano axial das dobras P_1	S1 // S0, variando de intensidade e morfologia	Dobras com eixo para sudoeste inicialmente passando para eixos NW, NE e EW em deformação progressiva	Deformação progressiva com evolução de níveis crustais inferiores para superiores
	P1 com dobras isoclinais pertencentes à Fm. Paracatu e à Fm. Lapa	Domínio 2 – clivagem ardosiana e foliação milonítica restrita. A lineação das micas é paralela ao estiramento de seixos	P1 com dobras isoclinais nos Grupos Canastra e Vazante	Alguns exemplos de dobras P1 isoclinais e intrafoliais		Dobramentos homoclinais descontínuos e basculamentos
		Falha de cavalgamento na base do Grupo Canastra	Foliação Sn milonítica desenvolvendo o sistema de falhas e empurrões – F_1		Cavalgamentos Paralelos às estruturas	Clivagem ardosiana (s1), clivagem espaçada (s2)
D2	S_2 representando clivagem de plano-axial e foliação milonítica	*Kink bands* e *tension gashes* conjugadas com clivagens de crenulação e	S_2 representando clivagem de crenulação e clivagem penetrativa de	Clivagem de crenulação S2 sobre o Grupo	Falhas Transversais.	Reticulado de falhas distencionais EW e NW que controlam, em

	dobras simétricas. Em um momento tardio clivagem de fratura em pares conjugados	plano-axial	Canastra	grande parte, o fluxo hidrológico nos aquíferos carsticos
P_2 representando dobras isoclinais centimétricas horizontais, apresentando assimentria (flanco longo-curto)		P_2 sendo grandes dobras de escala quilométrica, interpretadas na imagem de satélite	P2 dobras isoclinais assimétricas pouco inclinadas	

3. Metodologia

Para o presente trabalho foram utilizadas quatro técnicas distintas, sendo elas: estudo do fluxo de calor, interpretação de dados aeromagnetométricos, deconvolução de Euler e *Matched Filter*, descritas a seguir.

3.1. Estudos do Fluxo de Calor

Uma grande parcela do calor percebido na crosta terrestre é proveniente do calor gerado pela transformação da energia cinética das partículas emitidas e produzidas no decaimento radioativo dos radioisótopos naturais no processo de interação dessas partículas com os objetos terrestres.

Em uma bacia, parcelas do calor radiogênico produzidas pelas rochas do embasamento, pelas camadas sedimentares da própria bacia, somadas ao calor proveniente da astenosfera, desempenham papéis importantes em sua história térmica (Sapucaia et al., 2005).

O transporte de materiais enriquecidos em urânio, tório e potássio ocorre através de atuações diversas como processos metamórficos, de fusão crustal, metassomatismo e hidrotermalismo. A distribuição desses elementos nas várias litologias está diretamente ligada a estes processos, que normalmente ocorrem em diferentes profundidades na crosta terrestre e com variação na escala do tempo. A diferenciação magmática é responsável pela distribuição inicial desses mesmos radioelementos, sendo os dois últimos mais sensíveis aos vários processos dessa diferenciação (Adams & Gasparini, 1970). A atuação posterior de processos metamórficos altera a distribuição destes elementos enriquecendo alguns de seus níveis. Da mesma maneira, o hidrotermalismo tende a redistribuir estes elementos, trazendo-os para as porções mais externas da crosta (Figura 3).

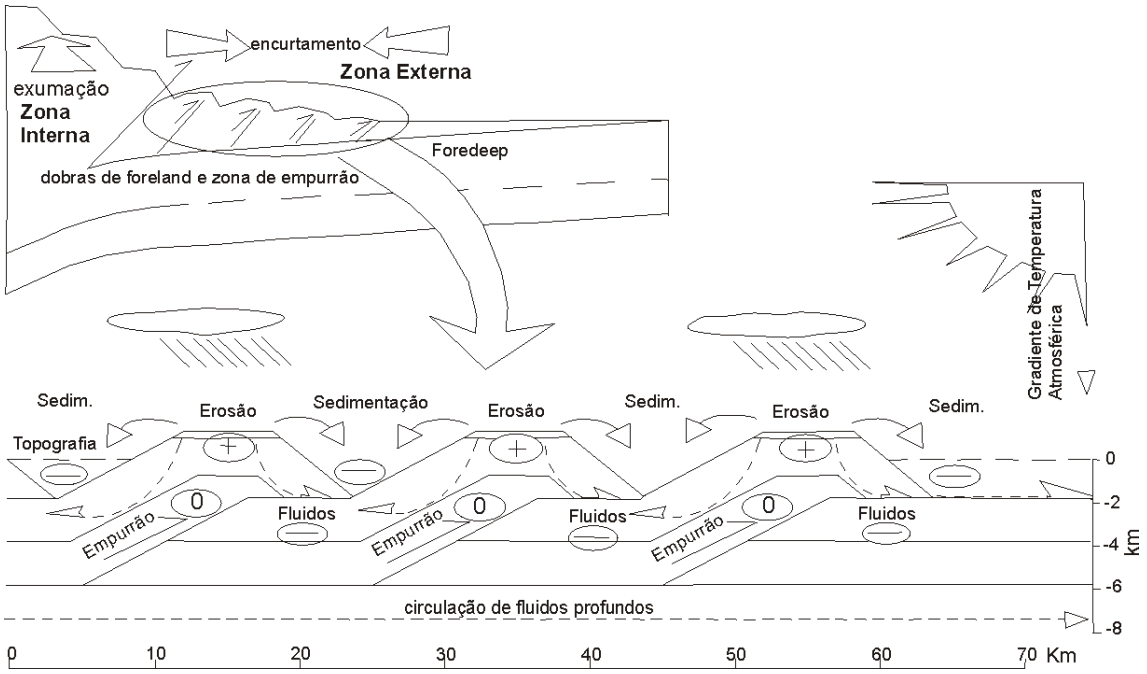

Figura 3– Corte transversal esquemático em uma região repleta de fronts de empurrão para explicar a dinâmica termal dos processos próximos à superfície.

Quatro radioisótopos – U^{238}, U^{235}, Th^{232} e K^{40}- ocorrem em abundância suficiente para contribuir com o orçamento térmico da litosfera. Esses elementos são referidos como elementos produtores de calor radiogênico.

Segundo a fórmula de Ryabach (1986), para uma amostra de rocha de densidade ρ (Kg/m³), o calor radiogênico (A) é dado por:

$$A(\mu W/m^3) = 10^{-5}\rho(9{,}52C_U + 2{,}56C_{Th} + 3{,}48C_K)$$

Onde C_U e C_{Th} são respectivamente a concentração em ppm de U e de Th e C_K é a concentração em porcentagem de K.

Ryabach (1986) derivou uma relação linear entre as leituras de raios gama (em unidades API) e A. Posteriormente ela foi aprimorada e chegou-se a simples relação:

$$A(\mu W/m^3) = 0{,}0158\ (CT(API) - 0{,}8)$$

Como pode ser visto, existe uma correlação excelente ao longo de toda a faixa de raios gama de quase 0 API em e rochas ultrmáficas e basálticas e de até 350 API para rochas graníticas. O coeficiente de regressão para a relação linear é que l = 0,98; a equação (2) dá as estimativas de A com um erro relativo inferior a 10% e está correta também para rochas sedimentares. Quanto mais próximo os raios potássio/urânio- e tório/urânio com as médias dos valores da crosta continental, menor é o erro. Com essa relação bem calibrada é possível derivar informações rapidamente significativas do fluxo de calor.

3.2.Processamento e Interpretação de dados aeromagnetométricos

Os dados brutos apresentam o Campo Magnético Anômalo (CMA), corrigido o IGRF (International Geomagnetic Reference Field) do Campo Magnético Total. Os dados do CMA foram gridados com uma célula de 125 m, que corresponde a ¼ do espaçamento da linha de vôo, pelo método de bigrid, que se mostrou mais eficiente que o mínima curvatura na correção linha a linha dos dados.

Após essa primeira etapa, foi feito o micronivelamento dos dados, a fim de melhorar o sinal por meio da filtragem de ruídos com direção coincidente com as da linha de vôo. A partir desse produto foram geradas as demais imagens, como exemplificado na Figura 4.

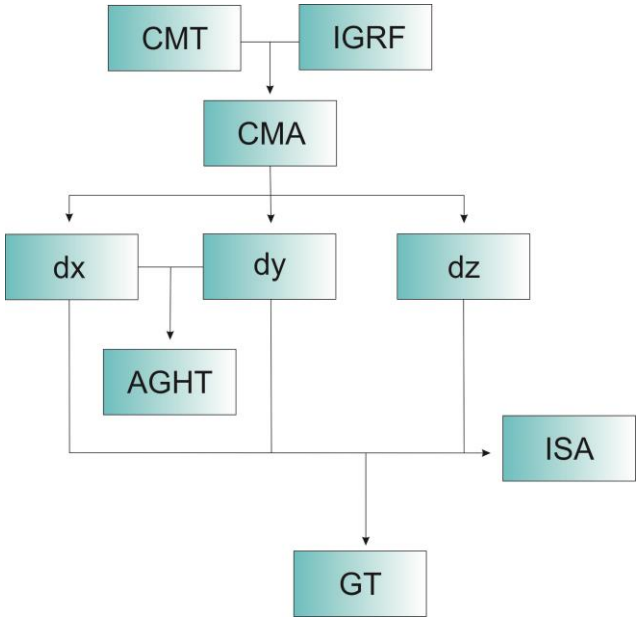

Figura 4- Fluxograma mostrando a dinâmica do processamento geofísico e os principais produtos gerados.

Para a interpretação dos produtos de magnetometria foi utilizado inicialmente o Espectro de Potência Radialmente ponderado da intensidade do Campo Magnético Total. Na forma proposta, com base no modelo espectral de profundidades, segundo Spector & Grant, (1970), trabalha-se com a hipótese de correlação entre as profundidades do topo das fontes magnéticas e as características do sinal medido, mais especificamente o comprimento de onda.

A partir dele foi possível subdividir as assinaturas magnéticas observadas em termos das profundidades relativas de suas fontes dadas pela análise do decaimento espectral de acordo com as faixas de profundidade de maior relevância no referido espectro.

Para a separação do espectro observado nas faixas de frequências espaciais (números de onda) correspondentes a cada família de fontes cujos topos estariam numa determinada profundidade foi feita com uma combinação do filtro passa-baixa do tipo Butterworth na intensidade do Campo Magnético Anômalo micronivelado. Na análise feita foram divisadas quatro faixas espectrais.

Sobre a separação espectral das diversas faixas de frequências espaciais condicionadoras foram gerados: Amplitude do Sinal Analítico (ASA) e Inclinação do Sinal Analítico (ISA), em primeiro momento, sequenciados pela geração das derivadas direcionais (x, y e z) e da Amplitude do Gradiente Horizontal Total (AGHT).

Os domínios magnéticos foram interpretados, em cada caso, a partir da Amplitude do Sinal Analítico do Campo Magnético Anômalo – ASA. Já os lineamentos foram baseados nas imagens da Inclinação do Sinal Analítico do Campo Magnético Anômalo – ISA.

A interpretação dos domínios magnéticos foi realizada a partir da análise dos tipos das anomalias de amplitude do sinal analítico do campo magnético anômalo – ASA, levando-se em conta os distintos comprimentos de onda e amplitude, além dos padrões característicos de cada domínio referente aos outros produtos derivados do Campo Magnético Anômalo – CMA, os quais são a Amplitude do Gradiente Horizontal Total – AGHT e Derivada Vertical - Dz. A opção pela ASA se deu pelo fato de os valores máximos de amplitude do sinal analítico representarem o centro do corpo magnético gerador da anomalia e as regiões de maior gradiente indicarem os seus respectivos limites.

O arcabouço magnético foi obtido a partir dos produtos derivados do Campo Magnético Anômalo micronivelado, mais especificamente a Inclinação do Sinal Analítico – ISA das bandas B0, B1, B2 e B3. Foi utilizada ainda composição ASA-ISA para aprimorar a compreensão do relevo e fonte magnética. A trama dos lineamentos magnéticos evidencia três sistemas com direção preferencial para N70ºE, além de estruturas N30ºE e N30ºW.

3.3.Deconvolução de Euler

A deconvolução de Euler, inicialmente desenvolvida por Thompson (1982) e posteriormente refinada por Reid et al (1990) e Reid (2003) é um método para uma rápida estimativa da profundidade de uma região, que para isso utiliza a equação da homogeneidade de Euler:

$$X-Xo(\partial T/\partial x)+Y-Yo(\partial T/\partial y)+Z-Zo(\partial T/\partial z)=N\ (B-T)$$

Sendo, **T** o campo regional, **B** o campo observado e **N** o índice estrutural.

Para isso, é preciso conhecer sua área de estudos (x, y, z) e o tamanho da anomalia e sua profundidade esperada. Para análise de dados magnéticos o índice estrutural varia de 0 a 3, sendo o 0 relacionado a estruturas planares, 1 a estruturas lineares, 2 a corpos bidimensionais e 3 a corpos tridimensionais.

Precisa ser testado também o tamanho da janela a ser processada e a porcentagem de tolerância admitida, sendo esses dois fatores associados ao problema analisado. O tamanho da janela influi nos tamanhos da anomalia estudada, ou seja, um aumento nesse valor resulta em maiores profundidades, mas diminui o número de soluções.

3.4.Matched Filter

No presente trabalho, a filtragem espectral foi feita através do método descrito por Phillips (2001), por meio de um algoritmo da USGS (Phillips, 1997). O seu filtro é escolhido interativamente através dos gráficos do programa MFDESIGN, ajustando a camada fonte equivalente ao log da potência RSP. O MFDESIGN também inclui um ajuste não linear dos parâmetros equivalentes da camada para o melhor ajuste do espectro analisado. A separação espectral e qualquer filtro azimutal são realizados no programa MFFILTER, o qual também calcula a transformada inversa de Fourier e remove os ruídos e as extensões colunares. Um quarto programa é utilizado MFPLOT para plotar as curvas de resposta dos filtros.

O número de onda mais alto a ser analisado é definido pela frequência de Nyquist. Haja vista que comprimentos de onda menores do que o dobro da distância entre amostras não poderão ser detectados, frequências maiores que a de Nyquist devem ser considerados ruídos aleatórios (Davis, 1986). Abaixo segue a relação entre profundidade da fonte geradora e o espectro radial de potência:

$$h= -(S/4\pi)$$

Onde, h é a profundidade da fonte e S é a inclinação de uma determinada reta no logaritmo de densidade de energia.

O espectro de potência radialmente ponderado – A frequência de Nyquist (fn) definida para o aerolevantamento foi de $1km^{-1}$, ou seja, um ciclo por quilômetro, tendo em vista que deve ser de duas vezes a distância entre os pontos de amostragem (Davis, 1986). Desta forma, foram considerados para análise somente os sinais inferiores a fn, pois aqueles maiores tendem a ser prováveis ruídos.

4. Escopo do Projeto

Conforme previsto no regulamento do Curso de Pós Graduação em Geologia da Universidade de Brasília e por sugestão do Orientador, esta dissertação de mestrado encontra-se estruturada na forma de artigos a serem submetidos para a publicação em periódicos científicos especializados sobre o tema. Estes se encontram apresentados na mesma forma em que serão submetidos.

No capítulo 5 é apresentado o paper de título "Fluxo de Calor em Bacias Precambrianas Associadas à Tectônica Thin Skin : A Sequência Paracatu-Vazante, Brasil Central". Os autores provavelmente submeterão esse artigo à revista *Tectonophysics*, publicada pela Elsevier, Holanda. Esse texto tem como objetivo principal o entendimento da Sequência Vazante-Paracatu através do desenvolvimento de estudos de fluxo de calor, em que foi explorada a técnica para a caracterização das diferentes unidades e litologias, bem como aplicar para o estudo das Bacias dos Grupos Canastra e Vazante, além do fluxo de calor em meio às mineralizações.

O Capítulo 6 apresenta o paper de título "Structural Geology of a Neoproterozoic Thin Skin Thrust Foreland System in Central Brazil: Depth of Sources Based on Airborne Survey and Field Relationships". Os autores provavelmente submeterão esse artigo à revista *Precambrian Research*, publicada pela Elsevier, Holanda. Esse texto tem como objetivo principal o estudo do arcabouço tectônico da porção central da Sequência Vazante-Paracatu, em que são definidas as estruturas principais e seu enquadramento tectônico na região, bem como o estudo de suas profundidades através da magnetometria.

Por fim, no capítulo 7 foi feita uma conclusão geral do projeto de mestrado e proposições de pesquisas futuras.

5. **Referências**

Adams, J.A.S. & Gasparini P. 1970. Gamma-Ray Spectrometry of Rocks. Methods in Geochemistry and Geophysics Series. Elsevier Publishing Company.

Affolter, T. and Gratier, J. (2004). Map view retrodeformation of an arcuate fold-and-thrust belt: The Jura case. Journal of Geophysical Research 109. doi: 10.1029/2002JB002270. issn: 0148-0227.

Almeida, F. F. M. 1967. Origem e Evolução da Plataforma Brasileira. Rio de Janeiro, DNPM/DGM.96 p. (Boletim 241).

Almeida, F. F. M. 1977. O Cráton do São Francisco. Rev. Bras. Geoc., 7(4): 349-364.

Almeida, F. F. M.; HASUI, Y; BRITO NEVES, B. B.; FUCK, R.A. 1981. Brazilian Structural Provinces: an introduction. Earth Sciences Rev.,v. 17, p. 1-29

Anudu, G. K., Stephenson, R. A., Macdonald, D. I. M. 2014. Using high-resolution aeromagnetic data to recognise and map intra-sedimentary volcanic rocks and geological structures across the Cretaceous middle Benue Trough, Nigeria. Journal of African Earth Sciences V. 99, Part 2, p. 625–636. Special Volume of the 24th Colloquium of African Geology.

Araújo Filho, J. O. 2000. The Pirineus Syntaxis: an example of the intersection of two Brasiliano fold-thrust belts in central brasil and its implications for the tectonic evolution of western Gondwana. Revista Brasileira de Geociências, v. 30, n. 1, p. 144-148.

Argollo, R. B., Marinho, M. M., Costa, A. B., Sampaio Filho, H. A., Santos, E. J., Coutinho, L. F. C. 2012. Modelo crustal e fluxo de calor nos domínios Estância, Canudos-Vaza-Barris e Macururé adjacentes às bordas emersas da Bacia Sergipe-Alagoas. B. Geoci. Petrobras, Rio de Janeiro, v. 20, n. 1/2, p. 283-304.

Bellahsen, N., L. Jolivet, O. Lacombe, M. Bellanger, A. Boutoux, S. Garcia, F. Mouthereau, L. Le Pourhiet, Gumiaux, C. 2012. Mechanisms of margin inversion in the external Western Alps: Implications for crustal rheology, Tectonophysics, 560–561, 62–83, doi:10.1016/j.tecto.2012.06.022.

Brito, D. C. 2014. Mapa Geológico da folha Serra da Tiririca. Ministério de Minas e Energia. Secretaria de Geologia, Mineração e Transformação Mineral. Belo Horizonte. Escala 1:100.000.

Bücker, C.; Rybach, L. 1996. A simple method to determine heat production from gamma-ray logs. Elsevier Science Publishers, v 13, n.4, p.373-375.

Campos Neto, M. C. 1979. Contribution à l'étude des Brasilides: Lithostratigraphie et Structure des Groupes Canastra, Paranoá et Bambuí dans l'ouest nord-ouest de l'Etat de Minas Gerais-Brésil. Dissertação de Mestrado. Université Pierre et Marie Curie, LISE / CNRS, França. 212 pp.

Campos Neto, M. C.. Geometria e fases de dobramentos brasilianos superpostos no oeste de Minas Gerais. Revista Brasileira de Geociências, São Paulo, Brasil, v. 14, n.1, p. 60-68, 1984.

Coelho, J. C. C.; Martins-Neto, M. A., Marinho, M. S. 2008. Estilos estruturais e evolução tectônica da porção mineira da bacia proterozóica do São Francisco. *Rev. bras. geociênc.* [online]. 38 (2): suppl.1, pp. 149-165. ISSN 0375-7536.

Cunha, I. A., Coelho, C. E. S., Misi, A. 2000. Fluid Inclusion Study of the Morro Agudo Pb and Zn deposit, Minas Gerais, Brazil. Revista Brasileira de Geociências 30, 318-321.

Cunha, I. A., Misi, A., Babinski, M. 2001. Lead isotope signature of galenas from Morro Agudo Pb-Zn deposits, Minas Gerais, Brazil. In: Misi, A., Teixeira, J. B. G. (Eds.), Proterozoic Base Metal Deposits of Africa and South Africa. Proceedings of the first IGCP 450 Field Workshop. CNPq/UNESCO/IUGS, Belo Horizonte and Paracatu (MG), Brazil, pp. 45-47.

Dahlen, F.A., 1990, Critical taper model of fold-and-thrust belts and accretionary wedges: Annual Review of Earth and Planetary Sciences, v. 18, p. 55–99

Dardenne M. A., Freitas-Silva F. H., Nogueira G. M. S., Souza J. F. C. 1997. Depósitos de fosfato de Rocinha e Lagamar, Minas Gerais. In: Schobbenhaus C., Queiroz E. T., Coelho, C. E. S., Principais depósitos minerais do Brasil, DNPM/CPRM, v.IV C, p.113-122.

Dardenne, M. A. & Freitas-Silva, F. H. 1998. Modelos Genéticos dos depósitos de Pb-Zn nos Grupos Bambuí e Vazante. Workshop Depósitos Minerais Brasileiros de Metais Base, Salvados, CPGG-UFBA/ADIMB, p.86-93.

Dardenne, M. A. 2000. The Brasilia Fold Belt. *In:* Cordani, E. G., Milani, E. J. Thomaz Filho, A., Campos, D. A. Tectonic evolution of South America. Rio de Janeiro: 31° International Geology Congress. p. 231-263.

Dardenne, M. A.; Faria, A. ; Magalhães, L. F. ; Soares, L. A. 1978. O tilito da base do Grupo Bambuí na Borda Ocidental do Craton São Francisco. Boletim Núcleo Centro Oeste - SBG, Goiânia, v. 7/8, p. 85-97.

Dardenne, M.A. 1978. Zonação tectôncia da borda ocidental do craton do São Francisco. In: CONGR. BRAS. GEOL., 30, Recife, 1978, Anais... Recife, SBG. V. 1, p. 299-308.

Dardenne, M.A. - 1979 - Les mineralisations de plomb, zinc, fluor du Protérozoique Superieur dans le Brésil Central.Thése de Doutorat d'Etat, Université de Paris VI, 251p, (inédito).

Davis, D., Suppe, J., Dahlen, F.A., 1983. Mechanics of fold and thrust belts and accretionary wedges. J. Geophys. Res. 88, 1153–1172.

Davis, J.C. 1986. Statistics and Data Analysis in Geology, 2nd edn. (646 pages). John Wiley & Sons: New York, NY.

D'el Rey Silva L.J.H.D., Oliveira I.L., Pohren, C. B., Tanizaki, M. L. N., Carneiro, R. C., Fernandes, G. L. F., Aragão, P. E. 2011. Coeval perpendicular shortenings in the Brasìlia belt: collision of irregular plate margins leading to oroclinal bending in the Neoproterozoic of central Brazil, Journal of South American Earth Sciences, 32, p. 1 -13.

Dias P.H.A. 2011. Estratigrafia e Tectônica da Faixa Brasília na Região de Ibiá, Minas Gerais: Estudo de Proveniência Sedimentar dos grupos Canastra e Ibiá, com base em estudos isotópicos U-Pb e Sm-Nd. Instituto de Geociências, Universidade Federal de Minas Gerais, Dissertação de Mestrado.

Espurt, N., Hippolyte, J.-C., Saillard, M., Bellier, O. 2012. Geometry and kinematic evolution of a long-living foreland structure inferred from field data and cross section balancing, the Sainte-Victoire System, Provence, France. Tectonics 31, TC4021. http://dx.doi.org/10.1029/2011TC002988.

Freitas-Silva F.H. 1991. Enquadramento lito-estratigráfico e estrutural do depósito de ouro de Morro do Ouro, Paracatu/MG. Dissertação de Mestrado, UnB-IG, 151p.

Freitas-Silva F.H. 1996. Metalogênese do Depósito do Morro do Ouro, Paracatu – MG. Tese de Doutorado, UnB-IG, 338 p.

Freitas-Silva, F. H. ; Dardenne, M. A. 1994. Proposta de subdivisão estratigráfica formal para o Grupo Canastra no oeste de Minas Gerais e leste de Goiás.. In: 4º Simpósio de Geologia do Centro-Oeste, Brasília. Anais. Resumos Expandidos. p. 161-163.

Freitas-Silva, F. H., Dardenne, M. A. 1998. Fluid inclusions and isotopic ^{18}O and ^{13}C geochemistry of zinc ore in Vazante, Vazante/MG Fluid inclusions and isotopic ^{18}O and ^{13}C geochemistry of zinc ore in Vazante, Vazante/MG. In: 40 CONGRESSO BRASILEIRO DE GEOLOGIA, 1998, Belo Horizonte. 40 CONGRESSO BRASILEIRO DE GEOLOGIA.

Fuck, R. A. 1994. A Faixa Brasília e a Compartimentação Tectônica na Província Tocantins. In: Simpósio de Geologia do Centro-Oeste, 4., Brasília. Atas... Brasília: SBG, 1994. p. 184-187.

Hasui, Y. & Almeida, F.F.M. 1970. Geocronologia do Centro Oeste Brasileiro. Bol. Soc. Bras. Geol., v. 19, n. 1, p. 7-26.

Kwon, S., Sajeev, K., Mitra, G., Park, Y., Kim, S.W., Ryu, I. C. 2009. Evidence for Permo-Triassic collision in far east Asia: the Korean collisional orogeny Earth and Planetary Science Letters, 279, pp. 340–349

Macedo, J.M. & Marshak, S. 1999. Controls on the geometry of fold-thrust belt salients. Geol Soc Am Bull 111: 1808-1822.

Madalosso, A. & Valle, C. R. O. 1978. Considerações sobre a estratigrafía e sedimentología do Grupo ambuí na Região de Paracatu – Morro Agudo (MG). In: Congresso Brasileiro de Geologia, 30. Anais. SBG, v.2, p. 622-631.

Madalosso, A. 1980. Aspectos da diagênese dos carbonatos do Grupo Bambuí na Região de Paracatu (MG). In: Congresso Brasileiro de Geologia, 31. Camboriú, 1980. Anais, Camburiú, SBG, v.4, p.2069-2081.

Marcia, L. 2014. Studio Geologico Strutturale del Settore della Faixa Brasiliana compreso tra Paracatù e Vazante (Minas Gerais - Brasile). Universita' degli Studi di Cagliari. Facolta di Scienze. 93 pp. (inédita).

Misi, A., Azmy, K., Kaufman, A. J., Oliveira, T. F., Sanches, A. L., Oliveira, G. D. 2014. Review of the geological and geochronological framework of the Vazante sequence, Minas Gerais, Brazil: Implications to metallogenic and phosphogenic models. Ore Geology Reviews v. 63, p. 76–90.

Misi, A.; Iyer, S. S S; Coelho, C. E. S; Tassinari, C. C. G; Franca-Rocha, W. J. S.; C., I. A.; Gomes, A. S. R.; Oliveira, T. F.; T., J. B. G. 2005. Sediment-Hosted Lead-Zinc Deposits of the Neoproterozoic Bambuí Group and Correlative Sequences, São Francisco Craton, Brazil: A Review and a Possible Metallogenic Evolution Model. Ore Geology Reviews, Amsterdam, v. 26, n. 3, p. 263-304.

Mitra, G. 1997. Evolution of salient in a fold-and-thrust belt: the effects of sedimentary basin geometry, strain distribution and critical taper, in: S. Sengupta, ed., Evolution of geological structures in micro-to-macro scales: London, Chapman & Hall, p. 59-90.

Monteiro L.V.S. 2002. Modelamento metalogenético dos depósitos de zinco de Vazante, Fagundes e Ambrósia, associados ao Grupo Vazante, Minas Gerais. 317 pp. Tese de Doutorado. Universidade de São Paulo.

Monteiro, L.V.S., Bittencourt, J.S., Juliani, C., de Oliveira T.F. 2006. Geology, Pethrography and mineral chemistry of the Vazante, Ambrosia and Fagundes Neoproterozoic carbonate-hosted Zn-Pb deposits, Minas Gerais, Brazil. Ore Geology Reviews v. 28, p. 201-234.

Neves, L. P. 2011. Características Descritivas e Genéticas do depósito de Zn-Pb Morro agudo, Grupo Vazante. Dissertação de Mestrado – Universidade de Brasília, Brasília – DF.

Pereira L.F. 1992. Relações tectono-estratigráficas entre as unidades Canastra e Ibiá na região de Coromandel, MG. Dissertação de Mestrado, UnB-IG, 73p.

Pereira, L.; Dardenne, M. A.; Rosière, C. A.; Pedrosa-Soares, A. C. 1994. Evolução Geológica dos Grupos Canastra e Ibiá na região entre Coromandel e Guarda-Mor, MG. Geonomos, v. 2, p. 22-32.

Philippe, Y., E. Deville, and A. Mascle.1998. Thin-Skinned Inversion Tectonics at Oblique Basin Margins: Example of the Western Vercors and Chartreuse Subalpine Massifs (SE France), Geol. Soc. London Spec. Publ., 134, pp. 239–262.

Phillips, J.D. 1997. Potential-field geophysical software for the PC, version 2.2. US Geological Survey Open-File Report 97-725.

Phillips, J.D. 2001. Designing matched bandpass and azimuthal filters for the separation of potential-field anomalies by source region and source type. Australian Society of Exploration Geophysicists, 15th Geophysical Conference and Exhibition, Expanded Abstracts CD-ROM, 4p.

Pimentel, M. M. 2000. The Neoproterozoic Goiás Magmatic Arc, Central Brazil: a Review and New Sm-Nd Isotopic Data. Revista Brasileira de Geociências, 30(1):035-039.

Pimentel, M. M. 2004. O embasamento da Faixa Brasília e o Arco Magmático de Goiás. In Capítulo XXI- Geologia do Continente Sul-Amercano : Evolução da Obra de Fernando Flávio Marques de Almeida. p. 325-369.

Reid, A. B., Allsop, J.M., Granser, H., Millett, A.J., Smerton, I.W. 1990. Magnetic interpretation in three dimensions using Euler deconvolution. Geophysics, 55, 80-91.

Reid, A.B. 2003. Euler magnetic structureal index of a thin bed fault. Geophysics, 68, 1255p. doi:10.1190/1.1598117

Ribeiro, J. H., Féboli, W. L. 2013. Mapa Geológico da folha Coromandel. Ministério de Minas e Energia. Secretaria de Geologia, Mineração e Transformação Mineral. Belo Horizonte, 2013. Escala 1:100.000.

Rigobello A. E. Branquinho J. A. Dantas M. G. S. Oliveira T. F., Neves Filho W. 1988. Mina de zinco de Vazante. In: C. Schobbenhause C. E. S. Coelho (eds): Principais Depósitos Minerais do Brasil. DNPM, Brasília, v. 3, p. 101-110.

Rodrigues, J. B. 2008. Proveniência de sedimentos dos grupos Canastra, Ibiá, Vazante e Bambuí – Um estudo de zircões detríticos e Idades Modelo Sm-Nd. 128 pp. Tese (Doutorado) – Universidade de Brasília.

Rostirolla, S. P., Mancini, F., Reis Neto, J. M., Figueira, E. G., Araújo, E. C. 2002. Análise estrutural da mina de vazante e adjacências: geometria, cinemática e implicações para a hidrogeologia. Revista Brasileira de Geociências, 32(1):59-68.

Rybach, L. 1986. Amount and significance of radioactive heat sources in sediments. In: BURRUS, J. (Ed.) Thermal Modeling in Sedimentary Basins. Paris: Technip, p. 311-322.

Sapucaia, N.S.; Argollo, R.M.; Barbosa, J.S.F. 2005. Teores de potássio, urânio, tório e taxa de produção de calor radiogênico no embasamento adjacente às bacias sedimentares de Camamu e Almada, Bahia, Brasil. Revista Brasileira de Geofísica, v. 23, p. 453-475.

Signorelli, N, Pinho, J. M. M., Tuller, M. P.; Baptista, M. C.; Brito, D. C. 2013 b. Mapa Geológico da folha Lagamar. Ministério de Minas e Energia. Secretaria de Geologia, Mineração e Transformação Mineral. Belo Horizonte. Escala 1:100.000.

Signorelli, N; Tuller, M. P.; Pinho, J. M. M.; Baptista, M. C.; Brito, D. C. 2013 a. Mapa Geológico da folha Arrenegado. Ministério de Minas e Energia. Secretaria de Geologia, Mineração e Transformação Mineral. Belo Horizonte. Escala 1:100.000.

Spector A., Grant F.S. 1970. Statistical models for interpreting aeromagnetic data, Geophysics, 35, 293–302.

Suppe, J. 1987. The active Taiwan mountain belt, in Schaer, J.P., and Rodgers, J., eds., Anatomy of mountain chains: Princeton, New Jersey, Princeton University Press, p. 277–293

Thompson, D.T. 1982. EULDPH: A new technique for making depth estimates from magnetic data. Geophysics 47, 31-37

Tuller, M. P. 2014. Mapa Geológico da folha Paracatu. Ministério de Minas e Energia. Secretaria de Geologia, Mineração e Transformação Mineral. Belo Horizonte. Escala 1:100.000.

Tuller, M. P.; Signorelli, N, Baptista, M. C., Brito, D. C. 2013. Mapa Geológico da folha Guarda-Mor. Ministério de Minas e Energia. Secretaria de Geologia, Mineração e Transformação Mineral. Belo Horizonte, 2013. Escala 1:100.000.

Uhlein, A., Fonseca, M. A., Seer, H. J., Dardenne, M. A. 2012. Tectônica da Faixa de Dobramentos Brasília – Setores Setentrional e Meridional. Geonomos, 20(2), 1-14.

Valeriano, C. M. A Faixa Brasília meridional com ênfase no segmento da Represa de Furnas: Estado atual do conhecimento e modelos de evolução tectônica. 1999. Tese (Livre Docência) – Universidade Estadual do Rio de Janeiro, Rio de Janeiro.

Valeriano, C.M., Pimentel, M.M., Heilbron, M., Almeida, J.C.H. & Trouw, R.A.J. 2008. Tectonic evolution of the Brasília Belt, Central Brazil, and early assembly of Gondwana. In: Pankhurst, R.J., Trouw, R.A.J., Brito Neves, B.B. & de Wit, M.J. (eds) West Gondwana: Pre-Cenozoic Correlations Across the South Atlantic Region. Geological Society, London. Special Publications, 294, 197-210.

Vasconcellos, R. M.; Metelo, M. J.; Motta, A. C.; Gomes, R. D. 1994. Geofísica em Levantamentos Geológicos no Brasil.CPRM, Rio de Janeiro.

6. Heat Flux in Precambrian Basins Related to Thin-Skin Tectonics: Paracatu-Vazante Sequence, Central Brasil

Abstract

We measured the heat flow in geological units of the External Zone of the Brasília Fold Belt, Neoproterozoic orogen tectonics dominantly thin skin type, to investigate the relationship between the two large basins - Canastra and Vazante Group, the different types of mineralization, tectonic environments in region, and to explore the method and its application. For calculating the heat flow, were used high resolution aero gamma-ray spectrometry data (survey line spacing of 250 m) to generate the average heat production estimate. The contribution of the heat flow range from 38 mW/m² for the Canastra Group and 48 mW/m² for Vazante Group. Within these units were found different production values for the various lithologies: siltstones (1.9 to 4.5 μW/m³), carbonates (2.1 to 3.9 μW/m³), black shales (2.2 to 4.5 μW/m³) and sandstones (1.9 to 5.3 μW/m³). The discrepancy between the results obtained for these two units indicate depositional environments and different deposition times, just being juxtaposed at the end of the Neoproterozoic, in addition to its sedimentary formations of different thicknesses. Locally, the gaps and percolation fluids are also responsible for the variation of the volumetric production of heat in this region. In addition, it was possible to filter through the volumetric heat flow lower values corresponding to the black shales and carbonates, host rocks of Pb-Zn mineralization and Au in the area, thus constituting an important prospective guide.

6.1. Introduction

A large portion of the thermal energy emitted by the Earth's crust originates from the transformation of the kinetic energy of particles that are emitted and produced during the radioactive decay of natural radioisotopes, keeping in mind that mass is converted into energy during this process. Four radioisotopes, U^{238}, U^{235}, Th^{232} and K^{40}, occur in sufficient abundance to contribute to the heat budget of the lithosphere. These elements are referred to as radiogenic heat-producing elements. According to Bodorkos et al. (2004), approximately two-thirds of all this energy is due to the presence of these three elements. Studies on heat flow variation are indirect methods used to understand what occurs in geothermal terms in a given region.

The surface heat flow generated in a region is the sum of six components: (i) heat generated by the radioactive decay of an unstable isotope in the crust; (ii) heat conducted to the crust from the underlying mantle; (iii) heat refracted in the crust by the structure of thermal conductivity; (iv) heat advected to the crust by magmatism; (v) heat advected inside the crust due

to tectonic deformation; and (vi) heat redistributed in the upper crust due to groundwater flow (Morgan, 2006).

Anomalies in the existing heat flow in a region can be related to several factors, particularly the tectonic environment in which the rocks were created. The heat flow in sedimentary basins is considered low compared with that of other types of geological environments due to the low density of the rocks deposited in these basins (Vilà et al., 2010; Salem et al., 2005; Andreescu et al., 2002). In passive margin basins, Pereira et al. (1986) found that heat conductivity is clearly associated with the granulometry of the sediment because the higher the granulometry is, the greater the capacity to concentrate radioelements in the rocks. Jessop and Majorovicz (1994) stated that heat flow abnormalities in sedimentary basins can be connected to the supply of heat from the basement and the water content within the basin. Intracratonic basins have uniform heat flow, which is dependent on the depth of the basement, whereas in passive margin basins and rift basins, there is a correlation between the heat flow, depth of the basin and distance from the shoreline (Jessop & Majorowicz, 1994).

Different tectonic regimes in orogenic or collisional systems influence the superficial response of heat flow in internal and external zones of orogenic belts. In internal zones of thrust systems, there is a concentration of heat flow in topographically elevated regions with increased radiogenic heat in areas with greater crustal thickening. In external zones, whose tectonics are characterized as thin-skin tectonic processes that affect only the sedimentary cover, the heat flow tends to be redistributed between layers that have undergone rapid sedimentation or erosion in foreland basins, where the deformation is concentrated in the horizontal strata (Dewey et al., 1999; Husson & Moretti, 2002). In the case of external zones, the erosion of mountain ridges, when active, may enhance the heat flow by two times in the first few kilometers of the basin's depth.

Locally, contractional faults, changes in surface morphology and percolation of fluids can also generate anomalies in high heat flows (Husson & Moretti, 2002).

The use of geophysical data as a methodology to calculate heat flow has been applied in various tectonic environments around the world (Bordokos, 2004; Salem et al., 2005). The comparison of the easy and low cost application of aerogeophysical data to understand basins (Husson & Moretti, 2002; Salem et al., 2005) with traditional methods (measurement of hand samples, wells and outcrops) has shown that high-resolution aerogeophysical data have good correlation with and similar accuracy as conventional data (Salem et al., 2005).

The use of this methodology is recommended and can bring a new perspective in the use of heat flow data in the South American platform (Argollo et al., 2012; Pereira, 1986; Cardozo &

Hamza, 2014). However, the approach used for ancient Brazilian Neoproterozoic basins still lacks more consistent models.

This study presents a heat flow analysis using aerogeophysical data in the western portion of the state of Minas Gerais, Brazil between the cities of Guarda-Mor, Vazante and Claro de Minas, i.e., the External Zone of the Brasília Belt. The Vazante Group is considered a passive margin basin inverted by thin-skin compression (Uhlein et al., 2012) and exhibits an unusual lithological variation with rocks typical of platform margin alongside rocks typical of a marine environment (Dardenne 1978; Dardenne 2000; Oliveira, 2013). The Canastra Group is interpreted as a passive margin regressive megacycle with a basal section rich in organic matter, interpreted as deep water, followed by turbidite levels and eventually shallow shelf sediments occurring (Dardenne, 2000, Pereira, 1992).

Economically, the study area has lead (Pb) and zinc (Zn) mines, i.e., Morro Agudo and Vazante, and is also close to one of the largest gold (Au) mines in the country, Morro do Ouro. The sedimentation and evolution of the host basins of these mineralizations have not been widely discussed, and there are few absolute consensuses. The data presented in this study provide new perspectives for evolutionary models in this important mining district and determine the paleoenvironmental conditions and the influence of the depositional substrate of these sedimentary basins; from this, data are generated to assist in the understanding of the depositional substrate conditions by considering the relationship between the topographic contrast of the substrate and the hydro-paleoflow, sedimentation, stratigraphy and thickening of the layers that occur in the sedimentary basins of the Vazante and Canastra Groups.

6.2. Regional Geology

The study area is located at the western end of the state of Minas Gerais near the cities of Guarda-Mor, Paracatu and Vazante and approximately 500 km from the capital, Belo Horizonte. The area is in the eastern portion of the Brasília Belt in its external zone (Dardenne, 2000), which is in the Tocantins Province (Figure 1).

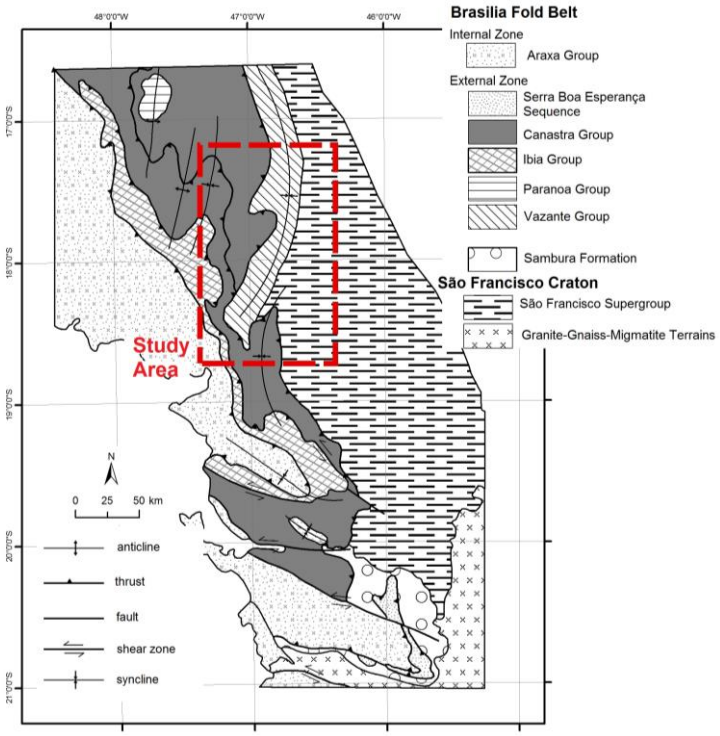

Figure 1- Study area location (red polygon, Figure 2) amid the Brasília Belt. (Tuller et al., 2013; Signorelli et al., 2013a; Signorelli et al., 2013b; Ribeiro & Féboli, 2013; Tuller, 2014; Brito, 2014, e Valeriano, 1999).

The Brasília Belt is partitioned based on the modern classification of collisional belts (Fuck, 1994; Dardene, 1978, 2000; Pimentel, 2004; Valeriano, 2008) and is divided into the following: (i) Goiás Massif, allochthonous sialic terrain, which contains granite gneiss terrains and greenstone belts and, to the south, associated mafic-ultramafic complexes; (ii) Goiás Magmatic Arc, separated into the Mara-Rosa to the north and Arenópolis to the south; (iii) the Internal Zone, represented by rocks of the Annapolis-Itauçu Complex metamorphosed in granulite facies and metasedimentary rocks of the Araxá Group, imbricated in the basement; (iv) the External Zone, represented by the Proterozoic metasedimentary stack, which includes the Paranoá, Canastra, Ibia and Vazante Groups, formed in a passive continental margin environment in addition to the Serra da Mesa and Natividade Groups; and v) the Cratonic Zone, located on the west edge of the São Francisco Craton, which includes sediment from the Bambuí Group and basement exposures (Almeida et al., 1981; Fuck, 1994; Pimentel, 2000).

The focus of this study is the External Zone (EZ) of the Brasilia Belt, which consists of metasedimentary units (Paranoá, Canastra, Ibia, Vazante and, locally, the Bambuí Groups) and portions of its basement. In this zone, sedimentary facies that correspond to the passive margin predominate, and the metamorphism is greenschist facies (Figure 1). Figure 2 shows the geology of the study area (CPRM, 2014) and the main thrust faults.

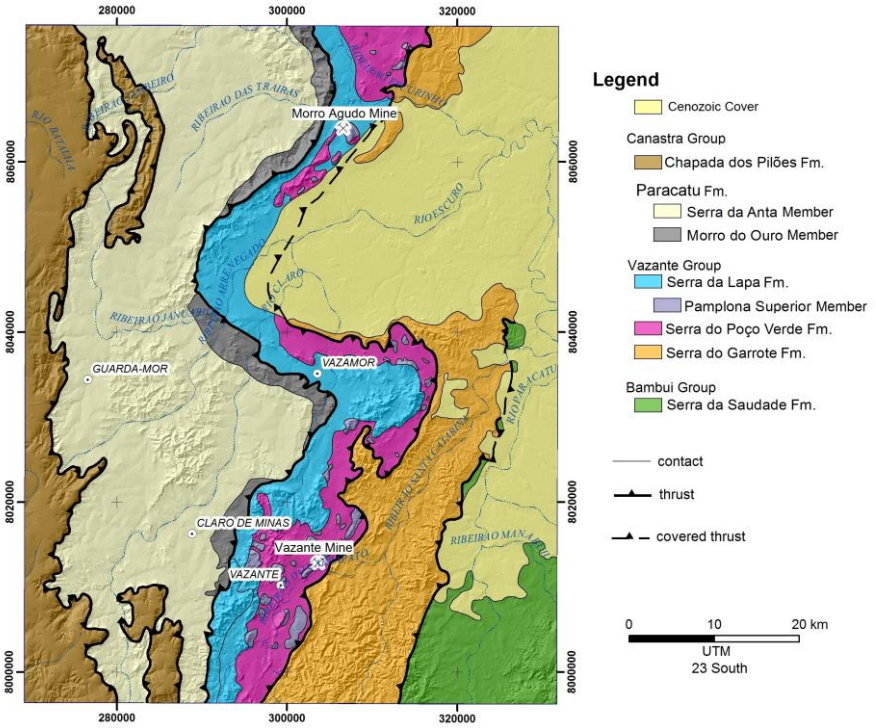

Figure 2 - Detail of Figure 1 with the geology and regional thrusts of the study area (Adapted from Tuller et al., 2013; Signorelli et al., 2013a; Signorelli et al., 2013b; Ribeiro & Féboli, 2013; Tuller, 2014; Brito, 2014).

The Vazante Group occupies an elongated N-S range with an approximate length of 250 km between the towns of Unai and Coromandel and consists of a thick clay-dolomite sequence (Dardenne et al., 1997). Oliveira (2013) stated that the basin was the result of a series of four distinct depositional and evolutionary stages: (i) deposition of silts and marine platform shales, (ii) development of carbonate ramp with the evolution of a sabkha tidal plain, (iii) emergence of a regional flood surface and (iv) the development of a barrier carbonate platform. According to Dardenne (2000), it can be divided into seven formations from bottom to top: the Retiro, Rocinha, Lagamar, Serra do Garrote, Serra do Poço Verde, Morro do Calcário and Serra da Lapa Formations. Misi et al. (2014) determined the Mesoproterozoic age using Re-Os dating, which ranges from 1.1 Ga to 1.3 Ga for the upper and middle portions of the group; however, the Neoproterozoic age was found to range from 600 Ma to 800 Ma (Rodrigues, 2008) for the lower portions, the Rocinha and Santo Antonio do Bonito Formations, which indicates tectonic contact from the base to the Lagamar Formation.

The Retiro, Rocinha, Serra do Garrote and Serra da Lapa Formations are part of the clay sequence of the Vazante Group, which range from rhythmites to slates, siltstones and phyllites and may contain lenses of quartzite and dolomite, generally in greenschist facies (Dardenne, 2000). The northern sequences, as opposed to the southern sequences, may also contain sandstones and conglomerates intercalated with slate (Rodrigues, 2008). The Lagamar Formation features a carbonate package that covers the pelites from the Retiro Formation.

The Serra do Poço Verde Formation corresponds to a predominantly dolomite sequence, which was initially described by Dardenne (1978, 1979) and subsequently incorporated into the Vazante Formation by Rigobello et al. (1988). This formation is divided into four members from the base to the top: Inferior Morro do Pinheiro, Superior Morro do Pinheiro, Inferior Pamplona and Middle Pamplona.

The Morro do Calcário Formation (Dardenne, 2000) or Superior Pamplona of the Serra do Poço Verde Formation (Rigobello, 1988; CPRM, 2014a, b, c) is characterized by dolomites interpreted as reef stromatolitic constructions of varying depths, between 100 and 200 m to the south and 650 m to the north. The flanks of this sequence contain oolitic and oncolytic dolarenite and dolomitic breccias, which are interpreted as intraformational breccias. The rocks of this formation host the Morro Agudo, Ambrosia and Fagundes deposits (Monteiro et al., 2006).

The Canastra Group occurs in a continuous strip between southwestern Minas Gerais and central and western Goiás. This group was studied by Freitas-Silva and Dardenne (1994) and, more specifically, in the region of Guarda-Mor and Coromandel, near the study area, was extensively studied by Pereira (1994). Its age is considered by several authors (Bertoni et al., 2014; Rodrigues, 2008; Azmy, 2008; Dias, 2011) to be approximately 1.0 Ga.

The Canastra Group consists primarily of quartzites, at times micaceous and phyllitic, sometimes black, and contains pyrite. Associated with these are carbonate, carbonaceous and mica rocks. All have undergone metamorphism in greenschist facies.

In the region of Paracatu and Vazante (Pereira et al., 1994), the Canastra Group was divided into three formations from bottom to top: Serra do Landim Formation – calciphyllites to calcisiltites; Paracatu Formation - divided into two members, the Morro do Ouro Member (quartzites at the base and carbonaceous phyllites at the top) and the Serra da Anta Member (phyllites with thin interbedded quartzites and carbonates); and the Chapada dos Pilões Formation - quartzites that may be interspersed with phyllites.

Determining the thickness of the formations that constitute the Vazante and Canastra Groups is hampered primarily by the thrust faults that affect the entire region, which often change the thickness of the layers. Figure 3 shows the stratigraphic stacking for the region according to Dardenne (2000) and Pereira et al. (1994).

	Formation		Thickness
Canastra Group	Chapada dos Pilões	Quartzite interbedded with phyllites Sandy Rhythmites with interbedded quartzites	550 m
	Paracatu - Serra da Anta Member	Sericite phyllite intercalated with carbonaceous phyllites and quartzite	600 m
	Paracatu - Morro do Ouro Member	Carbonaceous phyllites interlayered with quartzite and sericite phyllite	600 m
Vazante Group	Lapa	Slates Carbonated with sandy dolomite lens	500 m
	Morro do Calcário	Bioherma stromatolitic with rocks facies and sandy dolomite	250 m
	Serra do Poço Verde	Dolomites with stromatolites mats, barite nodules and dryness of crevasses	2250 m
		Slates with interleaving dolomites	
		Dolomites with stromatolites mats and bird's eyes	
		Dolomites with rocks and sandy dolomites	
	Serra do Garrote	Slates with rare lenses of quartzite	1000 m

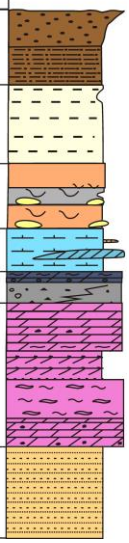

Figure 3 - Stratigraphic column adapted from Dardenne (2000) and Pereira et al (1994) for the study area having approximate thicknesses for each geologic unit.

The structure of this region is marked by thrust faults inverting the basin, known as the first deformational phase of this system, which also developed several shear zones and associated structures (Pereira, 1992). This caused the uplift of a paleohigh that, according to Campos-Neto (1979) and Freitas-Silva (1991), individualized the basin of the Vazante Group.

Using seismic data for the area, Coelho et al. (2008) defined the existence of two sets of faults with different depths, which indicates that for the majority of faults, there is no contribution from the basement, and therefore, they are only surface faults, i.e., primarily thin-skin deformations. The density of the basement and depth of the Moho were estimated using seismic and gravimetric data for the External Zone of the Brasília Belt by Ventura et al. (2011) and Silveira et al. (2012), respectively. A mean density of 2.57 g/cm^3, p-wave velocities of 7 km/s and vp/vs ratio of 1.72 suggest that the thickness of the crust in the region is 37.2 ± 2.4 km.

However, the thickness of the stratigraphic sequences and the variation in the depth of the basement within the Vazante and Canastra basins have yet to be measured empirically through lithostratigraphic sections (Dardene 1978, Dardenne 2000).

6.2.1. Mineralizations

The mineralizations in this zinc district are hosted amidst the carbonates in the Morro do Calcário and Serra do Poço Verde Formations. However, they are structurally distinct despite the physical proximity of the Vazante and Morro Agudo mines.

The mineralization in Vazante is associated with its namesake, the Fault Zone, has a ductile-brittle characteristic and is oriented approximately in the N50E/60NW direction. The host unit of these mineralizations corresponds to the Lower Pamplona Member, which consists of light gray, beige and rosy metadolomites interlayered with gray or green slate, metamarl,

sericite phyllite and lenses of intraformational breccias (Dardenne 1979; 2000, Pine, 1990). Willemite is the most important ore of the Vazante mine and occurs as pockets tectonically imbricated in brecciated metadolomites, metabasites and smaller bodies, which are tectonized and consist of sulfides. In sulfide bodies, willemite can occur along mylonitic foliation planes as part of two mineral associations (Monteiro, 2002).

In the Morro Agudo mine, the mineralizations are associated with the back-reef facies located on the western flank of the stromatolitic bioherm of the Morro do Calcário (Dardenne 1978; 1979; Madalosso & Valle, 1978; Madalosso, 1980; Bez, 1980; Dardenne & Freitas-Silva, 1998; Oliveira, 1998; Cunha, 1999). Morro Agudo Mine is controlled by a normal fault with an approximate N10W/75SW direction in addition to the contribution of a brittle-ductile NE-SW Transcurrent Zone, which bounds the ore bodies to the east and is part of a system of closely spaced normal faults that intersect the mineralized bodies. In all of the bodies of ores, sulfides fill late fractures that cut ooids and intraclasts and constitute the vein ore. Sulfide concentrations in secondary faults (Bez, 1980) and in the principal fault (Dardenne, 2000) are also common.

6.3.Methodology

The aero gamma-ray spectrometric data used in this study are from Area 1 of the Geophysical Survey Project of the State of Minas Gerais, a CPRM and CODEMIG partnership. The flight lines were raised in the N30W direction with a spacing of 250 m. The nominal height of the flight was 100 m with an average speed of 200 km/h. (CPRM/CODEMIG, 2001).

The pre-processed data were gridded with a cell size of 60 m using a minimum curvature algorithm from the software Oasis Montaj 7.2 - Geosoft (Figure 4). To conduct the study, two gamma-ray spectrometric data analysis techniques were used, as described below.

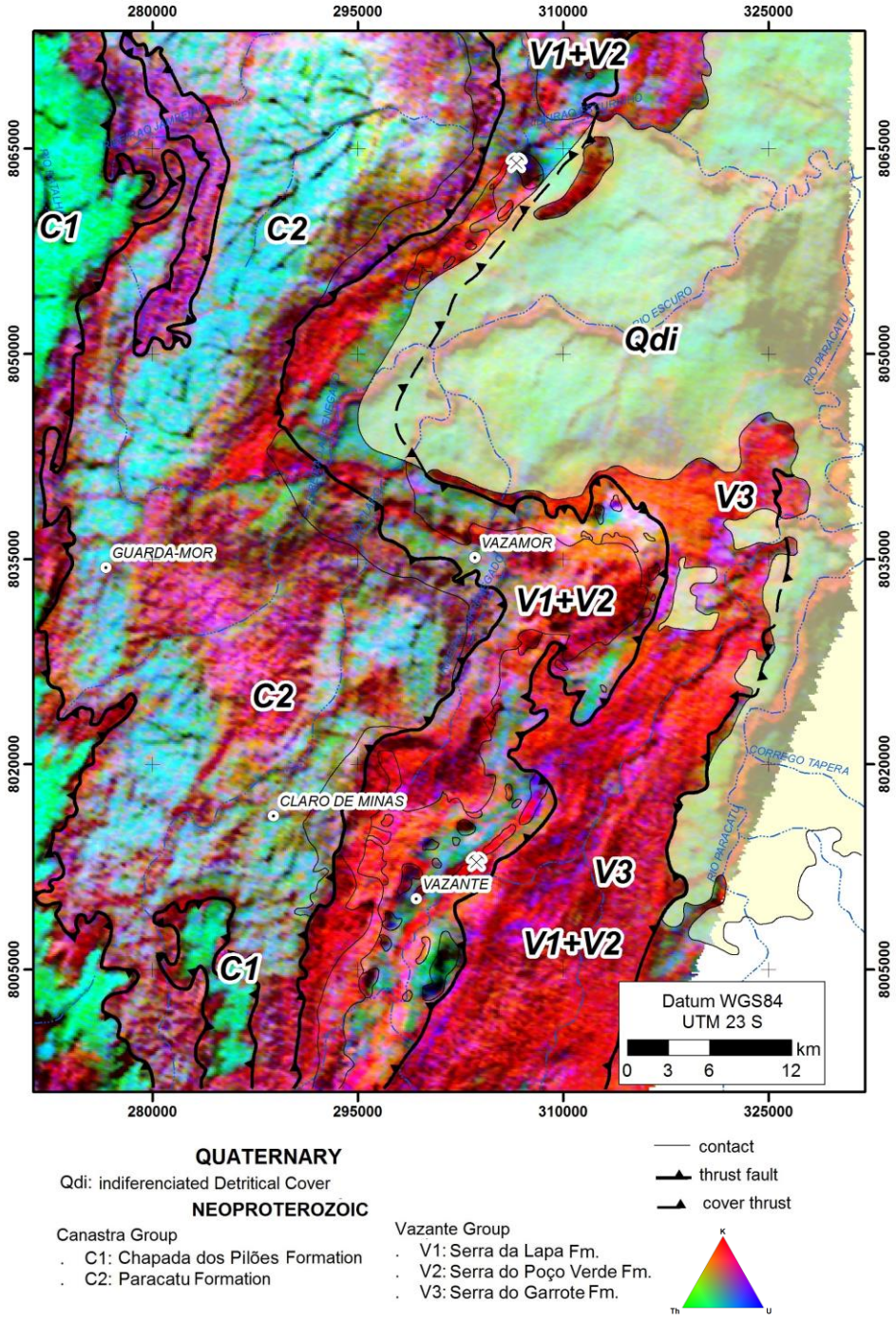

Figure 4 -Ternary composition for Study area with geological boundaries overlapping.

6.3.1. Volumetric Production of Radiogenic Heat

The volumetric heat production map was created using total gamma radioactivity count data (TC). The data unit was converted into API because its initial unit was in µR/h. According to Hilchie (1979), this conversion of units is dependent on the device's specifications. It is recommended to take the equivalent of 1 µR/h as 10 API (Russel, 1944).

In this way, the volumetric production of radiogenic heat channel (A) was obtained based on the simplified equation from Bücker and Ryabach (1996) (Equation 1).

$$A(\mu W/m^3) = 0.0158(TC(API) - 0.8) \quad \text{Equation 1}$$

where the total radioactivity count is given in the API (American Petroleum Institute) unit.

6.3.2. Surface Geothermal Flow

To calculate the heat flow *Q* produced by a block of rock, it is necessary to know the function of the vertical distribution of the heat production rate - A(z). Regarding function A(z), it is known only that this function depends primarily on the lithology and that it decreases with depth, though not systematically in metamorphic regions (Ashwal et al., 1987). Several authors (Hawkesworth, 1974; Fountain and Salisbury, 1981; Nicolaysen et al., 1981; Schneider et al., 1975; Reyes, 2008) have obtained this function by studying regions where a vertical crustal section is exposed on the surface by tectonics. In this case, A(z) is determined directly in samples taken from these sections. However, in this study, we followed the methodology of Bordokos et al. (2004), where these data are obtained through volumetric heat production maps, that were subsequently compared with the existing values in the literature to assess their validity.

To obtain A(z), the domains for each the individual heat contribution is being investigated - in our case, the basins of the Canastra and Vazante Groups - are typically evaluated separately. From this, the exponential fit functions are obtained, as described by Equation 2:

$$A(z) = \alpha + \beta e^{-\frac{z-x}{t}} \quad \text{Equation 2}$$

where α, x and t are parameters to be fit using experimental data, and β corresponds to the surface heat flow.

The use of exponential equations is important when working with heat flow, considering that it is the only way to preserve the linear relationship between heat flow and topography; i.e., they are valid even in areas affected by erosion (Turcotte & Schubert, 1982).

Knowing that the heat flow on the surface of the domains generated from the crust is the sum of the contribution of heat flow from the rocks plus the portion generated by the substrate (Argollo et al., 2012), an additional calculation is required for the basement under the domain and for the basal flow.

Rybach and Buntebartw (1984), related there is a relationship between geothermic flow and medium density for Paleoproterozoic rocks, in Fennoscandia, which we have applied as a estimative for our study area (Equation 3).

$$A = 21.4 - 8.15\rho \qquad \text{Equation 3}$$

where **A** is heat production in μW/m^3, and **ρ** is the density of the medium in g/cm³.

Therefore, knowing the function of the vertical variation in heat production A(z) in the domain and in its substrate and the thickness thereof, the heat flow Q produced by a block of rocks can be calculated with Equation 4:

$$Q = \int_{z_1}^{z_2} A(z)dz \qquad \text{Equation } \underline{4}$$

where the integral of A(z) is within the limits Z_1 and Z_2 of the block's thickness.

Finally, for the generation of geothermal flow on the surface, the contribution of the crust (basin and basement) must be added to the basal heat flow from the asthenosphere (Reyes, 2008).

6.4. Results

After initial processing, with the generation of K (%), Th (ppm) and U (ppm) and the total count maps, a map was generated with the volumetric heat production calculated for the study areas according to Equation 1 (Figure 5).

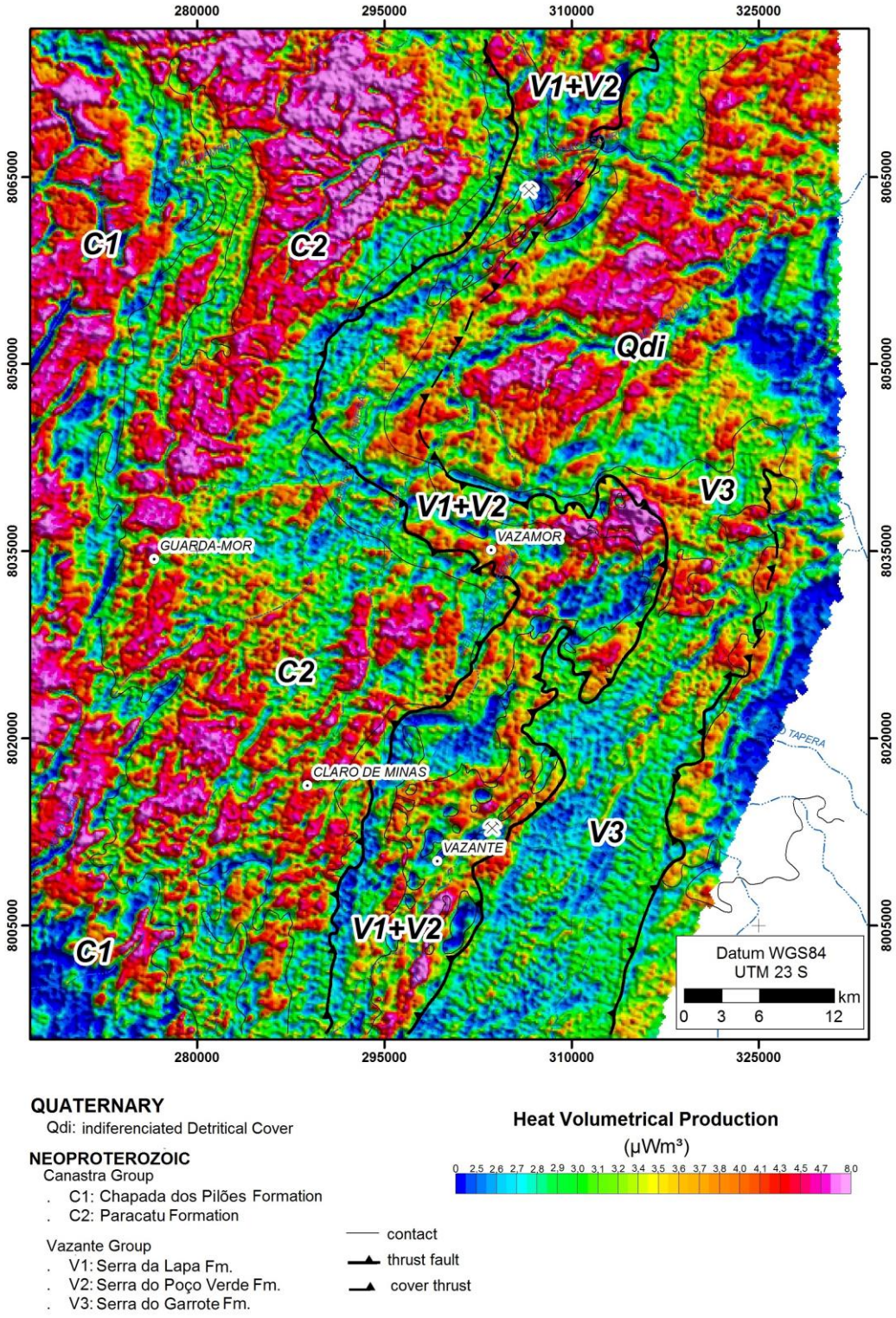

Figure 5 – Map of the volumetric radiogenic heat production generated in the study areas, which highlights the limits of the geological map at a 1: 100,000 scale, modified from Tuller et al., 2013, Signorelli et al., 2013a, Signorelli et al., 2013b, Ribeiro & Féboli, 2013; Tuller, 2014; Brito, 2014).

The volumetric heat production for the study areas ranged from 8 μW/m³ to 0 μW/m³ with a mean of 3 μW/m³ and with the highest amounts related to laterizations and sediments with

larger grain sizes, such as the Chapada de Pilões Formation, which is composed of sandstones, and the Paracatu Formation, which is formed by carbonates and phyllites but is extremely lateritized. The lowest values, those near 0, were related to rocks with only a slight presence of radioactive elements, which included the following: carbonates, black shales and siltstones in addition to the rivers of the region and recent sediments.

Based on the volumetric heat production data for the Canastra Group and Vazante Group, exponential fit functions were calculated for the vertical distribution of the volumetric rate of heat production (Equation 2). The following are the obtained values: Canastra Group: $A(z) = 3.7894e^{-1.10^{-4}x}$ and Vazante Group: $A(z) = 3.4256e^{-2.10^{-5}x}$.

Thus, after obtaining A(z), the contribution of each geologic unit to the surface heat flow can be calculated through an integral with intervals defined by the thickness of the groups (Equation 4), with 2 km for the Canastra Group and 4 km for the Vazante Group in the region (Pereira, 1992, 1994; Dardenne, 1978, 2000). Table 1 summarizes these data.

Table 1 – Heat Flux produced by each geological unit.

Geological Unit	Main Rocks	Max. And min. Of heat production (μW/m³)		Mean of heat production (μW/m³)	Heat flux for each domain (mW/m²)
Chapada dos Pilões Fm.	Arenitos e Quartzitos	1,9	5,3	3,798	6,63
Serra da Anta Mb.	Siltitos e Filitos Carbonosos	2,2	4,8	3,373	
Morro do Ouro Mb.	Filitos Carbonosos	2,2	4,5	3,222	
Serra da Lapa Fm.	Siltitos com intercalações de Carbonatos	2,1	4,9	3,373	17,13
Pamplona Superior Mb.	Carbonatos	2,1	3,9	3,395	
Pamplona Inferior Mb.	Siltitos com intercalações de carbonatos	1,9	5,3	3,323	
Serra do Garrote Fm.	Siltitos a Filitos rosados	1,9	5,1	3,211	

Based on the methodology of Reyes et al. (2008) for calculating the heat flow in the areas, the surface heat flow, the contribution from the basement, and the contribution from the crust were added to the basal heat flow from the asthenosphere.

To calculate the basement heat flow using Equation 3, the density value of 2.57 g/cm³ (Ventura et al., 2011) was used as the standard, and a volumetric heat flow contribution of 0.37 $\mu W/m^3$ was obtained for the region, which means a contribution of 13.13 mW/m² for the region of the Canastra Group and 12.4 mW/m² for the Vazante Group using 37.2 km as the average thickness of the crust (Silveira et al., 2012).

Because no data on the basal heat flow from the asthenosphere are available for this region, we used, as a standard, the value obtained by Reyes (2008) for the rift Camamu Almada Basin, i.e., 18.8 mW/m², because this basin was also developed on the São Francisco Craton.

As seen in Figure 3, the fault regions and shear zones have volumetric heat production ranging from low to extremely low; remember that because the values for lateritized portions and for larger particle-size formations within the Canastra Group were extremely high, the portions with moderate to high heat production presented themselves as low due to the interpolation of all the results along with the black shales, carbonates, drainages and sediments. Accordingly, the volumetric radiogenic heat production map shown in Figure 4 has been reprocessed with the exclusion of values greater than 3 µW/m³ and a 2% linear histogram enhancement of the values between 0 and 3 µW/m.

The resulting image (Figure 6) shows the exposure areas of the host rocks and Pb and Zn mineralizations in the region (black shales and limestones), which, as previously seen, have a low volumetric heat production rate. Thus, this image can be used as one of the elements to be considered in the search for new exploration targets (prospective guide).

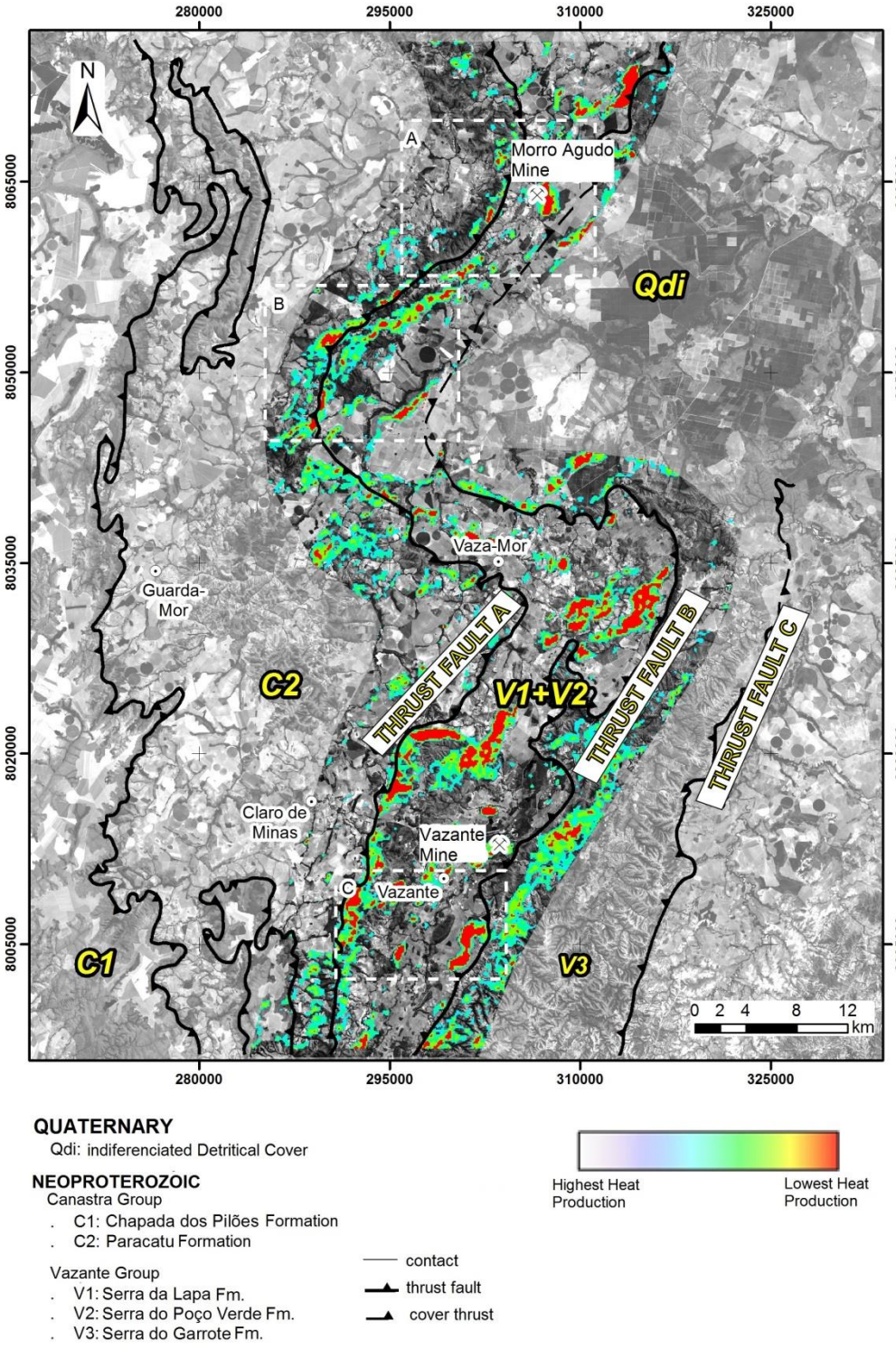

Figure 6 –Map of radiogenic heat volumetric production to the exclusion of values greater than 3 μW / m³ and linear histogramic enhancement 2% of values between 0 and 3 μW / m³. The lowest intensity anomalies (close to 0 μW / m³) have the colors red, given that the bodies of carbonates and black shales are associated with lower heat flux rates. The small rectangles dashes are related to the highlighted areas in Figure 7.

The areas indicated as A, B and C in Figure 6 are highlighted in Figure 7 and demonstrate the high correlation between low heat anomalies and outcrops of carbonate rocks and black

shales mapped by CPRM (2014). This indicates the reliability of this methodological approach to discriminate new targets.

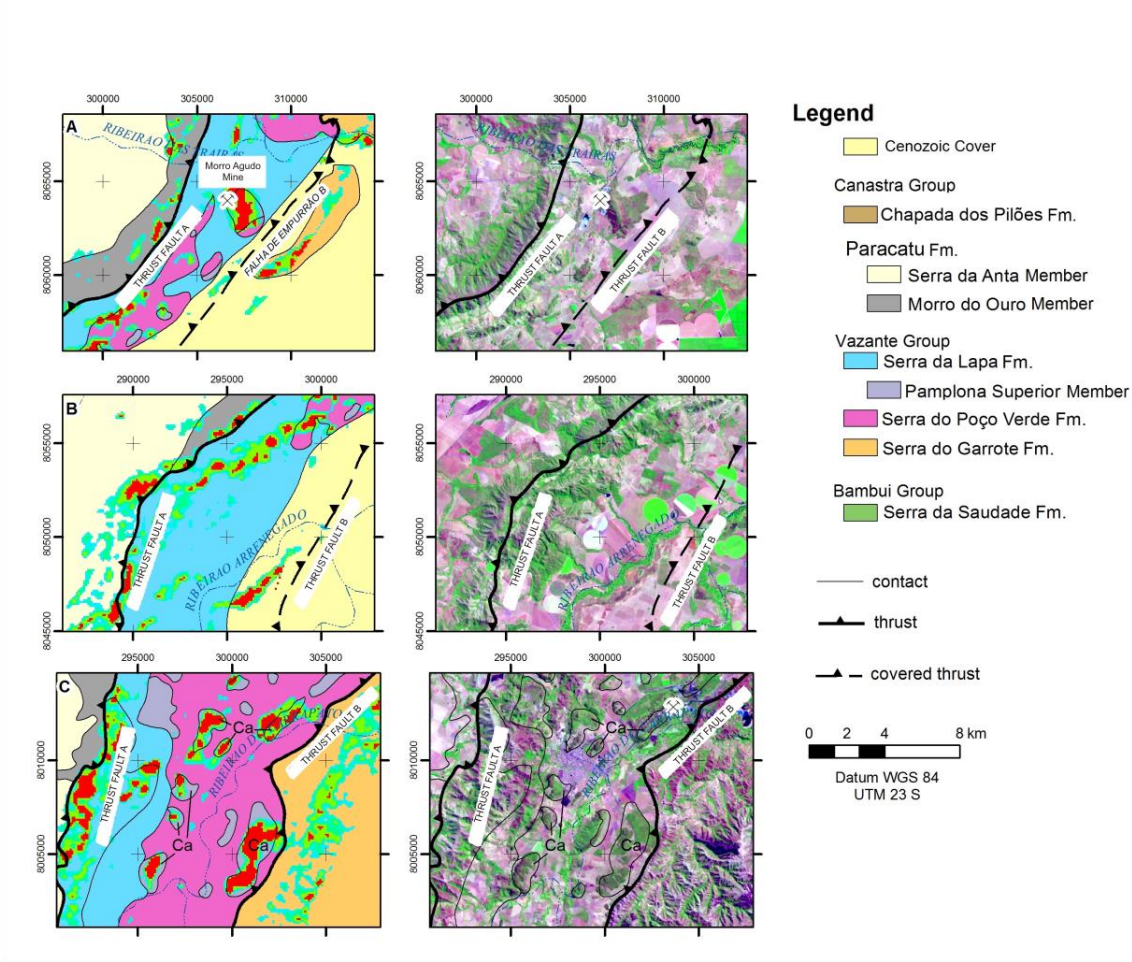

Figure 7 - Correlation between areas with low radiogenic heat and and Landsat 8.1colorful composition. Note the high correlation between low heat values and carbonate rocks and mapped shales. Location in Fig. 6 by dotted polygons.

The greatest anomaly is in **A**, which corresponds to the lowest heat flow value in the region of the Morro Agudo mine, showing the strong relationship of the carbonates with low heat flow and also minor anomalies in the black shales of the Paracatu Formation. In **B**, we identified anomalies in the Paracatu Formation, which correspond to the black shales, and in the Serra da Lapa Formation, which correspond to the carbonaceous portions. In **C,** the anomalies correspond exactly to the small carbonate hills mapped in the region in addition to black shales in the Paracatu Formation and carbonaceous portions in the Serra da Lapa Formation.

6.5. Discussion

6.5.1. Heat Flow and Sedimentation Environment

Because these are Neoproterozoic passive margin basins, the mean volumetric production of surface heat values were 3.33 μW/m³ for the rocks of the Vazante Group and 3.46 μW/m³ for the rocks of the Canastra Group. These values are high considering that the mean rates for

sedimentary rocks are approximately 0.8 μW/m³ for sandstones, 1.4 μW/m³ for mudstones and up to 1 μW/m³ for carbonate rocks (Vilà et al, 2010; Al-Alfy & Nabih, 2013). The high volumetric heat production value, particularly in the Canastra Group rocks, is explained by the considerable amount of uranium and thorium in the rocks, which are less mobile elements, related to the concentration of these elements in detritus, such as the sandstones of the Serra das Antas Formation and the high index of lateritization in the region. Lateritization is a chemical weathering process formed by leaching of the parent rock, which results only in insoluble ions, primarily iron and aluminum, and therefore prevents water penetration to depth levels greater than the laterite generated (Batista et al., 2008). In addition, the rocks of the Canastra Group have a larger grain size compared with that of the Vazante Group, particularly the Chapada dos Pilões Formation, which thereby allows a greater concentration of radiogenic elements (Pereira et al., 1986).

The heat flow for the entire Vazante Group is 48.33 mW/m² (Figure 7), which is similar to the values obtained in other basins with similar tectonic styles, such as in the orogenic region of the Arabian Shield, which varies from 39 to 73 mW/m² (Rolandone et al., 2013). The value for the heat flow of the Canastra Group basin is 38.56 mW/m², which corresponds to the values obtained for Neoproterozoic basins, such as the eastern Canadian Shield (Pinet et al., 1991).

It is believed that the large difference in heat flow between the basins of the Canastra and Vazante Groups, approximately 20%, is due to the differences in the depositional environment of these two basins. The Canastra Group has a shallower basin, approximately 2 km deep, formed by sandstones and black shales with thin-skin tectonics that pushes over the rocks of the Vazante Group, generating erosion in the first few kilometers of the crust and consequently deposition in the Vazante Group, which has a surface heat flux of 6.13 mW/m^2. The Vazante Group consists of a deeper basin, approximately 4,000 meters deep, formed by shallow water carbonates in the central portion (Dardenne, 1978, Dardenne, 2000, Oliveira, 2013) and deep water pelagic sediments in the distal portion, also with thin-skin tectonics that in turn pushes on the rocks of the Bambuí Group with a surface heat flow of 17.34 mW/m². Therefore, the heat flow is closely associated with the depth of the basin, related to the position of the basement in the system.

Thus, the two basins have different geothermal histories, which is consistent with the fact that they are of different ages and joined only at the end of the Neoproterozoic period, a time when the two were already well consolidated (Figure 8).

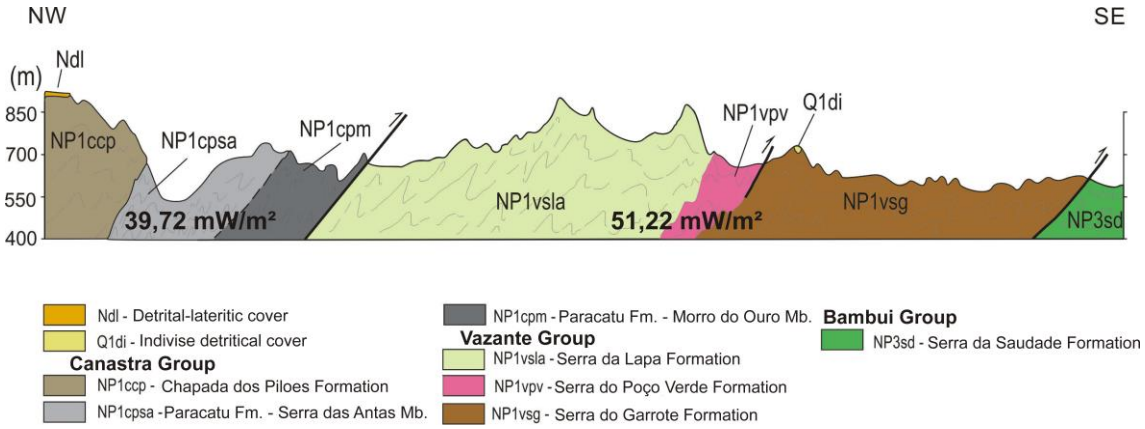

Figure 8 - Geological profile for the area of studies showing the heat flow generated by each of the basins.

Given that heat flow depends on the total thickness of the sediment deposited in the basin, each layer has an individual contribution to the system (Waples, 2002, Norden & Förster, 2006).

Due to the great variation in the volumetric production of internal heat flows to the basins with differences of 500%, their depositional history is thus complex (see Jessop & Majorowicz, 1994) with many associated events that caused their heat production to not be homogeneous. This is explained by the rocks typical of shallow environments, limestones with bioherms, adjacent to rocks from deep environments, siltstones and mudstones, showing that the depositional substrate of this basin was irregular.

Thus, younger rocks have higher radiogenic heat production rates than older rocks. This may be related to the gradual erosion of the upper crustal portions (which generates more radiogenic elements). Thus, although the basins of the Canastra and Vazante Groups have similar heat production rates, because they were formed in the Precambrian, their depositional history is different, and therefore, they have small variations that reflect the subsidence, deposition and also depth of the basement of each (Waples, 2002; Argolo et al., 2012; Beach et al., 1987; Morgan, 1995).

According to the studies of Coelho et al. (2008) for the Brasília Belt, Argolo et al. (2012) for the Sergipe Basin, and Matos et al. (2015) for the Canastra and Vazante Groups, and the heat flow results for the basins of the Canastra Group and the Vazante Group, we believe that the groups have different basement depths, where the basement superimposed on the Canastra Group is located in a portion higher than the basement superimposed on the Vazante Group.

There are also internal variations in heat production within the basins, which may also suggest different sediment deposition depths, such as the dolomites near the Morro Agudo Mine, with heat production values of 2.6 $\mu W/m^3$, and near the Vazante Mine, with values of 2.4 $\mu W/m^3$, that thus indicate the existence of shallow and deep sources in the basin at the time of its

deposition (Vitorello et al., 1980). However, there is no direct comparison between depth and heat flow considering that each rock, as well as each type of basin, has a relative contribution.

Considerable variations in heat flow are indicative of young volcanism or other heat sources that cause the heat flow to be extremely anomalous in relation to regional values obtained in the literature (Hu et al., 2000). The values found for the basins of the Canastra and Vazante Groups are in the acceptable range, and young volcanism has not been found in the study area. However, there is a Neocretaceous alkaline volcanism near the city of Catalão, Minas Gerais (MG), which can influence the heat flow throughout the entire region.

It is believed that the basement of the region is formed by felsic rocks, considering the moderate to high amount of heat flow found for the region; for basements formed by mafic rocks, the heat flow is well below the general average, such as in the Ural Mountains, which is a region formed by Island Arc-like tectonics with mafic magmatism (Kukkonen et al., 1997, Gazzas & Hashad, 1991).

The study area today is characterized as a stable region because it is a passive margin and was later deformed into a foreland system. Alexandrino & Hamza (2008), Hamza et al. (2005) and Vitorello et al. (1980) estimated the heat flow for South America, including the São Francisco Craton, the adjacent folded belts and points of interest, such as carbonates from the Vazante and Morro Agudo mines. The average values obtained by these authors were 50-70 for the rocks of the São Francisco craton, approximately 48 for the region of Tocantins Province, 53 mW/m^2 for the dolomites of the Morro Agudo mine and 44 mW/m^2 for the dolomites of the Vazante mine.

From the data on the average rate of heat production for each geological unit, it can be seen that the units belonging to the Vazante Group had a higher contribution than those belonging to the Canastra Group. The Superior Pamplona Member belonging to the Serra do Poço Verde Formation was the unit with the greatest influence on the high heat flow of the Vazante Group, which may be related to its higher crustal thickening and high circulation of different types of associated fluids as well as erosion and recent sedimentation. The Lower Pamplona Member had a lower average rate, which may be related to its smaller thickness within the set.

Because the study area was deformed with thin-skin tectonics, the thrust faults are shallow, and the seismics indicate that faults and deformation occur only in the most superficial levels. The heat flow values may be compared with those of other basins that exhibit this deformation style, such as in the orogenic region of the Arabian shield, which shows heat flow

variations of 39 to 73 mW/m² (Rolandone et al., 2013), or the Andean subregion of Bolivia, with variations ranging from 50 to 55 mW/m² (Husson & Moretti, 2002).

Thus, according to Husson & Moretti (2002), under regular conditions in external zones of orogenic belts, where portions of the thrust fault are not as thick, the thermal field is not generally affected. Thus, because the volumetric heat production corresponding to thrust faults B and C of the study area were low, it is believed, according to the models of Coelho et al. (2008) and Matos et al. (*in press*), that these structures are more superficial. They are related to the first system described by Coelho et al. (2008) without the contribution of the basement; i.e., they are restricted only to the first few kilometers of the crust and correspond to the thin-skin deformation model.

6.5.2. Fluids and Ductile-Brittle Shear Zones

Despite the low level of heat production from the Vazante and Morro Agudo mines, quantitatively, the heat flow around the Morro Agudo Mine has higher responses than those of the Vazante deposit, which may be related to the fact that because the mineralization of Vazante is predominantly silicatic, it provides a lower response to the radiogenic elements (Figure 9). This relationship between heat flow and metal mineralization has been found in other parts of the world (Gazzaz & Hashad, 1991) and could be an effective tool in further exploration studies in the Vazante-Paracatu Range.

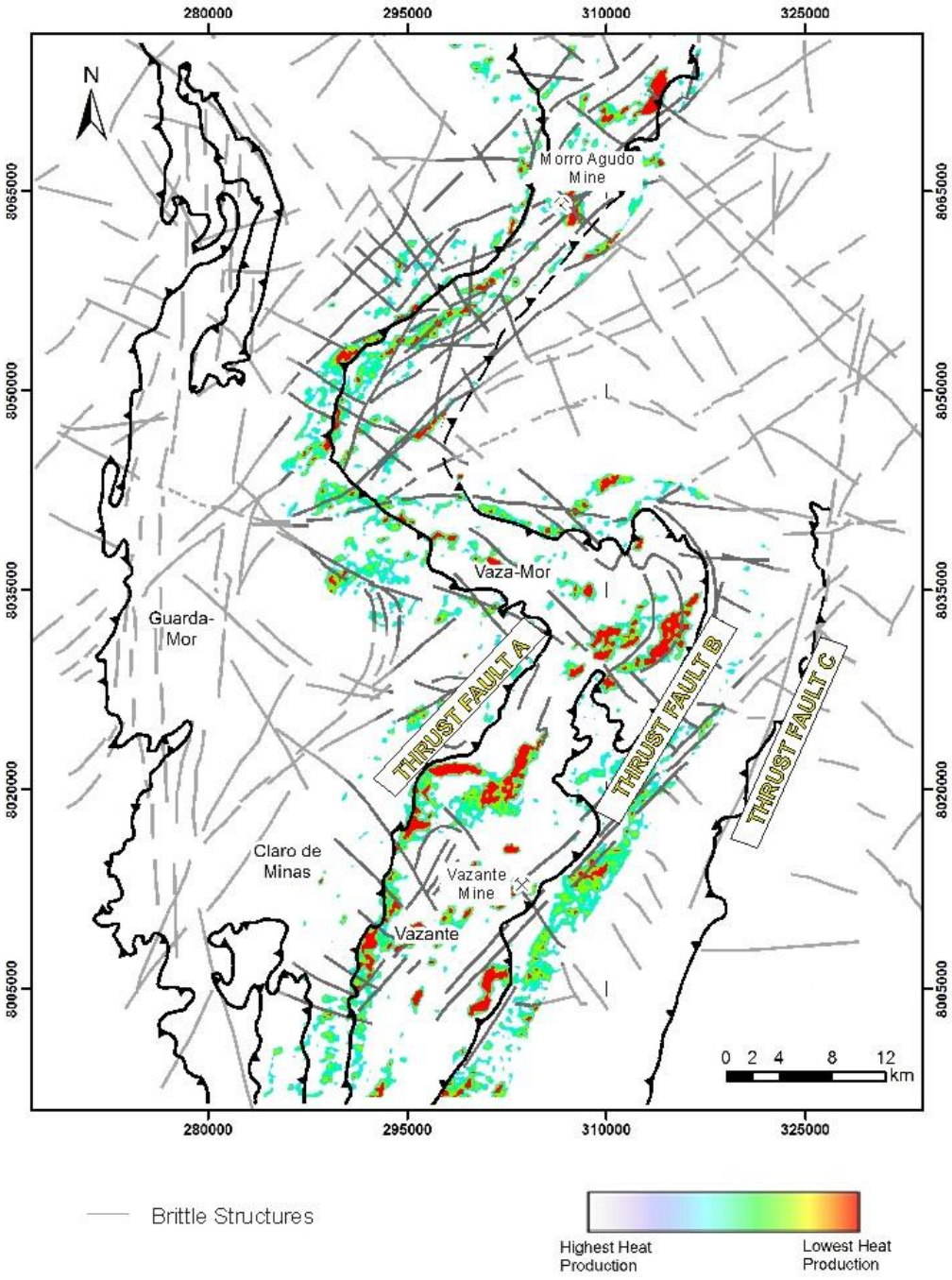

Figure 9 – Relationship between heat production and the main faults and brittle structures.

Fracture zones in the subsurface have been associated with high concentrations of U due to its mobility during the movement of hydrothermal fluids (McKay et al., 2014). Thus, it is thought that in fracture zones, there is increased heat flow, which contributes to the generation of mineralizations and also becomes a key factor for individualizing hydrothermal areas feeding the system (Brow et al., 1980; Gazzaz & Hashad, 1991).

In areas with high heat flow, i.e., greater than 60 mW/m^2 and reaching 150 mW/m², there is an associated increase in heat production related to the generation of metal mineralizations (Brown et al., 1980, Wikinsion, 2014), which makes the heat generation rates of these regions

extremely anomalous compared to the regional averages. Although the basins of the Canastra and Vazante Groups do not reach these high heat flow values, the heat production of their rocks have values above the regional average, which can also be explained by their mineralizations.

In the study area, the heat production near the regions of the Vazante and Morro Agudo mines is higher than the mean for the rocks of the Vazante Group, ranging from 2.6 μW/m³ for the Morro Agudo Mine and 2.4 μW/m³ for the Vazante Mine, which is in accordance with the literature on this type of environment.

Thus, as shown in Figure 6, the method has good applicability because it allowed effective observation of the fact that the low heat flow anomalies may be related in the area of study to the black shales and carbonates. Thus, this is an additional prospective guide for the region given that these are the lithologies that host the mineralizations in the region.

In addition, the results contribute to a prospective heat flow signature by distinguishing the host rocks of the mineralization considering the great similarity of the heat production map with the lithologic map.

6.6.Conclusions

1- A great similarity was found between the heat flow results obtained in this study using high-resolution aerogeophysics and those obtained by conventional methods; thus, greater use of this technique in Precambrian regions is recommended.

2- There is a wide variation in results between the basins of the Canastra and Vazante Groups, which may be related to the fact that they are from different ages and environments and were joined only at the end of the Neoproterozoic period, which is a time when the two were already well consolidated.

3- Because, according to Husson & Moretti (2002), under regular conditions in external zones of orogenic belts, where portions of the thrust faults are not as thick, the thermal field is not generally affected, the low heat productions corresponding to thrust faults B and C are related to the first fault system according to the Coelho et al. (2008) model without the contribution of the basement; i.e., they are restricted to the first few kilometers of the crust only.

4- The volumetric heat production of the Vazante Mine is greater than that of Morro Agudo, which indicates that the silicate (willemite) ore from the Vazante mine has a greater response to radioactive elements than the ore from Morro Agudo, which is sulfidic.

5- The method had good applicability in the region and can serve as a prospective guide because it was able to locate the main ore host rocks of the region and can provide information regarding their associated structures.

6.7.Acknowledgements

The authors would like to thank CNPq process 550259-2011-2 that financially supported this research.

6.8.References

Adams, J.A.S. & Gasparini P. 1970. Gamma-Ray Spectrometry of Rocks. Methods in Geochemistry and Geophysics Series. Elsevier Publishing Company.

Al-Alfy, I. M., Nabih, M. A. 2013. 3D slicing of radiogenic heat production in Bahariya Formation, Tut oil field, North-Western Desert, Egypt. Applied Radiation and Isotopes v. 73, p. 68–73.

Almeida, F. F. M.; HASUI, Y; BRITO NEVES, B. B.; FUCK, R.A. 1981. Brazilian Structural Provinces: an introduction. Earth Sciences Rev.,v. 17, p. 1-29

Almeida, R E M. 1967. Origem e Evolução da Plataforma Brasileira. Rio de Janeiro, DNPM/DGM.96 p. (Boletim 241).

Almeida. F. F. M. 1977. O Cráton do São Francisco. Rev. Bras. Geoc., 7(4): 349-364.

Araújo Filho, J. O. 2000. The Pirineus Syntaxis: an example of the intersection of two Brasiliano fold-thrust belts in central brasil and its implications for the tectonic evolution of western Gondwana. Revista Brasileira de Geociências, v. 30, n. 1, p. 144-148.

Argollo, R. B., Marinho, M. M., Costa, A. B., Sampaio Filho, H. A., Santos, E. J., Coutinho, L. F. C. 2012. Modelo crustal e fluxo de calor nos domínios Estância, Canudos-Vaza-Barris e Macururé adjacentes às bordas emersas da Bacia Sergipe-Alagoas. B. Geoci. Petrobras, Rio de Janeiro, v. 20, n. 1/2, p. 283-304.

Ashwal, L. D.; Morgan, P.; Kelley, S. A.; Perciva, J. A. 1987. Heat production in an Archean crustal profile and implications for heat flow and mobilization of heatproducting elements. Earth and Planetary Sciences Letters, Amsterdam, v. 85, n. 4, p. 439-450.

Azmy, K., Kendall, B., Creaser, R.A., Heaman, L., de Oliveira, T.F., 2008. Global Correlation of the Vazante Group, São Francisco Basin, Brazil: Re-Os and U–Pb radiometric age constraints. Precambrian Research, 164: 160–172.

Baptista, G. M. M. Filtragens. *In:* Meneses, P. R., Almeida, T. 2012. Introdução ao Processamento de Imagens de Sensoriamento Remoto, Universidade de Brasília. p. 168-190.

Beach, R.D.W., Jones, F.W. and Majorowicz, J.A. 1987. Heat flow and heat generation estimates for the Churchill basement of the Western Canadian basin in Alberta, Canada, Geothermics, 16 No. 1. , p. 1-16.

Bertoni, M. E., Rooney, A. D., Selby, D., Alkmim, F. F., Le Heron, D. P. 2014. Neoproterozoic Re–Os systematics of organic-rich rocks in the São Francisco Basin, Brazil and implications for hydrocarbon exploration. Precambrian Research, v. 255, Part 1, p. 355-366.

Bez, L. 1980. Evolução Mineralógica e geoquímica do depósito de zinco e chumbo de Morro Agudo, Paracatu, MG, In: Congresso Brasileiro de Geologia, 31. Balneário Camboriú, 1980. Anais. Balneário Camburiú, SBG, v.3, p. 1402-1416.

Bodorkos, S.; Sandiford, M; Minty, B.R.S; Blewett, R.S. 2004. A high-resolution, calibrated airbone radiometric dataset applied to the estimation of crustal heat production in the Archean northern Pilbara Craton, Weastern Australia. Elsevier Science Publishers – Precambrian Research 128, p. 57-82.

Brito, D. C. 2014. Mapa Geológico da folha Serra da Tiririca. Ministério de Minas e Energia. Secretaria de Geologia, Mineração e Transformação Mineral. Belo Horizonte. Escala 1:100.000.

Bücker, C.; Rybach, L. 1996. A simple method to determine heat production from gamma-ray logs. Elsevier Science Publishers, v 13, n.4, p.373-375.

Clark, R. N.; Gallagher, A. J.; Swayze, G. A. 1990. Material absorption band depth mapping of imaging spectrometer data using a complete band shape least-squares fit with library reference spectra. In: Airborne Visible/Infrared Imaging Spectrometer (Aviris) Workshop, 2., Pasadena. Proceedings... Pasadena: Jet Propulsion Laboratory, 1990. p. 176-186. (Publication, 9054).

CPRM/CODEMIG. 2001. Relatório final do levantamento e processamento dos dados magnetométricos e gamaespectrométricos, área 1, Unaí-Paracatu-Vazante-Coromandel [Belo Horizonte], CPRM/CODEMIG.

Cunha, I. de A. 1999. Estudos de inclusões fluidas e de isótopos de enxofre dos corpos de minério de Morro Agudo, Minas Gerais. Salvador, 105 p. Dissertação de mestrado, Universidade federal da Bahia.

Dardenne M. A., Freitas-Silva F. H., Nogueira G. M. S., Souza J. F. C. 1997. Depósitos de fosfato de Rocinha e Lagamar, Minas Gerais. In: Schobbenhaus C., Queiroz E. T., Coelho, C. E. S., Principais depósitos minerais do Brasil, DNPM/CPRM, v.IV C, p.113-122.

Dardenne, M. A. & Freitas-Silva, F. H. 1998. Modelos Genéticos dos depósitos de Pb-Zn nos Grupos Bambuí e Vazante. Workshop Depósitos Minerais Brasileiros de Metais Base, Salvados, CPGG-UFBA/ADIMB, p.86-93.

Dardenne, M. A. 2000. The Brasilia Fold Belt. *In:* Cordani, E. G., Milani, E. J. Thomaz Filho, A., Campos, D. A. Tectonic evolution of South America. Rio de Janeiro: 31° International Geology Congress. p. 231-263.

Dardenne, M.A. - 1978 - Zonação tectôncia da borda ocidental do craton do São Francisco. In: CONGR. BRAS. GEOL., 30, Recife, 1978, Anais... Recife, SBG. V. 1, p. 299-308.

Dardenne, M.A. - 1979 - Les mineralisations de plomb, zinc, fluor du Protérozoique Superieur dans le Brésil Central.Thése de Doutorat d'Etat, Université de Paris VI, 251p, (inédito).

Dias P.H.A. 2011. Estratigrafia e Tectônica da Faixa Brasília na Região de Ibiá, Minas Gerais: Estudo de Proveniência Sedimentar dos grupos Canastra e Ibiá, com base em estudos isotópicos U-Pb e Sm-Nd. Instituto de Geociências, Universidade Federal de Minas Gerais, Dissertação de Mestrado.

Fountain, D. M.; Salisbury, M. H. 1981. Exposed crosssections through the continental crust: implications for the crustal structure, petrology and evolution. Earth and Planetary Sciences Letters, Amsterdam, v. 56, p. 263-277.

Freitas-Silva F.H. 1991. Enquadramento lito-estratigráfico e estrutural do depósito de ouro de Morro do Ouro, Paracatu/MG. Dissertação de Mestrado, UnB-IG, 151p.

Freitas-Silva, F. H.; Dardenne, M. A. 1994. Proposta de subdivisão estratigráfica formal para o grupo Canastra no oeste de Minas Gerais e leste de Goiás. In: Simpósio de Geologia do Centro-Oeste, 4., 1994. Brasília. Atas... Brasília: SBG. p. 164-165.

Fuck, R. A. 1994. A Faixa Brasília e a Compartimentação Tectônica na Província Tocantins. In: SIMPÓSIO DE GEOLOGIA DO CENTRO-OESTE, 4., Brasília. Atas... Brasília: SBG, 1994. p. 184-187.

Gazzaz, M. A., Hashad, A. H. 1991. Radiogenic heat production and heat flow in the northern Arabian Shield. Journal of African Earth Sciences (and the Middle East). V. 13, Issues 3–4, pp. 323–332.

Hasui, Y. & Almeida, F.F.M. - 1970 - Geocronologia do Centro Oeste Brasileiro. Bol. Soc. Bras. Geol., v. 19, n. 1, p. 7-26.

Hawkesworth, C. J. 1974. Vertical distribution of heat production in the basement of the Eastern Alps. Nature, v. 249, n. 5456, p. 435-436.

Hilchie, D.W., 1979, Old electrical log interpretation: Golden, Colorado. 161 pp.

Husson, L., Moretti, I. 2002. Thermal Regime of Fold and Thrust belts – na application to the Bolivian sub Andean Zone. Tectonophysics, 345 p. 253–280.

Jessop A. M. And Majorowicz J. A. 1994. Heat transfer in sedimentary basins. In: Geofluids: Origin, Migration and Evolution of Fluids in Sedimentary Basins (ed. J. Parnell). Geol. Soc. Spec. Publ., 78: 43–54. The Geological Society. London.

Madalosso, A. & Valle, C. R. O. 1978. Considerações sobre a estratigrafía e sedimentología do Grupo ambuí na Região de Paracatu – Morro Agudo (MG). In: Congresso Brasileiro de Geologia, 30. Anais. SBG, v.2, p. 622-631.

Madalosso, A. 1980. Aspectos da diagênese dos carbonatos do Grupo Bambuí na Região de Paracatu (MG). In: Congresso Brasileiro de Geologia, 31. Camboriú, 1980. Anais, Camburiú, SBG, v.4, p.2069-2081.

Misi, A., Azmy, K., Kaufman, A. J., Oliveira, T. F., Sanches, A. L., Oliveira, G. D. 2014. Review of the geological and geochronological framework of the Vazante sequence, Minas Gerais, Brazil: Implications to metallogenic and phosphogenic models. Ore Geology Reviews v. 63, p. 76–90.

Misi, A.; Iyer, S. S S; Coelho, C. E. S; Tassinari, C. C. G; Franca-Rocha, W. J. S.; C., I. A.; Gomes, A. S. R.; Oliveira, T. F.; T., J. B. G, 2005. Sediment-Hosted Lead-Zinc Deposits of the Neoproterozoic Bambuí Group and Correlative Sequences, São Francisco Craton, Brazil: A Review and a Possible Metallogenic Evolution Model. Ore Geology Reviews, Amsterdam, v. 26, n. 3, p. 263-304.

Monteiro L.V.S. 2002. Modelamento metalogenético dos depósitos de zinco de Vazante, Fagundes e Ambrósia, associados ao Grupo Vazante, Minas Gerais. 317 pp. Tese de Doutorado. Universidade de São Paulo.

Monteiro, L.V.S., Bittencourt, J.S., Juliani, C., de Oliveira T.F. 2006. Geology, Pethrography and mineral chemistry of the Vazante, Ambrosia and Fagundes Neoproterozoic carbonate-hosted Zn-Pb deposits, Minas Gerais, Brazil. Ore Geology Reviews v. 28, p. 201-234.

Morgan, P., Heat flow in rifts, in K. H. Olsen (ed.), Continental Rifts: Evolution, Structure, Tectonics, Elsevier, Amsterdam, 99-101, 1995.

Nicolaysen, L. O.; Hart, R. J.; Gale, N. H. 1981. The Vredefort element profile extended to supracrustal strata et Carletonville, with implications for continental heat flow. Journal of Geophysical Research, Malden MA, v. 86, n. B11, p. 10653-12218.

Oliveira, G. D. 2013. Reconstrução Paleoambiental e Quimioestratigrafia dos Carbonatos Hospedeiros do depósito de Zinco Silicatado de Vazante, MG. 79 pp. Dissertação (Mestrado) – Universidade de Brasília.

Oliveira, T. F. de. 1998. As Minas de Vazante e de Morro Agudo. In: Workshop Depósitos Minerais Brasileiros de Metais Base, Salvados, CPGG-UFBA/ADIMB, p.48-57.

Pereira L.F. 1992. Relações tectono-estratigráficas entre as unidades Canastra e Ibiá na região de Coromandel, MG. Dissertação de Mestrado, UnB-IG, 73p.

Pereira, L.; Dardenne, M. A.; Rosière, C. A.; Pedrosa-Soares, A. C. 1994. Evolução Geológica dos Grupos Canastra e Ibiá na região entre Coromandel e Guarda-Mor, MG. Geonomos, v. 2, p. 22-32.

Pimentel, M. M. 2000. The Neoproterozoic Goiás Magmatic Arc, Central Brazil: a Review and New Sm-Nd Isotopic Data. Revista Brasileira de Geociências, 30(1):035-039.

Pimentel, M. M. 2004. O embasamento da Faixa Brasília e o Arco Magmático de Goiás. In Capítulo XXI- Geologia do Continente Sul-Amercano : Evolução da Obra de Fernando Flávio Marques de Almeida. p. 325-369.

Pinet, C., Jaupart, C., Mareschal, J., Gariepy, C., Bienfait, G. and Lapointe, R. 1991. Heat flow and structure of the lithosphere in the eastern Canadian shield. Journal of Geophysical Research, v. 96, Issue B12, pp. 19941–19963.

Pinho, J. M. M. 1990. Evolução Tectônica da mineralização de zinco de Vazante, Brasília, 115p. Dissertação de Mestrado, Universidade de Brasília.

Reyes, L. M. G. 2008. Distribuição vertical da taxa volumétrica de produção de calor radiogênico no Cráton do São Francisco. 156 pp. Tese (Doutorado) – Universidade Federal da Bahia, Bahia.

Ribeiro, J. H., Féboli, W. L. 2013. Mapa Geológico da folha Coromandel. Ministério de Minas e Energia. Secretaria de Geologia, Mineração e Transformação Mineral. Belo Horizonte, 2013. Escala 1:100.000.

Rigobello A. E. Branquinho J. A. Dantas M. G. S. Oliveira T. F., Neves Filho W. 1988. Mina de zinco de Vazante. In: C. Schobbenhause C. E. S. Coelho (eds): Principais Depósitos Minerais do Brasil. DNPM, Brasília, v. 3, p. 101-110.

Rodrigues, J. B. 2008. Proveniência de sedimentos dos grupos Canastra, Ibiá, Vazante e Bambuí – Um estudo de zircões detríticos e Idades Modelo Sm-Nd. 128 pp. Tese (Doutorado) – Universidade de Brasília.

Rolandone, F., Lucazeau, F., Leroy, S., Mareschal., J. C., Jorand, R., Goutorbe, B., Bouquerel, H. 2013. New heat flow measurements in Oman and the thermal state of the Arabian Shield and Platform. Tectonophysics. v. 589, pp. 77–89.

Rybach, L. 1986. Amount and significance of radioactive heat sources in sediments. In: BURRUS, J. (Ed.) Thermal Modeling in Sedimentary Basins. Paris: Technip, p. 311-322.

Rybach, L., Buntebarth, G. 1984. The variation of heat generation, density and seismic velocity with rock type in the continental lithosphere. Tectonophysics, Volume 103, Issues 1–4, Pages 335-344.

Sapucaia, N.S.; Argollo, R.M.; Barbosa, J.S.F. 2005. Teores de potássio, urânio, tório e taxa de produção de calor radiogênico no embasamento adjacente às bacias sedimentares de Camamu e Almada, Bahia, Brasil. Revista Brasileira de Geofísica, v. 23, p. 453-475.

Schneider, R. V.; Roy, R. F.; Smith, A. R. 1975. Investigations and interpretations of the vertical distribution of U, Th and K: South Africa and Canada. Geophysical Research Letters, v. 14, n. 3, p. 264-267.

Signorelli, N, Pinho, J. M. M., Tuller, M. P.; Baptista, M. C.; Brito, D. C. 2013 b. Mapa Geológico da folha Lagamar. Ministério de Minas e Energia. Secretaria de Geologia, Mineração e Transformação Mineral. Belo Horizonte. Escala 1:100.000.

Signorelli, N; Tuller, M. P.; Pinho, J. M. M.; Baptista, M. C.; Brito, D. C. 2013 a. Mapa Geológico da folha Arrenegado. Ministério de Minas e Energia. Secretaria de Geologia, Mineração e Transformação Mineral. Belo Horizonte. Escala 1:100.000.

Silveira, R. T. G., Albuquerque, D. F., Pavão, C. G., França, G. S., Santos, I. G. 2012. Comparação Entre a Função do Receptor no Domínio do Tempo e da Frequência para o Cálculo de Espessura Crustal. *In:* Lopes, F. C., Andrade, A. I., Henriques, M. H., Quinta-Ferreira, M., Barata, M. T. & Pena dos Reis, R. Para Conhecer a Terra Memórias e Notícias de Geociências no Espaço Lusófono. Universidade de Coimbra. p. 79-86.

Tuller, M. P. 2014. Mapa Geológico da folha Paracatu. Ministério de Minas e Energia. Secretaria de Geologia, Mineração e Transformação Mineral. Belo Horizonte. Escala 1:100.000.

Tuller, M. P.; Signorelli, N, Baptista, M. C., Brito, D. C. 2013. Mapa Geológico da folha Guarda-Mor. Ministério de Minas e Energia. Secretaria de Geologia, Mineração e Transformação Mineral. Belo Horizonte, 2013. Escala 1:100.000.

Turcotte, D. T., Schubert, G. 1982. Geodynamics: Applications of continuum physics to geological problems, 450 pp. John Wiley, New York.

Uhlein, A., Fonseca, M. A., Seer, H. J., Dardenne, M. A., 2012. Tectônica da Faixa de Dobramentos Brasília – Setores Setentrional e Meridional. Geonomos, 20(2), 1-14.

Valeriano, C. M. A Faixa Brasília meridional com ênfase no segmento da Represa de Furnas: Estado atual do conhecimento e modelos de evolução tectônica. 1999. Tese (Livre Docência) – Universidade Estadual do Rio de Janeiro, Rio de Janeiro.

Valeriano, C.M., Pimentel, M.M., Heilbron, M., Almeida, J.C.H. & Trouw, R.A.J. 2008. Tectonic evolution of the Brasília Belt, Central Brazil, and early assembly of Gondwana. In: Pankhurst, R.J., Trouw, R.A.J., Brito Neves, B.B. & de Wit, M.J. (eds) West

Gondwana: Pre-Cenozoic Correlations Across the South Atlantic Region. Geological Society, London. Special Publications, 294, 197-210.

Ventura, D. B. R., Soares, J. E. P., Fuck, R. A., Caridade, L. C. C. 2011. Caracterização sísmica e gravimétrica da litosfera sob a linha de refração sísmica profunda de Porangatu, Província Tocantins, Brasil Central. Revista Brasileira de Geociências. 41(1): 130-140.

Vilà, M., Fernández, M., Jiménez-Munt, I. 2010. Radiogenic heat production variability of some common lithological groups and its significance to lithospheric thermal modeling. Tectonophysics v. 490, pp. 152–164.

Waples, D.W., 2002. A new model of heat flow in extensional basins: estimating radiogenic heat production. Nat. Res. Res., 11, 125–133.

7. Structural Geology of a Neoproterozoic Thin Skin Thrust Foreland System in Central Brazil: Depth of Sources Based on Airborne Survey and Field Relationships

Abstract

We studied the tectonic framework of the central portion of the Paracatu-Vazante sequence located at the External Zone of the Brasília Belt, Neoproterozoic orogeny, thin skin tectonics dominantly, in order to understand the relationship between the Canastra, Vazante and Bambuí groups, the tectonic environments and exploit the matched filter and Euler deconvolution methods. It was possible to recognize four deformational phases distinct and progressive in region, as well as individualization, by magnetometry and structural field data. Also it was possible to delimit five structural-geophysical domains related to differences in structural behavior of different mapped lithological units and magnitude, recognize dip of the S2 main foliation and differences in the magnetic relief, and the limits of the areas represented by thrust faults of N-S direction- Coromandel, NE-SW direction - Serra das Araras, Serra das Antas, Extremo Nort and Lagamar, transcurrent shear zones of NE -SW direction - Paracatu, Vazante, Morro Agudo and Arrenegado, E-W direction - Januário, and structural highs that serve as contact between the Canastra, Bambuí and Vazante groups. From the application of Euler deconvolution and matched filter in magnetic data the depths of the great structures that control the region could be estimated, namely: Coromandel Thrust Fault with approximately 1.2 - 9 km, Serra Araras Thrust Fault approximately 9 km, Serra das Antas Thrust Fault with 9 km, Arrenegado Shear Zone with 1.2 km, Morro Agudo Shear Zone 1.2 km, Januário Shear Zone with 9 km, Vazante Shear Zone with 1.2 to 9 km, Paracatu Shear Zone with 1 km, Extremo Norte Thrust Fault to 1.2 km and Lagamar Thrust Fault with 1 km. Thus, it is clear that the contact between the Canastra and Vazante groups is about 9 times deeper than the contact between the Vazante and Bambuí groups and the structures of the region can be divided into two distinct groups, the first formed by the structures over the western area of greater depth involving the basement and the second formed by the structures further east area, shallower, and only affecting coverage. Therefore, it is proposed that there is a thinning of the sedimentary thickness from west to east of the study area, which is in accordance with interpretations of seismic lines in the region.

7.1.Introduction

"Foreland thrust-fold belts," or simply "thrust belts," are thrust and fold systems between orogenic belts and sedimentary basins that are formed by large thrust faults with convergence to the foreland and usually mark the outer edges of converging orogens. The term was first used by Price and Mountjoy (1971), and these systems are considered to be natural laboratories for the study of rock architectures, deformation and tectonic evolution (Macedo & Marshak, 1999; Kwon et al., 2009). In a convergent tectonic context, the lithosphere is subjected to horizontal foreshortening, and the progression of deformation produces a series of structural styles that involve folds and thrust faults in many levels in the lithosphere (Pfiffiner, 2006). The shortening of these areas is marked by a state of compressional stress, which occurs in different geodynamic contexts such as accretionary wedges, subduction and collisional thrust belts (Dahlen, 1990, Davis et al., 1983, Suppe, 1987).

The depth of influence of a thrust and fold belt depends on the presence of a horizontal detachment that allows the mechanical disengagement of the upper and lower units; thus, the terms "tectonic thin-skin" and "tectonic thick-skin" were created to describe the involvement of basement rocks and supracrustal coverage in the deformational processes at different levels of the earth's crust.

The term "tectonic thick-skin" is used to describe a structural style whereby individual thrust faults or folded structures affect a wide range of continental crust to uplift the basement on a large scale. Likewise, "tectonic thin-skin" is used to describe a thrust ramp architecture with 5-8 km thick friable rocks such as shales and evaporites that are located at or near the base of the sedimentary cover and the presence of rocks immediately below the level of detachment, including basement that remains undisturbed (Butler et al, 2006). The deformation of a thick skin type involves the deformation of the whole package ensemble, including the underlying basement (Espurt et al, 2012; Bellahsen et al, 2012.). Both definitions encompass a variety of structural styles that are related to the geometry of the layers involved and the type of internal strain.

In the last three decades, tectonic thin skins have been considered to be more suitable for developing foreland thrust-and-fold belts, but an increasing number of studies have discussed the fact that thin skin deflections in conjunction with thick skin structures, either well developed or hybrid, are also common in many fold-thrust complexes (Butler et al., 2004, Coward et al., 1999, McDowell, 1997, Giambiagi et al., 2008).

Foreland Basins or Foreland Basin systems (BF) are, by definition, sedimentary basins that form adjacent or parallel mountain chains and are formed by the regional isostatic compensation generated in the crustal thinning of the lithosphere, which is necessary for the formation of mountain chains. Thus, it is considered that during the filling of the basins, a large amount of the sediment burden comes from the erosion of adjacent mountain ranges (Dickinson, 1974).

BFs consist of four discrete depozones: wedge-top, foredeep, forebulge and back bulge (DeCelles and Giles, 1996). The type of sedimentation in these basins suggests that the decrease in the grain size of the deposited rocks is directly proportional to the distance from their source.

The reactivation of preexisting crustal structures has been considered one of the key components in the geological evolution of structures and the development of the continental lithosphere (Butler and Mazzoli, 2006, Crawford et al., 2010, Sykes, 1978). In general, the reactivation of basement faults results in the location of structures such as thrusts and folds in the developing thrust wedges on reverse extensional faults, can induce an out-of-sequence thrust, can create accommodation structures such as lateral ramps and often lead to the development of

basement uplift (Boyce and Morris, 2002, Giambiagi et al., 2008, Brown et al., 1999, Butler et al., 1997).

The joint implementation of structural studies and geophysical methods to research fold and thrust belts, foreland systems and deformations in general basins has been widely used in recent years in all parts of the world (Bader, 2009, Brown et al., 1999, Ndougsa-Mbarga et al., 2012); magnetometry, in particular, is considered to be one of the best geophysical techniques to delineate structures in the subsurface (Zhang et al., 2015, Thompson et al., 1982). It provides a link between rocks from outcropping and surface, provides a connection between detailed observations on outcrop scale and regional standards for aeromagnetic data and can be used to generate 3D lithospheric architectures at any desired scale (Stewart et al., 2009, McLean and Betts, 2003). In thin-skin systems, where there is no influence from the basement, the tectonic structures are generally shallow (less than 10 km deep), which enables their characterization using high-resolution aero-magnetometry data (Ross et al., 2006).

Estimating the depths of large structures, understanding tectonic frameworks in areas with basements and studying structural extensions in the subsurface are among the challenges that aero-magnetometry has been used for, based on the large differences in magnetic susceptibilities between the host rocks and structures (Hoover et al., 1992 Dufréchou et al., 2014), and it has become an important tool for tectonic analyses (Jessel et al., 1993, Betts et al., 2003, Direen et al., 2005).

For this results, the magnetometric signal must be filtered to different depths using techniques that include the fractal distributions of the magnetic sources, spectral analyses of aeromagnetic data (Nwankwo, 2015) and interpretations that combine magnetometry with competent geological data for generating models (Direen et al., 2005), in view of the relationship between the depth of the basement, and the magnetic susceptibilities in regions with shallower basements tend to be the average magnetic susceptibilities in a region.

The use of magnetic data as guides for mapping shear zones has been a customary application (Boyce and Morris, 2002, Crawford et al., 2010), as long as the magnetite has been increased or decreased by fluids that have passed through the structure (Grant, 1984/1985). However, to determine a shear zone's expression in the subsurface, additional calculations are required, including the Fourier transform, which is the main constituent of the most advanced methods for determining the depths of magnetic sources (Aboud, 2005).

Examples of magnetic data applications in foreland basins can be found in northern China in the Kuqa Foreland Basin, where a systematic study of the transverse faults in the region was made to understand the role and significance of the basin-mountain system (Cai & Lü, 2015). In the Younghae Foreland Basin in South Korea, various types of filters were applied to the

magnetic data to determine the depths of large magnetic anomalies that are present in the region, and the depths were estimated to be between 63 and 354 meters (Abdallatif & Lee, 2001). In the Trans-North China Orogen, which was formed by several foreland basins, a study of the tectonic framework was made using aeromagnetic data to refine the crustal profile of the region, with a possible integration of the shallow and deep structures in the region, and resulted in a tectonically consistent model (Zhang et al., 2015).

Thus, the objective of this work was to study the tectonic framework of the central portion of the Vazante-Paracatu Sequence, which is located in the Outer Range of the Brasilia Thrust and Fold Belt (an important Neoproterozoic Orogen); the studied area is defined as a foreland basin (Coelho et al., 2008; Uhlein et al., 2012), in which systems of thrust faults and shear zones tectonically superimpose the Canastra, Vazante and Bambuí Groups.

The Vazante-Paracatu sequence is a thrust and fold belt with extensive longitudinal thrust faults that reverse the sequence of Canastra and Vazante Groups (Campos Neto, 1979; Freitas-Silva, 1991; Pereira, 1992), and its central portion is marked by the inflection of that sequence. Many studies have been conducted in this region, especially in the host carbonates of Pb and Zn mineralization and in the ore itself (Dardenne & Freitas-Silva, 1998; Misi et al., 2005, Cunha et al., 2000 and 2001; Neves, 2011), but integrated studies of the structural geology and airborne geophysics are still a novelty.

Through a seismic line that crossed the study area, Coelho et al. (2008) suggested the existence of two sets of structures at different depths; the first domain is restricted to sedimentary covers, and the second one extends to the basement, comprising strips of thin and thick skins.

The existence of sedimentation models, sparse seismic reflection data and high resolution aero-magnetometry data for the Vazante-Paracatu sequence make this area a natural laboratory for regional tectonic framework and evolution studies. In this work, we introduced new models of the tectonic architecture of the Vazante-Paracatu system using different magnetometric patterns that represent areas with different deformation styles and tectonic stress that are limited by shear zones, faults and fractures, as well as the delineation of faults in the subsurface and their continuity on the surface. We then discuss the implications of those data in seismic models built by Coelho et al. (2008) and Alvarenga et al. (2012).

The geological units under study host the largest zinc mine in Brazil and, in addition, major gold, zinc and lead mines (Dardenne, 1979, 2000).

7.2.Regional Geology

The study area is located in the central portion of the Paracatu-Vazante sequence in the far west of the state of Minas Gerais, near the cities of Guarda-Mor, Paracatu and Vazante. It lies

in the eastern part of the Brasília Fold Belt, in its outer zone (Dardenne, 2000), or southern part (Araújo Filho, 2000), which is inserted in the Tocantins Province.

The External Zone of the Brasília Belt is comprised of metasedimentary units (the Paranoá, Canastra, Ibia, Vazante Groups and, locally, the Bambuí Group) and portions of its basement. It is dominated by sedimentary facies that correspond to the passive margin, and metamorphism is represented by greenschist facies (Figures 1 and 2).

The Vazante Group occupies an elongated N-S range, with an approximate length of 250 km between the cities of Unai and Coromandel-MG, and consists of a thick clay-dolomite sequence (Dardenne et al., 1997). Oliveira (2013) stated that the basin was the result of a series of four depositional and evolutionary stages: (i) the deposition of silts and marine platform shales, (ii) the development of a carbonate ramp with the evolution of a plain tide sabkha type, (iii) the emergence of a regional flood surface and (iv) the development of a carbonate platform barrier. According to Dardenne (2000), the basin can be divided from bottom to top into seven formations: Retiro, Rocinha, Lagamar, Serra do Garrote, Serra do Poço Verde, Morro do Calcário and Serra da Lapa. Using Re-Os dating, Misi et al. (2014) determined a Mesoproterozoic age of 1.1 Ga to 1.3 Ga for the upper portions and averages of that group, but found a Neoproterozoic age of 600 Ma to 800 Ma (Rodrigues, 2008) for the lower portions, the Rocinha and Santo Antonio do Bonito formations, which indicates a tectonic contact from the base to the Lagamar Formation.

The Canastra Group occurs in a continuous strip from the southwest of Minas Gerais to the center and west of Goiás. This group was studied by Freitas-Silva and Dardenne (1994) and more specifically in the region of Guarda-Mor and Coromandel, which is near the study area, by Pereira (1994). Its age is considered by many authors (Bertoni et al., 2014, Rodrigues, 2008, Azmy, 2008, Dias, 2011) to be approximately 1.0 Ga. The Canastra Group is comprised mainly of micaceous quartzite and possibly some black phyllites that contain pyrite. They are associated with carbonate rocks that contain carbonaceous materials and mica. They have all suffered metamorphism of the greenschist facies.

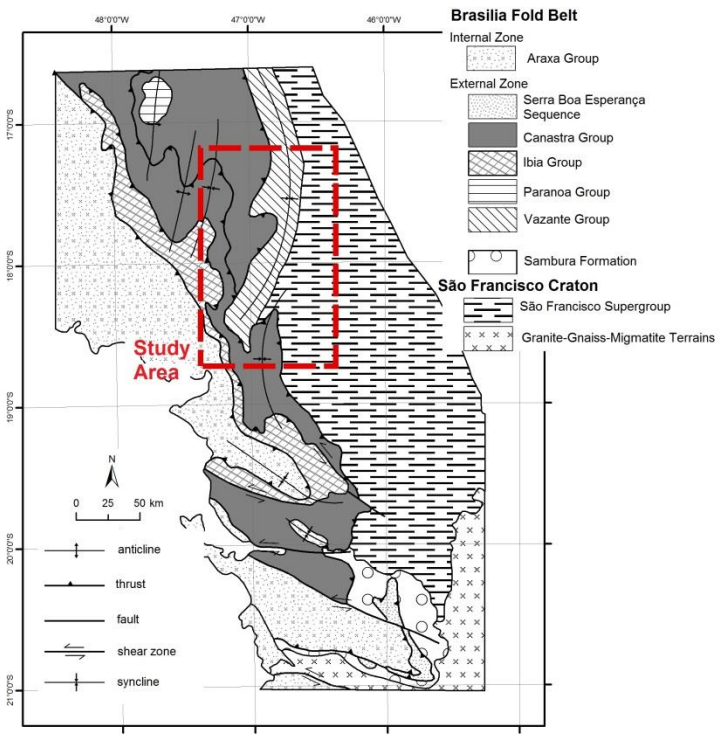

Figure 1 – Location of the study area (dotted red line) amid the Brasília Belt. (Based on Tuller et al, 2013; Signorelli et al, 2013a; Signorelli et al, 2013b; Ribeiro and Féboli, 2013; Tuller, 2014; Brito, 2014 and Valeriano, 1999).

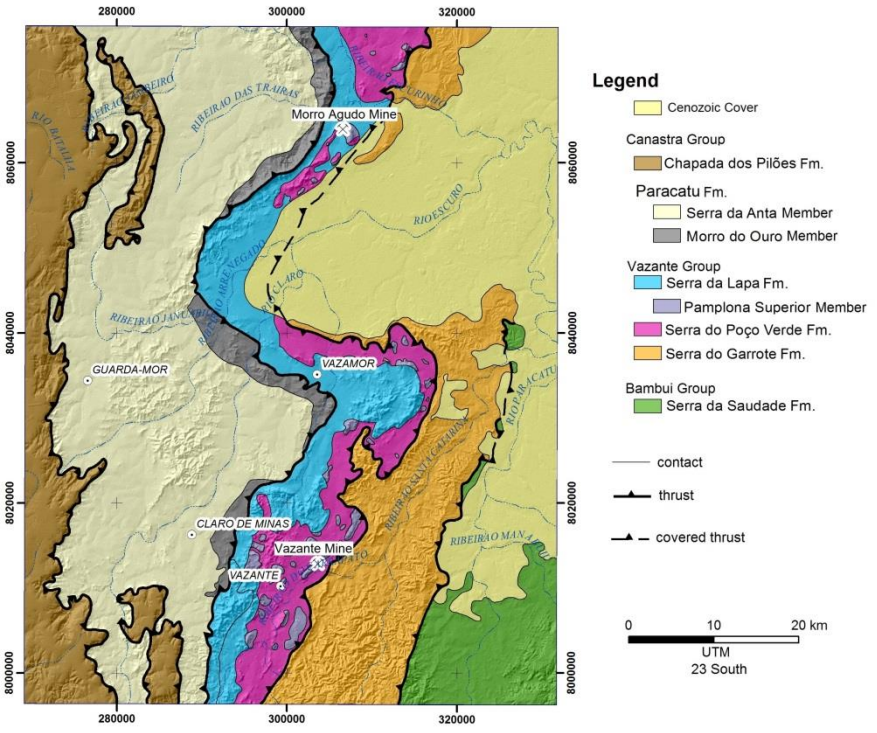

Figure 2 – Detail of the study area showing the geology and regional thrusts in the study area.

Dardenne (1978, 2000), Fuck (1994), and Pimentel (2000) considered the external zone of the Brasília Belt to be a typical fold and thrust belt foreland that was produced by the reversal of a Neoproterozoic passive margin on the western edge of the São Francisco craton.

According to Uhlein et al. (2012), the deformation style of the Brasília Belt varies with its crustal level, and the external domain of the Range is therefore dominated by a thin-skinned style (the Canastra, Bambuí and Vazante Groups), whereas the ductile deformation zones in the internal domain appear to be more intense and wide, with metamorphism in the higher facies (thick-skinned style - Araxá Group and Anapolis-Ituaçu Sequence).

Silva et al (2011) stated that the Brasilia dome tectonic structures recorded a polyphase deformation that was comprised of a ductile flow (D1/D2) and shortening (D3). Nevertheless, the D3 structures characterize shortening in the WNW and ESE (D3N) directions, which is typical of the northern segment of the Brasília Belt, and in the SW-NE direction (D3S), which is found exclusively in the southern segment.

Pereira and Dardenne (1994), who studied the Paracatu-Vazante sequence between Coromandel-MG and Guarda-Mor-MG, argued that the evolution of this portion was caused by two (2) different structural domains: one to the south, which had the greatest deformation, and another to the north, which suffered less deformation. In addition, the identified geometric elements were related to a single progressive deformation event (E1) with two distinct stages. The first deformation stage (D1) was a warp-intensive, ductile, simple shear component and is represented by the development of folds and shear zones structures in addition to the thrust fault that overlays the Canastra-Ibiá groups to the Vazante-Paracatu unity. Its late stage (D1-late) is represented by the development of a folding stage that was responsible for generating a large number of folds with a general east convergence.

The second stage (D2) is characterized by a pure shear component and a compressive component already in a ductile-brittle condition that produced kink bands and tension gashes, usually in conjunction with pairs of shear zones with pervasive crenulation cleavages with upright dips in the N-S direction and some symmetrical mesoscopic folds in chevron, which also have a vertical axial plane and a N-S axis.

Freitas-Silva (1991, 1996) stated that the Vazante Group was affected by progressive deformation during the Brasiliano cycle and displays a typical deformation style in the regions at the front of thrust, which are dominated by a pure shear component, with the following sequence: F1 as an intrastratal slip that was generated at the beginning of the reversal of the Brasília Belt, F2 as a flexural folding generation NNE-SSW, especially in pelites, axial cleavage and reverse faults, with a NNE-SSW orientation subparallel to the plan axis of the folds. In addition to the flexural folds and reverse faults, the accommodation of the deformation during

phase F2 was complemented by directional faulting with predominantly NE-SW NW-SE, and E-W directions, which could have been true shear or just lateral to the general mass transport ramps to the east. As the strain was facilitated, the F3 phase structures were generated, which are characterized by the formation of soft folds and conjugated kinks, and the interference of their folding generated a typical dome and basin pattern that accounts for the great dispersion and double trim of their axes. Phase F4 is characterized by normal faulting and fracturing of brittle widespread basis in response to the decompression Paracatu-Vazante sequence, and the Vazante Fault was one of the major faults in this phase.

Marcia (2014), who studied the region near Paracatu-MG, suggested the existence of two deformational phases: D1 and D2. D1 is characterized by the formation of a slate cleavage and the axial plane foliation of the isoclinal folds P1, in addition to generating a secondary mylonitic foliation associated with the F1 slip fault system. The second deformation phase, D2, is related to the formation of a crenulation cleavage, a penetrative cleavage and kilometric axial folds that were individualized in the satellite image.

Table 1 shows the tectonic evolution in regions close to the study area in the view of six authors: Freitas-Silva (1991), Pereira (1994), Marcia (2014), Silva et al. (2011), Campos-Neto, 1984 and Rostirolla et al. (2002).

Table 1 - Summary of structural stages in regions close to the area of study according to Freitas Silva (1991) - Morro do Ouro, Pereira (1994) - Guarda-Mor to Coromandel, Marcia (2014) region of Paracatu, Silva et al. (2011) in Brasilia Dome, Campos Neto (1984) in western Minas Gerais and Rostirolla et al (2002) in Vazante mine.

Events	Freitas Silva (1991)	Pereira (1994)	Marcia (2014)	Silva et al. (2011)	Campos Neto (1984)	Rostirolla (2012)
D1	S_0 transposed and the development of a recrystallization through a metamorphic differentiation	Domain 1 – isoclinal folds with axial-plan foliation. On late step asymmetrical soft folds tending to E	S1 formed by a slate cleavage, being S1 the axial plane of the folds P1	S1 // S0, varying in intensity and morphology	Folds with a southwesterly axis initially going to axes NW, NE and EW in progressive deformation	Progressive deformation with evolution of lower crustal levels to higher
	P1 – isoclinal folds belonging to Paracatu Fm. and Lapa Fm	Domain 2 – slaty cleavage and restrict mylonitic foliation. Mica lineation is parallel to the pebbles stretch	P1 represented by isoclinal folds on Canastra and Vazante Groups	Some examples of isoclinals folds P1		Discontinuous homoclinal Folds and tiltings
		Thrust Fault at the base of Canastra Group	Mylonitic foliation Sn, developing thrust faults systems – F1		thrusts parallels to structures	Slaty cleavage (s1), spaced cleavage (s2)
D2	S_2 representing axial-plan cleavage and mylonitic foliation	*Kink bands* and *tension gashes* combined with crenulation cleavage and symmetrical	S_2 representing crenulation cleavage and penetrative cleavage of axial plane	Cleavage crenulation S2 on Canastra Group	Transverse faults	Reticulated of SW and NW extensional faults controlling largely the hydrologic flow in karst aquifers

	folds. At one point late cleavage fracture in conjugate pairs		
P_2 representing centimetric horizontal isoclinal folds, presenting asymmetry		P_2 represented by large folds of kilometrical scale, interpreted on satellite image	P2 isoclinal asymmetric inclined folds

In addition, Muzzi Magalhães (1989) observed intense brittle slip faults with a predominant direction of N60W, which affect the basement in the Paracatu-Vazante Sequence.

Using regional seismic data, Coelho et al. (2008) proposed a compressive event linked to the Brazilian Cycle that was responsible for the formation of a foreland basin in the São Francisco Craton (Basin of Bambuí, Vazante and related) and two foreland belts. One of the foreland belts has folds and reverse faults that represent eastward convergence, involved the basement on the edge of the basin and has a thin-skinned area, and the second foreland belt to the east presents folds and thrust faults with generally east convergences.

Coelho et al. (2008) recognized two sets of faults at different depths from the seismic profile corresponding to Paracatu-Vazante Sequence. One set only affected the Bambuí sequence (Bambuí and Vazante Groups) at lower depths, but the other set deeply affected the basement.

However, there are no structural maps at an appropriate scale in the central portion of Paracatu-Vazante sequence, and one of the intentions of this study was therefore the characterization of the tectonic framework in this region, targeting the major faults and shear zones both at the surface and at depth to understand its characteristics as a tectonic thin-skin within the fold belt and faults of the Brasília belt and further define the Canastra and Vazante limits.

7.3.Magnetic Data

The magnetic data used in this study are from the Geophysical Survey Project of the State of Minas Gerais, area 1 (CPRM and CODEMIG, 2001). The data were acquired with a survey line spacing of 250 m toward N30W and a sampling interval of approximately 4 meters. The data were subtracted from IGRF and gridded with a cell size of 60 m using the minimum curvature algorithm in the software Oasis Montaj from Geosoft (GEOSOFT, 2008). The following images were obtained from that process: first order derivatives (x, y and z), Total Gradient (TG), Total Horizontal Gradient (THG) and Tilt Derivative (TDR) (Figure 3).

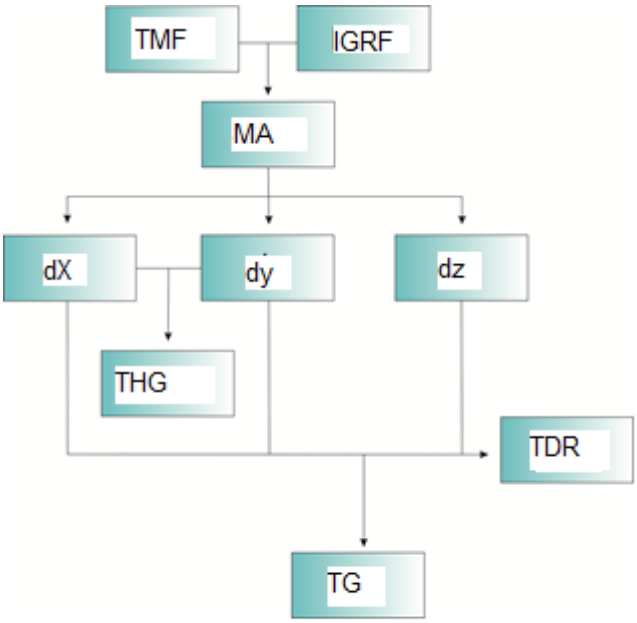

Figure 3 - Flow chart showing the dynamics of the geophysical processing and the main products that were generated.

The integration and interpretation of the magnetometric domains were conducted by analyzing magnetic anomalies, respecting the distinct wavelengths and amplitudes in addition to the representative features of each area related to the other products derived from the Magnetic Anomaly (MA), which were the Total Horizontal Gradient (THG) and Vertical Derivative (Dz).

The magnetic framework was derived from the anomalous magnetic field, mainly from Tilt Derivative (TDR), the first vertical derivative (Dz) and the TG.

The matched filter (Phillips 2001), was applied by means of the USGS algorithm (Phillips, 1997). This filter is chosen interactively through program graphics by adjusting the layer source equivalent to RSP power log. The spectral separation and any azimuthal filter are made and then computed the inverse Fourier transform and removed noise and the columnar extensions.

Euler deconvolution initially developed by Thompson (1982) and enhanced by Reid et al (1990) and Reid (2003) is a method for fast estimation of a region depth, for it utilizes the Euler homogeneity equation. For this, you need to know your study area, the size of the anomaly and its expected depth. For analysis of structural magnetic data, index ranges from 0 to 3, with 0 being related to planar structures, the linear structures 1, 2 and 3 the two-dimensional bodies and three-dimensional bodies.

7.3.1. Interpretation

The geophysical interpretation was performed on maps at a 1:100,000 scale. Using all of the generated products (Figure 4), TG was considered to be of major importance for the interpretation of the magnetic domains, and the Tilt was important for the interpretation of the magnetic lineaments.

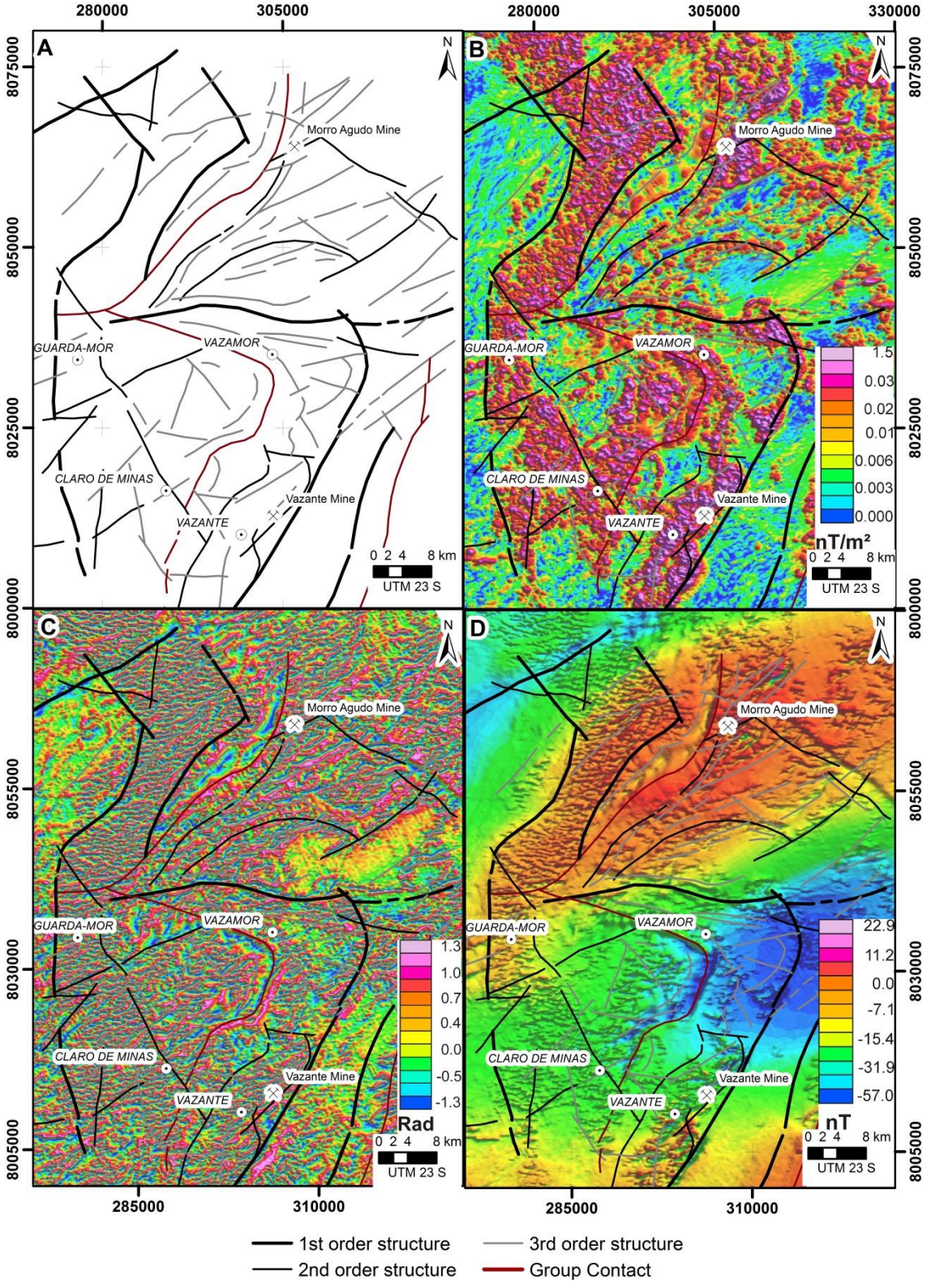

Figure 4 - Magnetic interpretation with the identification of the regional and other magnetic lineament structures: (A) interpretation; (B) interpretation superimposed on the Total Gradient image, highlighting the magnetic sources;

(C) interpretation superimposed on the Tilt gradient image, highlighting the magnetic lineaments; and (D) interpretation superimposed on the image of the magnetic anomaly, highlighting the large dipole generated in the region.

This interpretation permitted to identify magnetometric lineaments that represent the main structural controls in the region, namely the shear zones and regional thrust faults and the definition of geophysical-tectonic blocks.

Thus, major structures that trended NE-SW, E-W and NW-SE were identified. These structures are called first order magnetic domains and exist as separate distinct portions with different magnetic signatures with different wavelengths and extend over a wide range. The secondary structures are less frequent, do not properly define magnetic domains and can cut the first-order structures and the third-order structures are internal to the domains, related to its internal behavior (Figure 5). The individualization of structures following their order of importance is necessary, considering that the second-order structures are considered to be the main conduits of mineralization (Airo and Leväniemi, 2012).

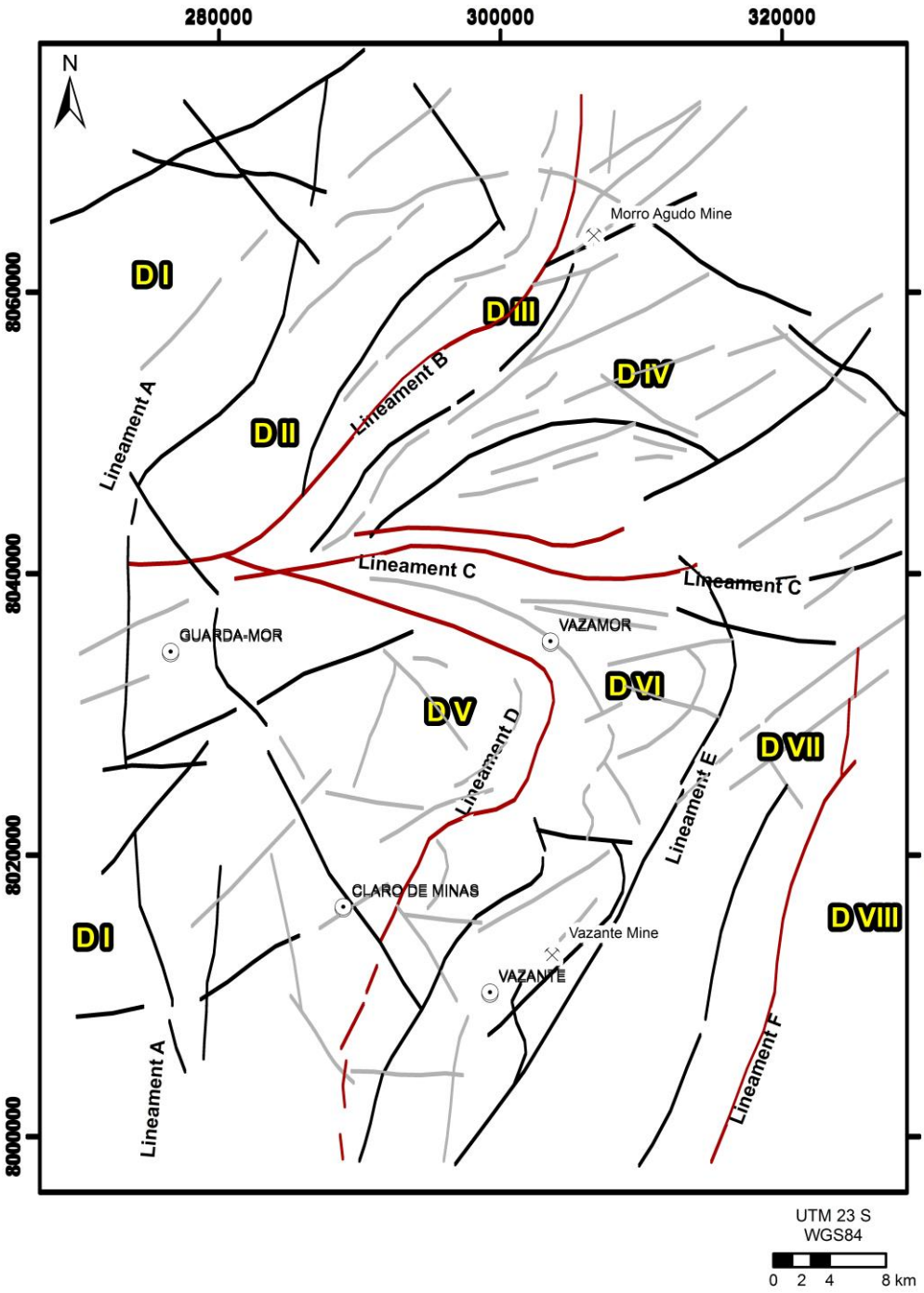

Figure 5 - Geophysical interpretation map showing the different areas and the first, second and third order structures. The first-order structures define the major lineaments. The rosette diagrams for all of the magnetic structures in the area are also presented and indicate a dominant NE-SW direction, followed by the E-W and NW-SE directions.

The area was divided into eight (8) different magnetic domains that are associated with lineaments and different magnetic reliefs (Figure 5). Domain I is characterized by a soft magnetic relief, a rare presence of magnetic high-frequency sources, predominating long wavelength anomalies that are more easily identified than in areas that are magnetically more disturbed, and the lack of the presence of lineaments that are predominantly NE-SW (Figure 5).

The boundary between domains I and II is given by lineament A. Lineament A is curved and often intercepted by the lineaments of the second order, and it separates areas of high and low magnetic relief (Figure 4b).

Domain II is characterized by a rugged magnetic relief (Figure 4b) and is intercepted by E-W, NE-SW and NW-SE second order lineaments (Figure 5). NE-SW lineament B forms the boundary between domains II and III, separates areas of greater and lesser magnetic relief and is defined by a low magnetic relief region.

Domain III is characterized by a soft magnetic relief, although it does contain some medium intensity magnetic sources (Figures 4b, c). The Morro Agudo mine is located in this domain. Its lineaments are predominantly NE-SW and often are truncated by lineaments with NW-SE directions. NE-SW lineament C forms the boundary between domains III and V and separates areas of very low and low magnetic relief.

Domain IV is characterized by a soft magnetic relief without the presence of high frequency magnetic sources (Figure 4b, c). The lineaments are only in the NE-SW direction. Lineament C forms the boundary of domains IV and V.

Domain V is characterized by a magnetic relief that ranges from rough to very rough and is defined mainly by NE-SW magnetic lineaments that are truncated by NW-SE lineaments (Figure 5). NE-SW lineament D forms the boundary of domains V and VI. It smoothly separates intermediate relief magnetic regions and has a length of approximately 20 km.

Domain VI is defined by a magnetic relief that is relatively disturbed by the presence of several magnetic sources of intermediate frequency and has a high density of primary lineaments in the NE-SW direction and secondary lineaments in the NW-SE direction (Figures 4b, c). E-W lineament E separates domains VI and VII (Figure 5) and separates magnetic low relief areas from intermediate and high relief areas.

Domain VII is comprised of a soft magnetic relief embossed with the rare presence of magnetic sources (Figure 4 b, c). It is cut by major NE-SW lineaments, which are often cut by NW-SE lineaments and E-W lineaments that correspond to the Serra do Garrote Formation of the Vazante Group. Lineament F divides domains VII and VIII (Figure 5) and is curved and separates areas of high and intermediary magnetic relief.

Domain VIII has a very rugged magnetic relief (Figure 4b, c), is curvilinear and contains NE-SW and NW-SE lineaments. The Vazante Mine is located in this domain.

According to the geological history of the zones associated with the various geophysical responses in each associated domain, the magnetometric data – magnetic anomaly map, were ordered and filtered to discover the depths of the different magnetic domains and their boundaries using the Euler and matched filter methods.

7.3.2. Matched Filter

The filter results indicated three magnetic source depths: 222 m (Figure 6), 1258 m (Figure 7) and 9268 m (Figure 8). Therefore, tilt maps were generated to those depths highlighting the main structures for each depth.

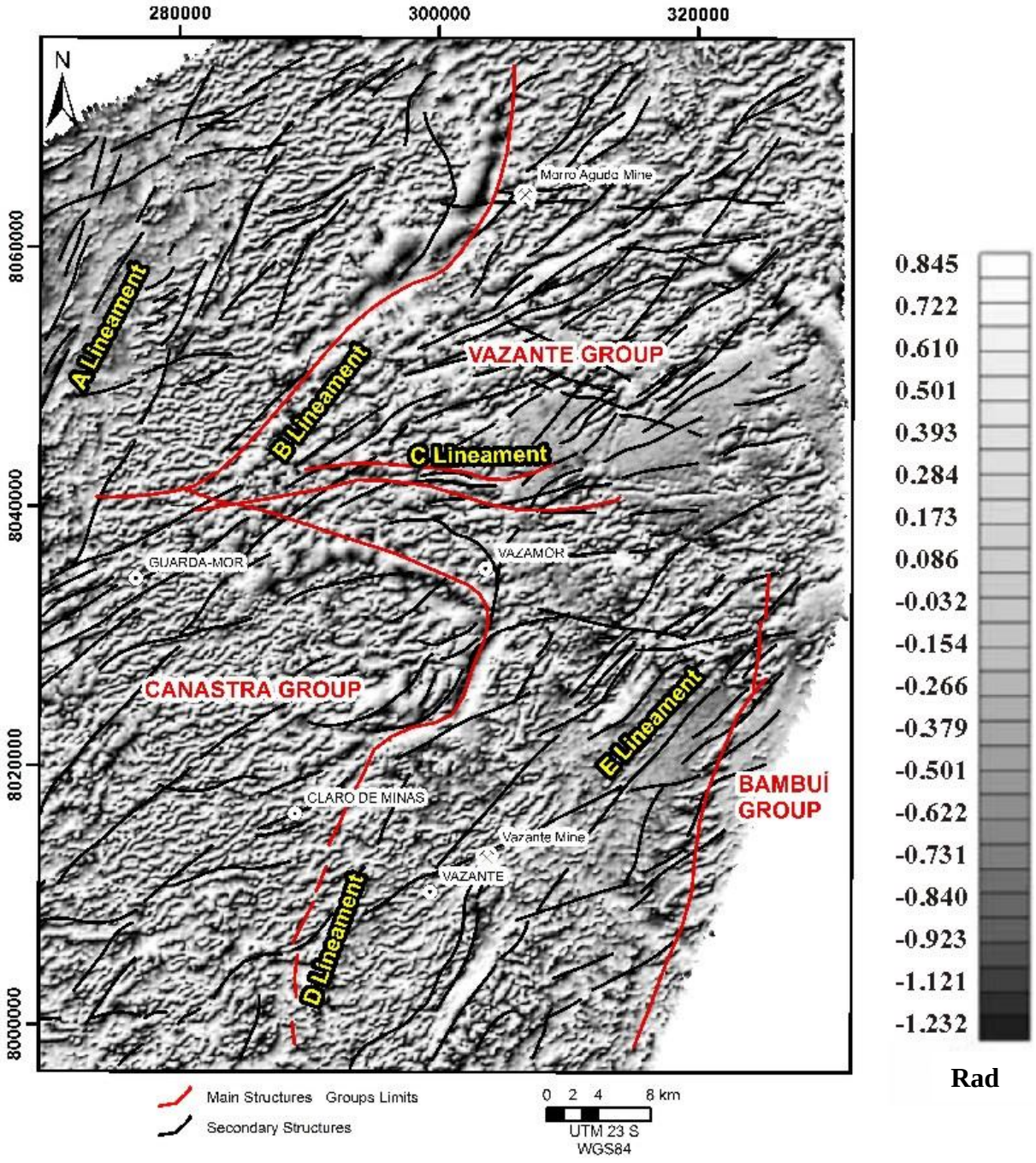

Figure 6 – Tilt derivative to a depth of 222 meters and the main structures that were obtained.

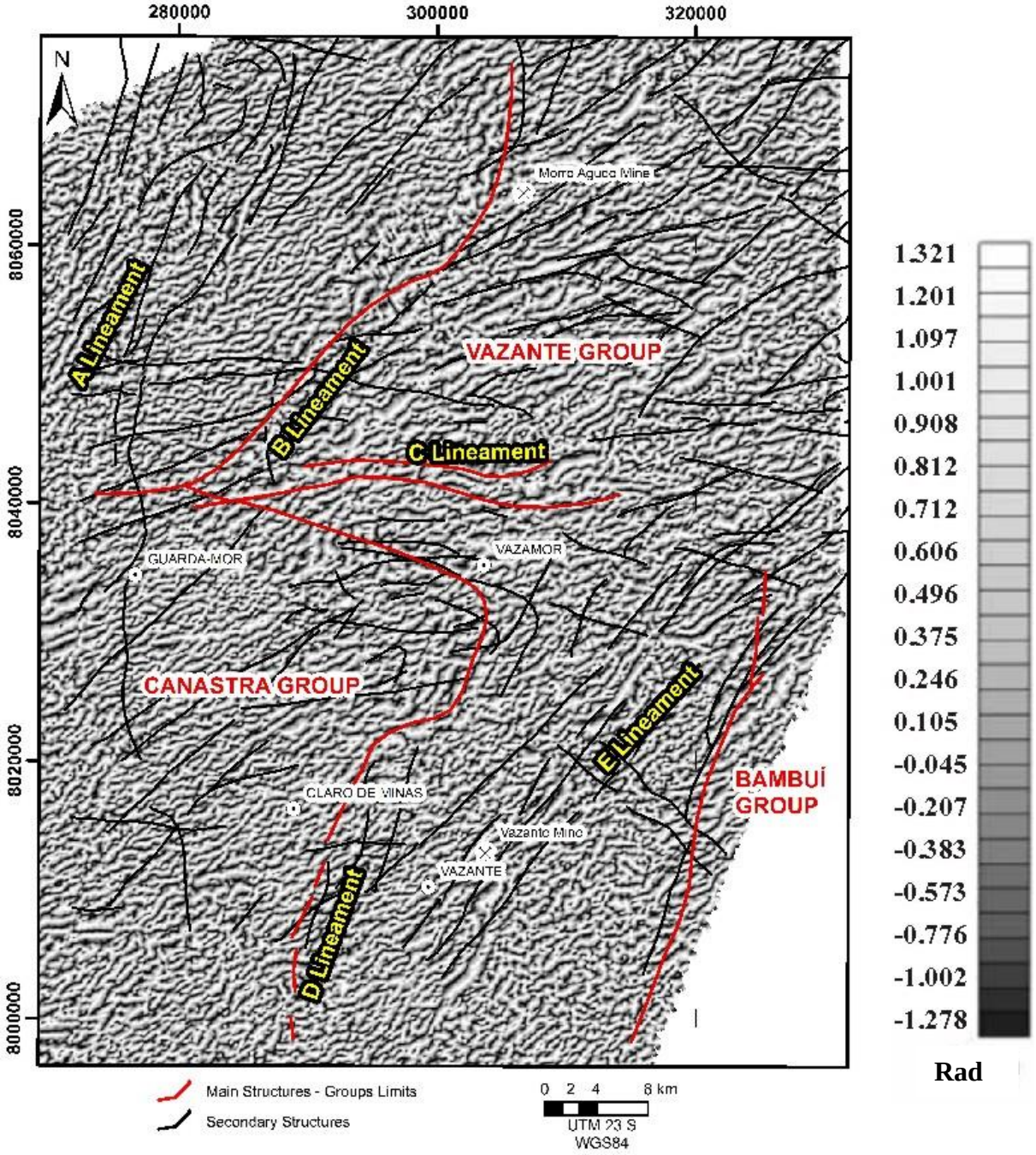

Figure 7 – Tilt derivative to a depth of 1258 meters and the main structures that were obtained.

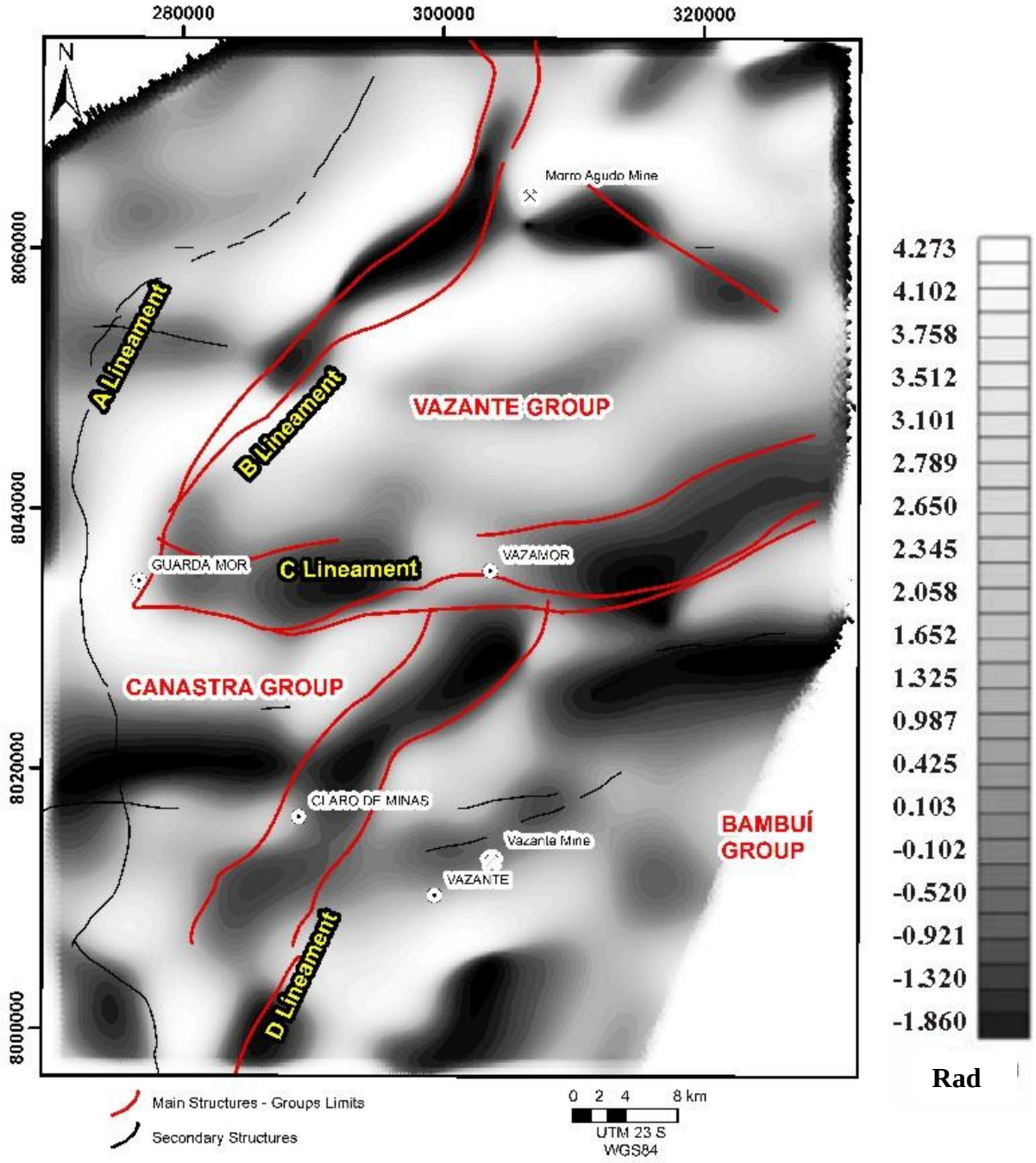

Figure 8 – Tilt derivative to a depth of 9268 meters and the main structures that were obtained.

We therefore associated the lineaments recognized using the magnetic data with their sources at depth, Figures 6, 7 and 8. Table 2 shows these associations.

Table 2 - Relations between the lineaments recognized using the matched filtered magnetic data with their sources at depth.

Lineament	Magnetic Source Depth (m)
A	222
B	222
C	1258 to 9268
D	1258

E	222 to 1258
F	222 to 1258

7.3.3. Euler deconvolution

For the Euler deconvolution applied in the study area, several tests were made between structural indexes 0, 1 and 2 with window sizes of 420 m, 600 m and 900 m. The best result was obtained with index 1 and the 600 m window. The anomalies were divided into four categories related to depth: less than 200 m, between 200 m and 500 m, between 500 m and 1000 m and between 1000 m and 5000 m. Figure 9 shows the results of the Euler deconvolution overlaid on the tilt image, which highlights the image's subsurface structures.

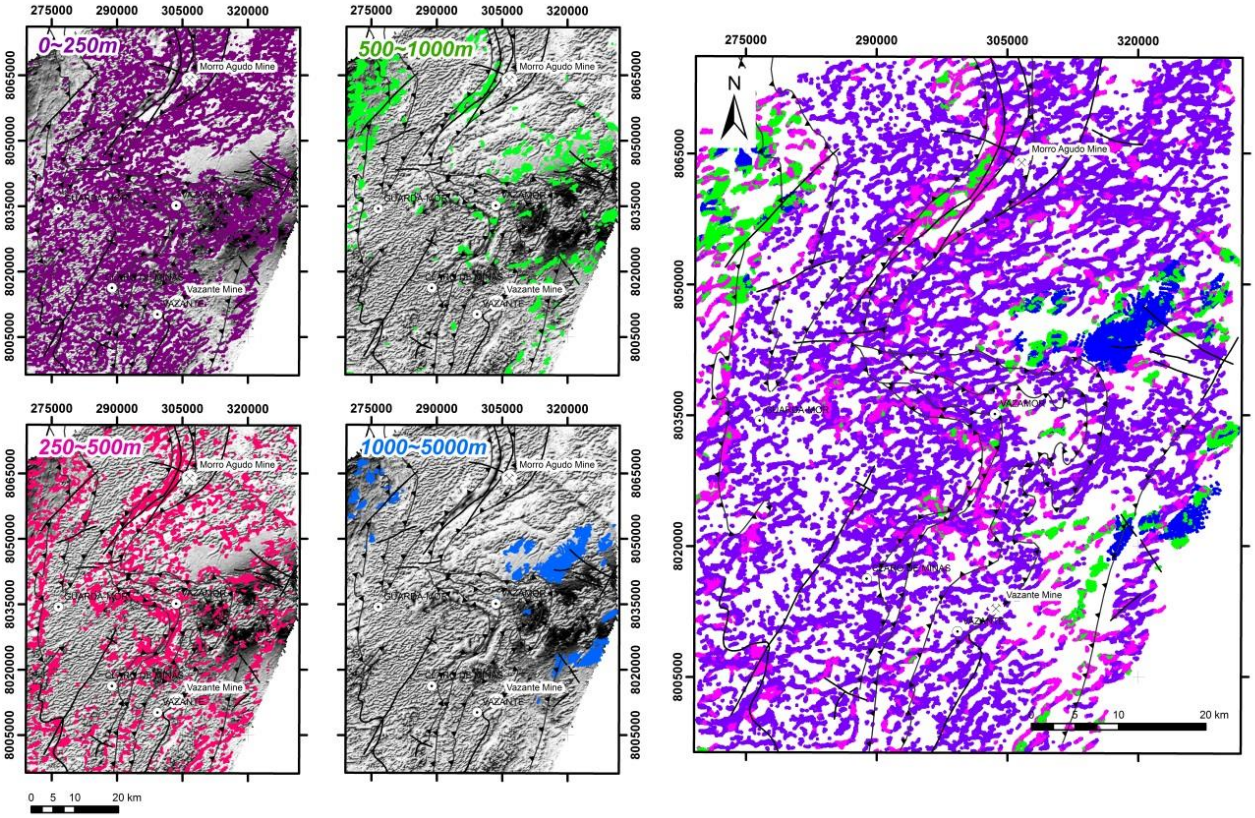

Figure 9 - The response of the Euler method in the study area and divided into 4 different depth groups. The first is 0-250 m (in purple), the second is 250-500 m (in pink), and the third and fourth are 500-1000 m (in green), 1000-5000 m (in blue), respectively. Euler solutions were plotted over tilt derivative.

From depths of 0 to 250 m, we found different magnetic sources that were spread across almost the entire area, except for the northwestern, southeastern and central-east parts of the area. From depths of 250 to 500 m, the magnetic sources are located in the far west and northeastern parts of the area and especially along the thrust faults. From depths of 500 to 1000 m, the magnetic sources are located in the extreme northwest of the area, and some thrust faults are located in the northern and east-central parts of the area. From depths of 1000 to 5000 m,

magnetic sources were found in the extreme northwestern, east-central and southwestern parts of the area.

7.4.Structural Framework of the area

The 1:100,000 structural map and detailed field surveys at a scale of 1:50,000 revealed a complex structure in the Guarda-Mor region and Vazante.

Four deformation phases were defined in the region. The D1 phase is marked by a intrastratal slip that generated a low angle foliation (S1) with a NS-NW dominant direction and dipping to the west. Generally, the foliation is represented by slate cleavage parallel to the bedding planes (S1 // S0), but in most cases, it was observed that the foliation can cut the bedding, causing an evident intersection lineation. The lodging can be recognized by compositional and textural variations in the pelitic rocks, meta-rhythmites and carbonates of the region. Folds closed at isoclinal recumbent folds in the lodging are the result of shortening associated with a low temperature ductile regime that affects the rocks of the region. Recrystallization of sericite, chlorite and quartz, and characteristic mylonitic features are concentrated in localized shear zones and form narrow strips of tens of meters, and the E-W L1 stretching lineation is frequently seen only in the vicinity of high strain zones.

Figure 10 - Representative portions of Stage E1. 1 - rhythmites related to the Serra do Poço Verde Formation of the Vazante Group, in which can be seen S1 // S0. 2 - Hill related to the Chapada dos Piloes Formation of the Canastra Group, with its sub-horizontal layers and the generation of the Coromandel Thrust Fault. 3 - rosy Siltstone, presenting well marked foliation associated with the Serra da Lapa formation, from Vazante Gr., related to E1 phase of deformation, with recumbent fold E-W axis. 4 - Carbonated Siltstone of Serra do Poço Verde Formation, from Vazante Gr., with main foliation S2 dipping about 20° N. 5 and 6- Thin section of a siltstone from Serra da Lapa Formation, Vazante Group, presenting a chlorite and a sericite recrystallization, besides mylonites features as mica fishes.

Phase D2 is responsible for the main foliation recorded in the Brasília Belt (S2) and is oblique to foliation S1 and transposes it, forming a penetrative NW plans direction with a trend ranging from 280° to 330°. The foliation cleavage may occur as spaced and slate foliations, depending on the lithology in which it is printed and the intensity of the deformation area. This phase is defined as flexural folding that is widespread at all scales from regional to microscopic features with a predominant style in the symmetrical folds and the asymmetrical long and short

sides with a convergence to the east. Transposition into the fold flanks resulted in faults and generated thrust areas.

The D2 deformational event ductile-brittle system is focused on WSW-ENE thrust faults mapped in the region and that occur in the contacts between the different units of the Vazante and Canastra Groups. The mylonitic areas are characterized by a lineation of penetrative NE-SW stretching, and the main cinematic related indicators include mica fish, pressure shadow porphyroclasts and sulfides and foliation SC, which suggest tectonic transport of the top to the NE. The stretch lineation is represented by micas and quartz grain recrystallization.

The thrust zones can be considered to be obliquous movements in the direction of the tectonic motion tangential to the main foliation in the region. The observed bending of the foliation and lineations from the NW to the NE, and the thrust fronts, which have associated large folds on the order of a kilometer, also suggest tectonic transport from the WSW to ENE. The thrust areas are characterized by the common transposition of the foliation and the generation of drag folds and recumbent isoclinal folds that can evolve locally to sheath folds. In general, the folds are asymmetrical with convergence to the east, and the rotation axes of the folds cause sheaths due to the differential movement in the thrust fronts.

The final pulse of the tangential tectonics was given by directional faults and NE-SW and E-W lineaments and suggests the jostling of contemporary transcurrent systems. The ductile shear zones are in NE direction and contain stretched quartz grains and micas and narrow mylonite groups that range from millimeters to tens of meters. Lineations that intersect and stretch together on the same outcrop are common in transitional environments between the thrusts and transcurrences.

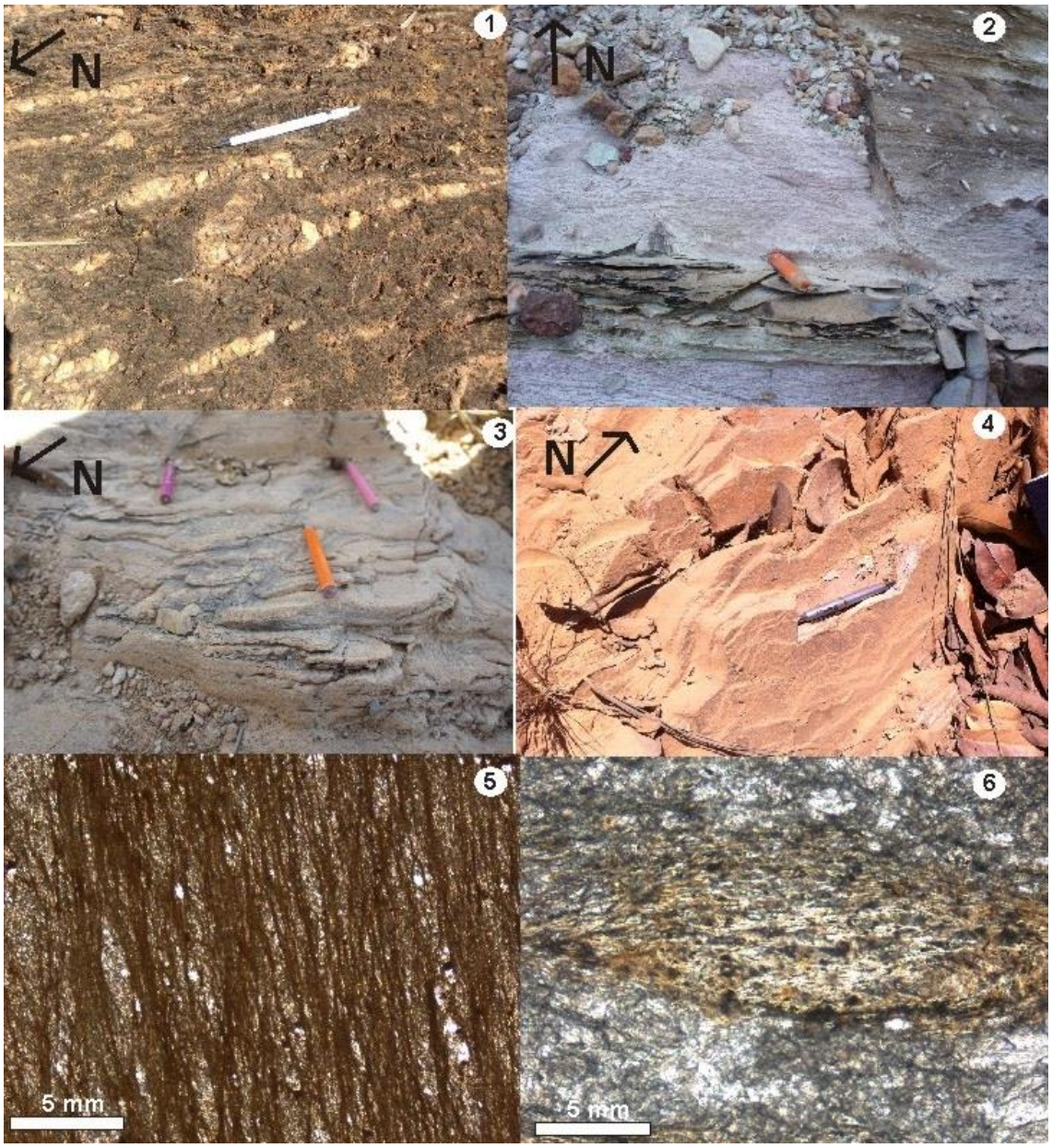

Figure 11 - Representative portions of the E2 Phase. 1 – Outcrop near the road connecting Guarda-Mor to the village of Vazamor with sigmoidal quartz veins of sinistral sense, N-S direction, penetrative and vertical in view of the proximity to the Paracatu Shear Zone. 2 – Rhythmites from the Serra da Lapa Formation of the Vazante Group, showing lithological and rheological variations that have the highest intensity of deformation, and the main foliation - S1, dips to the NW. 3 - Outcrop on the edge of road that links Guarda-Mor to Morro Agudo, which belongs to the Serra da Lapa Formation of the Vazante Group, with the main foliation - S2 presenting crenulation, E-W axis; 4 - Reddish siltstone of the Serra do Garrote Formation, from Vazante Group, with main penetrative foliation - S2 and slate cleavage, dipping to the west. 5 - Low temperature mylonite related to the E2 phase, with pronounced stretching, reaching a dextral sense sigmoid, in association with the Vazante Shear Zone. 6 - Photomicrograph of a siltstone related to the Serra da Lapa Formation of the Vazante Group and affected by the Morro Agudo Shear Zone, in the presence of S- C type foliation and a strong upside stretch.

Phase D3 is marked by an attenuation of the deformation in the N-S direction, the generation of open folds with N-S axes and the generation of spaced crenulation cleavages and intersecting lineations parallel to the axes of the crenulations (Figure 12). Foliation S3 is subvertical, with dips ranging from 60 to 90 degrees, and trims to the west. Open large folds that are kilometric up to hundreds of meters involve synclines and anticlines and do not generate

axial plane foliations. They are the result of a strong component of the further shortening of the thrust faults. Thus reverse and slip faults were formed by the accommodation of the deformation at the end of the tangential tectonic and now occur at a shallower crustal level than previous strains in the essentially brittle-ductile environment. The faults are associated with the reactivation of strike-slip shear zones in the NE, which now have a brittle character and sinistral kinematics. The interference between deformation stages D1, D2 and D3 created interference patterns of mushroom and dome and basin types, which suggest refolding during the course of progressive deformation in the same shear stress field in the region. Therefore, the D3 shortening phase of the bending of the mylonite shear zones formed in D1 / D2.

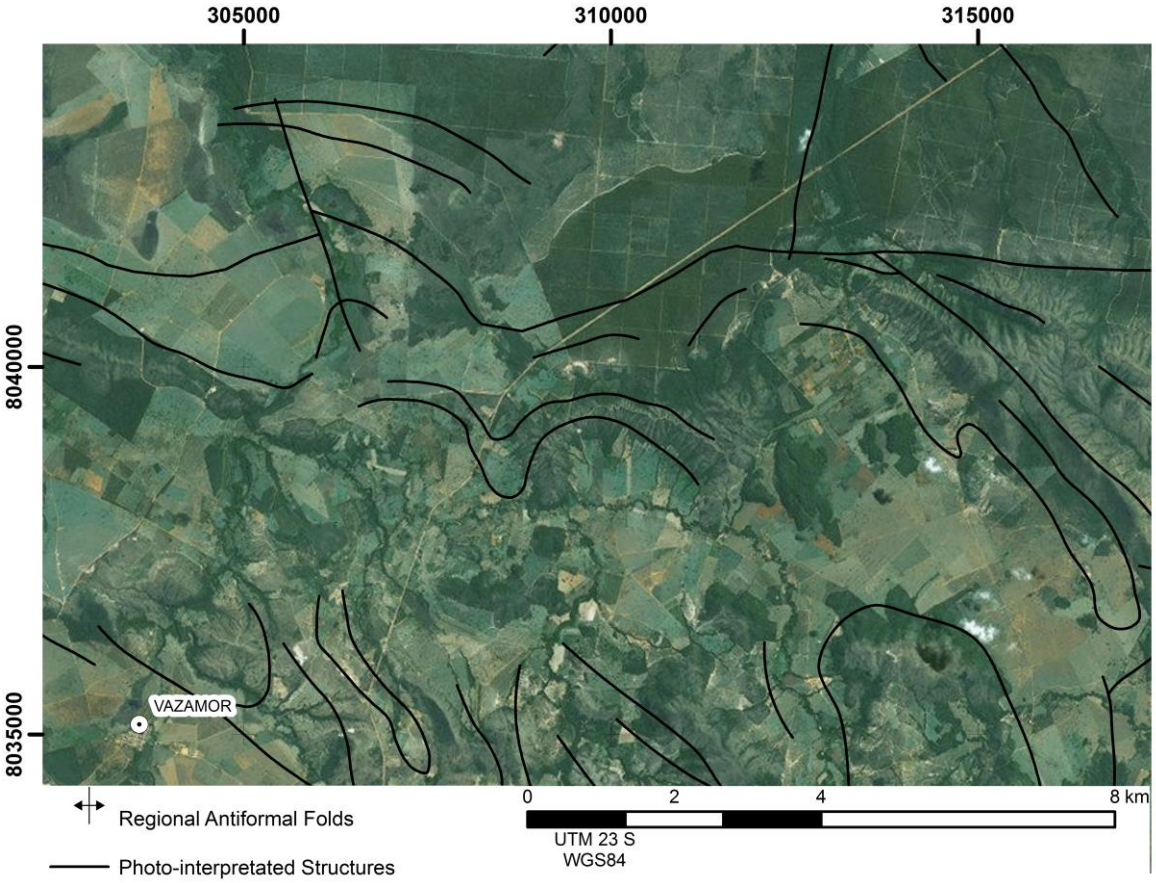

Figure 12 – Image of the regional open folds interpreted to be related to deformational phase E3.

In addition, this phase is related to the occurrence of symmetrical folds and the chevron and normal faults locally associated with the kink bands structures with E-W directions or conjugate pairs with WNW-ESE and WSW-ENE directions and is responsible for the main foliation S2 crenulation (Figure 13). The axes of microfolds that developed associated kinks generated a parallel crenulation cleavage there.

The generation of intense cleavage fracture faults and D3 tension gashes in this stage may be associated with a pure shear component in the region. There is also a presence of fault breccias and cataclasite in the NE and NW directions.

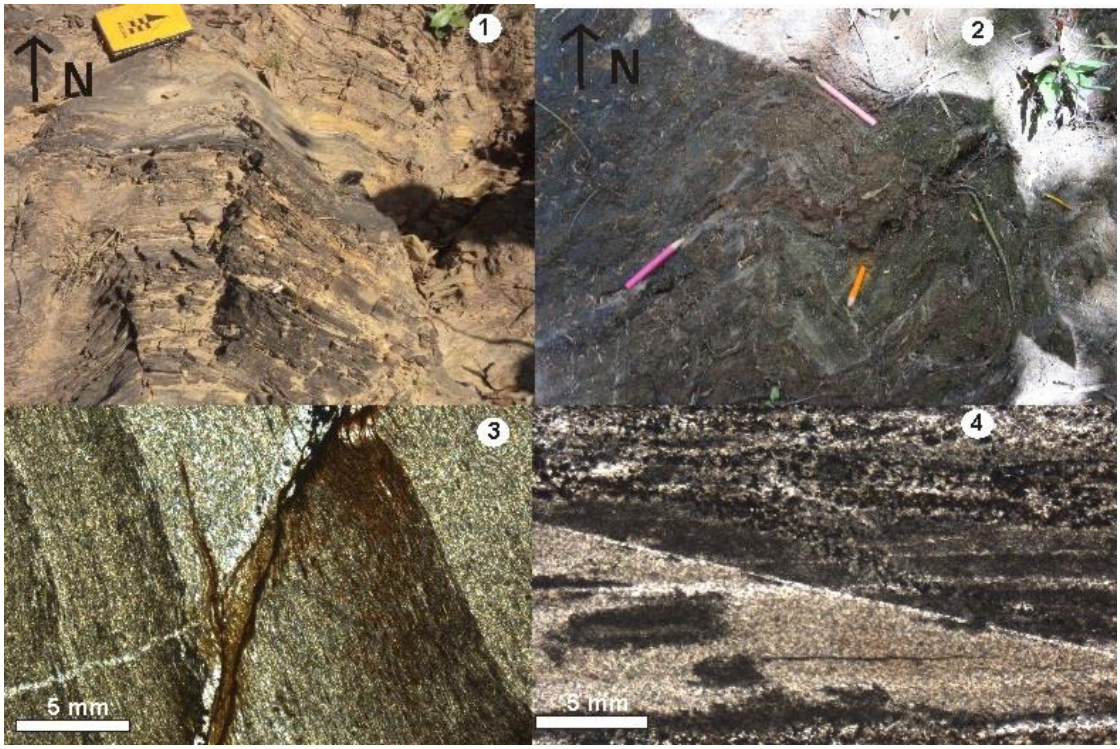

Figure 13 – 1- Yellow siltstone of Serra da Lapa Formation, Vazante Gr., presenting a symmetrical N-S axis open fold. 2- Kink bands along a NW-SE axis related to the E3 phase of deformational event D1 in the Serra do Poço Verde Formation, Vazante Gr. 3 - silt-clay particle size related to the Serra das Antas formation of the Canastra Gr., indicating a slight brecciation, and related to of the Arrenegado Shear Zone. 4 – Banded siltstone of Serra da Lapa Formation, Vazante Gr., presenting a reverse fault between the bands.

The D4 phase is characterized by normal fault systems and an essentially NE, NW and EW brittle transcurrent. The event generated an extensional and interconnected fault system and the Zn and Pb mineralization in the region, which generated different types of faults holes, cataclasite zones and a powerful system of fractures and joint strains.

The faults and fractures are irregular, and the kinematic indicators include anastomose lineaments, generation pods and features of type S-C, with dextral and sinistral kinematics. The main direction of the structures in this case is NW. This event may be associated with the tectonic relaxation of the Brasilia Fold belt and its reactivation in the Cretaceous and more recent times (Figure 14).

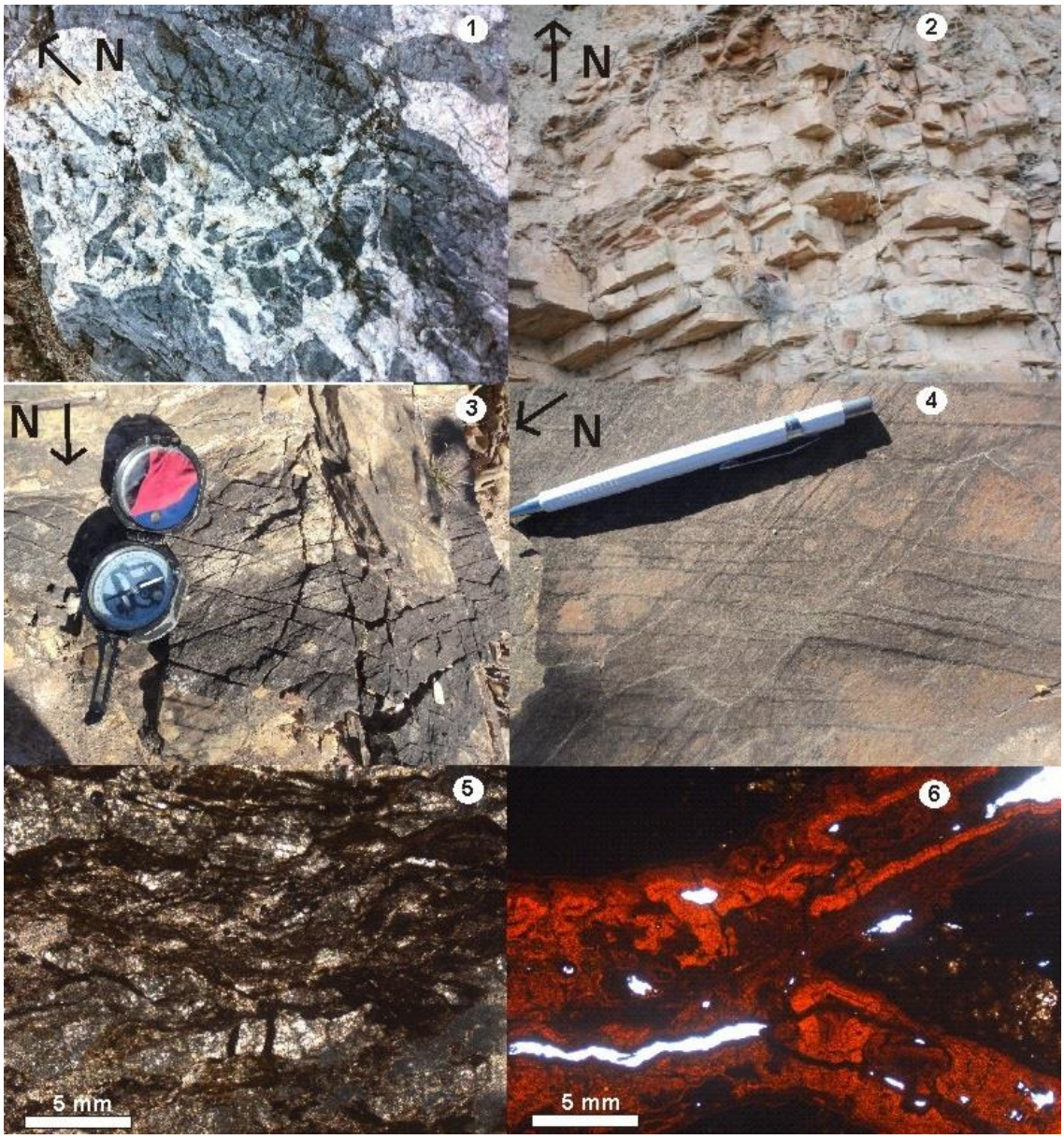

Figure 14 - Representative outcrops of the deformational E4 stage. 1 - Carbonate of the Serra do Poço Verde Formation, which is intensely breached and filled with alkaline fluid. 2 - Yellowish siltstone in the Serra da Lapa Formation, with well pronounced main foliation S2 that dips to the W and is cut by three fracture directions (N-S, NW-SE, and NE-SW). 3 - Carbonated siltstones in the Morro do Pinheiro formation of the Vazante Group, with a fracturing system with conjugate pairs in the N-S direction. 4 - Outcrop related to the Serra da Lapa Formation presenting small discrete joints at NE-SW and NW-SE, related to the E4 stage. 5 - Sample photomicrograph related to the Serra da Lapa Formation of the Vazante Group, in which can be seen a pronounced billing with percolating fluids that are rich in organic matter and form gaps. 6 - Sample photomicrograph related to Serra do Poço Verde Formation, in which iron rich fluids percolate through the rock's gaps.

A summary of the events and the proposed deformation phases for the region are presented in Table 3.

Table 3 - Summary of the events and proposed deformation phases for the region.

	D1 Event		D2 Event
E1Phase	**E2 Phase**	**E3Phase**	**E4 Phase**
Ductile	**Ductile-Brittle**	**Brittle-Ductile**	**Brittle**
Interfoliation slip Axial plane mylonitic foliation, S1 and S0 //	Low angle main foliation; Thrust faults, directional shear faults NE-SW, N-S e E-W	Attenuation of deformation. Crenulation generation in the main foliation S2.	Generation of fractures, joints and essentially brittle faults.
isoclinal recumbent folds at local scale	Generalized folds, mainly symmetrical chevrons, verging to east.	Open folds and kink bands E-W Mushroom type of interference pattern.	Small-scale drag folds.

The central portion of the Paracatu-Vazante sequence is divided into six structural-stratigraphic domains that are related to differences in the structural behaviors of the different mapped lithological units as well as the magnitude and dip of the main foliation S2. Each domain is separated by different deformation regimes and differences among the main foliations, dip angles and rheologies of the geological units. The boundaries of the fields are represented by thrust and strike-slip faults and high structural shear zones. Those areas are illustrated in Figure 15.

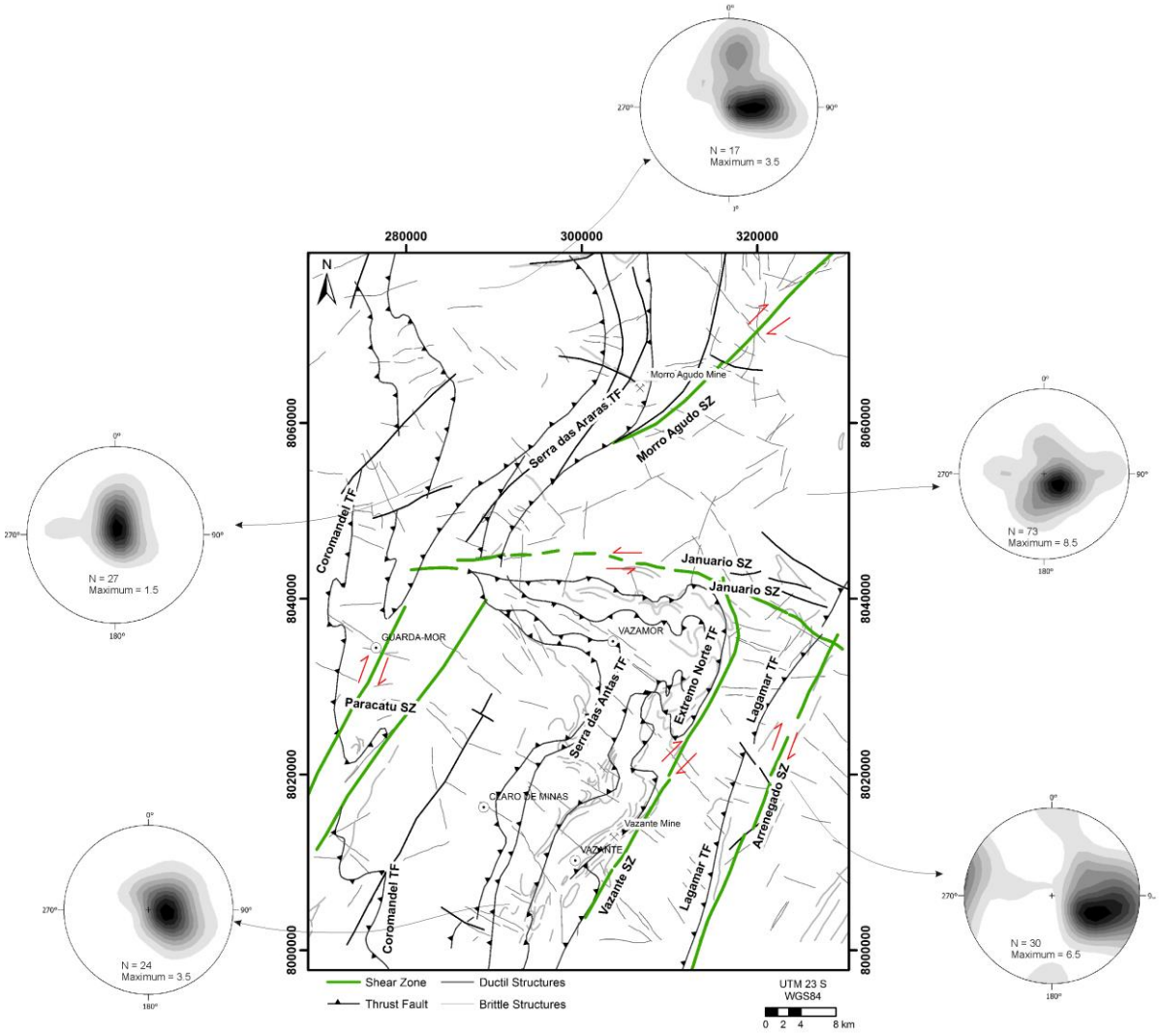

Figure 15 - Structural map of the study area showing the 6 structural-stratigraphic domains for the region and highlighting the five shear zones, which are: Paracatu Shear Zone, Morro Agudo Shear Zone, Januário Shear Zone, Vazante Shear Zone, and Arrenegado Shear Zone.

Domain I is located at the western end of the area and is formed by a structural high that is related to a sub-horizontal plateau represented by Chapada dos Pilões Formation of the Canastra Group, and most of the outcrops on slopes of the Chapada dos Pilões are in contact with Paracatu formation. There is an extensive lateritic cover in the middle of the plateau. Domain I is characterized by a foliation with a predominantly medium to high angle (40° to 90°), which is oriented ENE-WSW, dips westward and generally cuts the layering to the south (Figure 15), which produces a N-S intersection lineation (sub-horizontal) and one NE-SW stretch/mineral lineation (sub-horizontal) (Figure 16). The folds have a flexural flow feature axis with an approximate N-S direction and centimetric to metric dimensions, monoclinic symmetry, sub-recumbent spaced hinges and converges to the east. The main foliation is well marked, penetrative, can be crenulated, usually dips to the west (Figures 17-2).

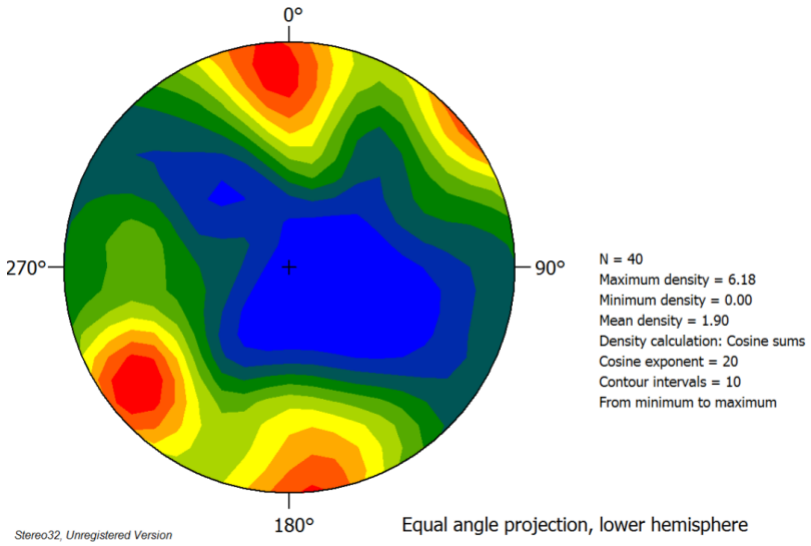

Figure 16 - Stereogram of the stretching lineations of Domain I. It is important to note that the diving gradient is not very high and the preferred directions are N-S and NE-SW.

Figure 17 - Outcrops with typical structures in Domain I. 1- Hill located at north of Guarda-Mor related to the Serra das Antas Formation of the Canastra Group, in which can be seen the main foliation - S2, dipping to the west. 2 - Reddish siltstone related to the Chapada dos Piloes Formation, Canastra Group, with an E-W asymmetrical fold axis, which is related to the event D1 of the deformation regime.

The contact of this domain with domain II is given by Coromandel Thrust Fault. The Coromandel Thrust Fault (Pereira, 1992), which has a roughly NS alignment and an irregular design, is characterized in the study area as a frontal thrust ramp, and the block ceiling is located in Paracatu formation with mass transport from the SW to the NE. Note the low angle foliation; the orientation is in the N-S direction with a trim of approximately 10-20° dipping westward.

Paracatu shear zone is comprised of a series of small structures with N-S directions and sub-vertical plunges that are approximately 60 ° to the west. It is responsible for generating a penetrative foliation that is accompanied by a stretching lineation with N-S direction and a gentle 5° to 20° dip to the south. In the field, the typical features are sigmoidally shaped mylonite and the presence of S-C foliation, which suggests a dextral kinematics. Normal and reverse faults to

the NE-SW and N-S with centimetric scarp are present in many outcrops of Domain I and II. A system of joints and NW-SE dominant fractures also appear in the domain.

Domain II is formed by Paracatu Fm., from Canastra Group. Does not present a significant relief, it consists of a largely devastated area, which are found scarce outcrops. However, the domain II is characterized by a well-marked, predominantly medium to high angle foliation (35° to 80°), with ENE-WSW direction dipping westward, Morro Agudo and Arrenegado shear zones make this foliation domain vertical in some points (Figure 15), which can generate mineral stretching lineations with east-west sub-horizontal and dip to the west (5° to 35°) (Figure 18), as can be seen in Figure 19.

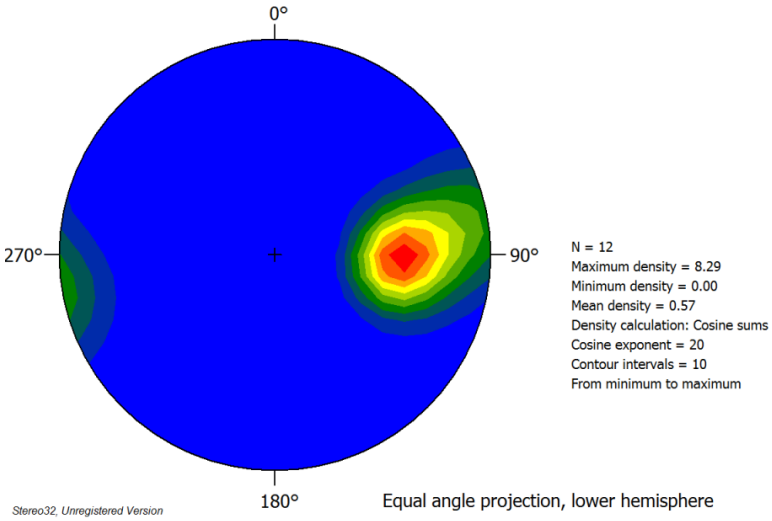

Figure 18 - Stereogram of the stretched mineral lineations for Domain II. It is important to note the main direction of the lineation is E-W and the gentle dip is to the W.

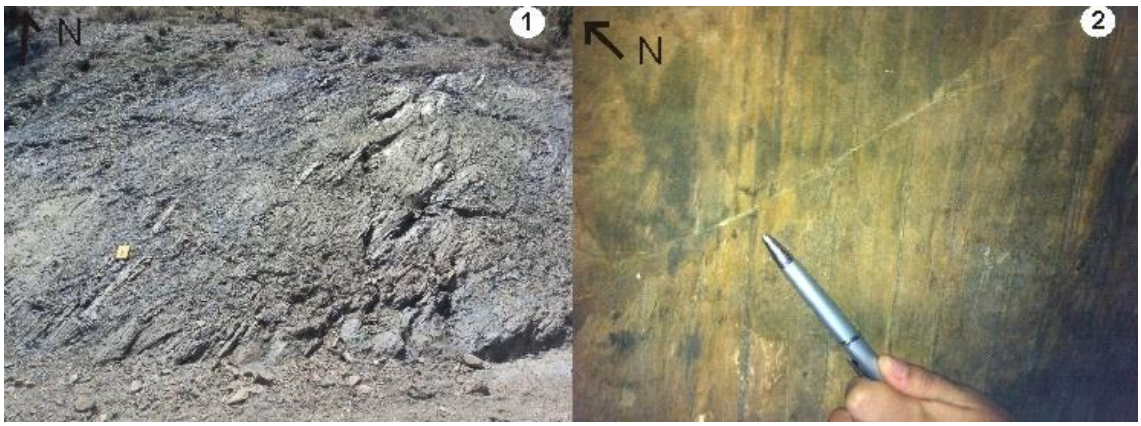

Figure 19 - Outcrops of Domain II. 1 - Outcrop amid the Paracatu Formation, Morro do Ouro Member, with main foliation - S2, penetrative, dipping westward, and fractured in the E-W direction Outcrop amid the Paracatu Formation, Morro do Ouro Member, with main foliation - S2, penetrative, dipping westward, and fractured in the E-W direction; 2 – Sub-vertical Rhythmites from the Serra da Lapa Formation of the Vazante Group, showing inverse faulting related to Serra das Araras Thrust Fault.

The Serra das Araras Thrust Fault System forms the contact between domains II and III, has an approximate NE-SW alignment, and is formed by several thrust fronts. Its roof block is located in the Serra da Lapa Formation of the Vazante Group, trends NW-SE, and represents the regional contact between the Vazante and Canasta groups.

Domain III is characterized by very significant relief that consists of a set of NE-SW aligned hills. It is bordered by the Serra das Araras Thrust Fault System and the Morro Agudo shear zone. It is characterized by medium-high angle foliation (42° to 88°), with the main WNW-ESE direction dipping to NW-W, that caused a vertical foliation next to the strike-slip shear zones and reverse faults (Figure 15 and 21-1), it can be, sometimes, intensively deformated because of the interactions of these structures (Figure 21-2). In this area, the main foliation appears as slate cleavage and crenulation and axial-plane weakly asymmetrical or symmetrical folds and can cut the layering. Therefore, it produces a NNW-SSE intersecting lineation (sub-horizontal) and a WSW- ENE mineral stretch lineation (average dip of 30°) (Figure 20). The folds are flexural, with monoclinic symmetry, recumbent semi-recumbent, and mesoscopic verging eastward, because the Serra das Araras Thrust Fault System is the contact between the Canastra Group and the Vazante Group in the northern portion of the area.

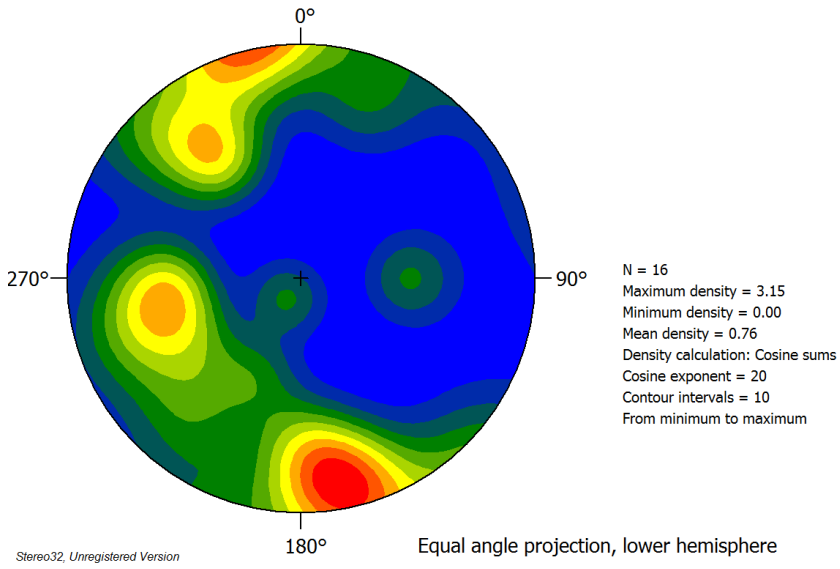

Figure 20 - Stereogram lineations in domain III. Two main directions of stretching in the minerals are noted: NNW-SSE and WSW-ENE.

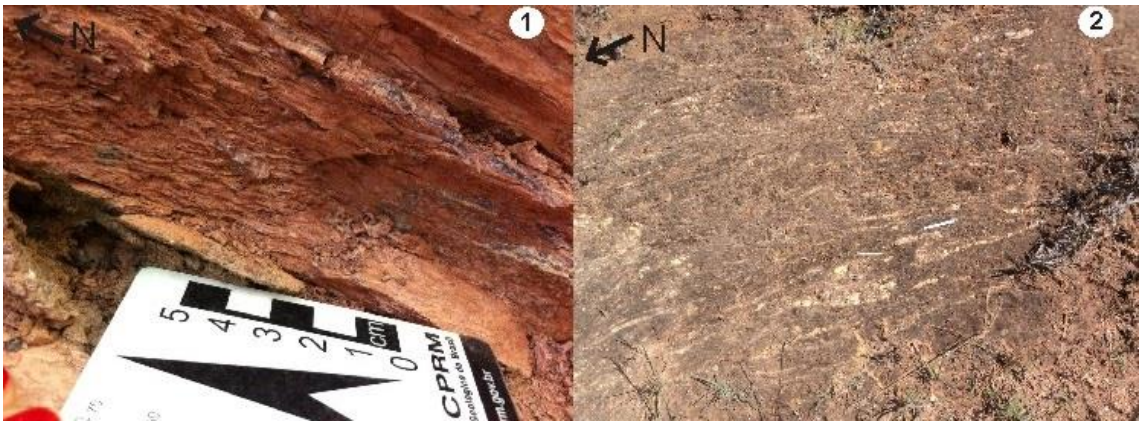

Figure 21 - Outcrops of Domain III. 1 - Reddish siltstone from the Serra da Lapa Formation of the Vazante Group, with penetrative foliation S2, dipping southwestern; 2 - Outcrop near the road that connects Guarda-Mor and the town of Vazamor with plenty of sigmoidal quartz veins of sinistral sense that are related to the E2 phase.

The Morro Agudo shear Zone is responsible for generating a series of NE-SW lineaments and dips approximately 60° to the west, with a dextral sense and lineation in the same direction dipping 20° SW, which affects the units of the Canastra Group and Serra da Lapa and Serra do Poço Verde Formations of Vazante Group. In some parts, there is an overlap between this shear zone and the Serra das Araras Thrust Fault System, which generates overlapping features in the same shear stress field during the continuous processes of a progressive and heterogeneous deformation such as sheath folds. All of these features suggest oblique movements that are related to tectonic thrust in the region. Reverse faults associated with this domain have more brittle characteristics, with well-defined and cohesive foliation and intense fracturing in the E-W and N-S directions. In thin sections, its breached nature is very evident, as is the enrichment in organic material and the presence of a filled discordant shaft, which is often filled by a fluid rich in iron (Figure 14-6).

The contact between Domain III and Domain IV, that can be easily seen in satellite imagery and digital terrain models, is defined by topographical differences and the Morro Agudo Shear Zone. The flat terrain portion corresponding to the region is filled with a Quaternary basin. Near the city of Guarda-Mor - MG, the set of E-W sinistral lineaments that dip approximately 70° south and a ENE-WNW lineation that plunges approximately 15° to the west and cuts across all geological units in the area is designated as the Januário Shear Zone. Its influence in the central portion of the area generates a strong inflection to the NE in the E-W foliation, that truncates it.

Domain IV extends over the entire eastern portion of the study area and is characterized by a low to moderate angle (15° to 60°) foliation to the west, which is usually subparallel to the lodging with ENE-WSW (Figure 15 and 22-1) symmetrical folds and closed isoclines that typically have E-W axes (Figure 22-2). The Lagamar Fault and Vazante Shear Zone, which has

mylonitic features in local reverse faults, form the southern boundary between domains IV and V. The mylonites are characterized by S-C foliation, with the presence of portions that are rich in organic matter. Brittle reactivation in this area is evidenced by faults and cataclasite.

Figure 22 - Outcrops of Domain IV. 1- Quartzite from the Domain Formation Serra da Lapa, the Gr Vazante in the Escuro River drainage border with penetrative foliation S2 that dips westward; 2- Reddish siltstone related to the Serra do Garrote Formation, Vazante Group, with an E-W asymmetrical fold axis.

The Escuro River Basin format suggests recent tectonic control that was reactivated by the use of old structures, which were notably related to the orientations of the Lagamar fault, Extremo Norte Thrust Fault and Serra das Araras Thrust Faults System. The Escuro River is controlled by a dominant NE fracture system and a secondary NW fracture system, which should reflect the deep structure in the basin.

The Lagamar thrust fault (Freitas-Silva, 1991) is approximately aligned N-S, and the ceiling block is located in the Bambuí Group, the W mass transit of the E. Vazante Shear Zone consists of several small structures towards the NE-SW, and the great faults of Vazante cut the Serra do Garrote and Serra do Poço Verde Formations. This thrust fault is characterized as simple shear, brittle-ductile, heterogeneous and progressive and is mainly responsible for the control of zinc mineralization in the area (Pinho, 1990, Rostirolla, 2002).

The Extremo Norte Thrust Fault is curvilinuos, being aligned N-S at its southern part and E-W folded at its northern part. It represents the interference between deformation stages D1, D2 and D3 as interference pattern of mushroom type, which suggest refolding during the course of progressive deformation in the same shear stress field in the region.

Domain V is characterized by the significant relief in the southern part of the area, which includes the city of Vazante and can be easily seen in the Ground Digital Model because it is delimited by the Serra da Lapa Thrust Fault System, Paracatu Shear Zone and Lagamar Thrust Fault. The area is characterized by medium-high angle foliation (45° to 80°) to the W and SW (Figure 15), with preferred directions ranging from the NW-SE to the NS (Figure 24), presenting

mineral stretching lineation east to northeast direction (sub-horizontal, with gentle dips between 8° and 35°) (Figure 23), that are generally parallel to the lodging, and verticalization that is close to the transcurrent shear zones, generating mylonits related to Arrenegado Shear Zone.

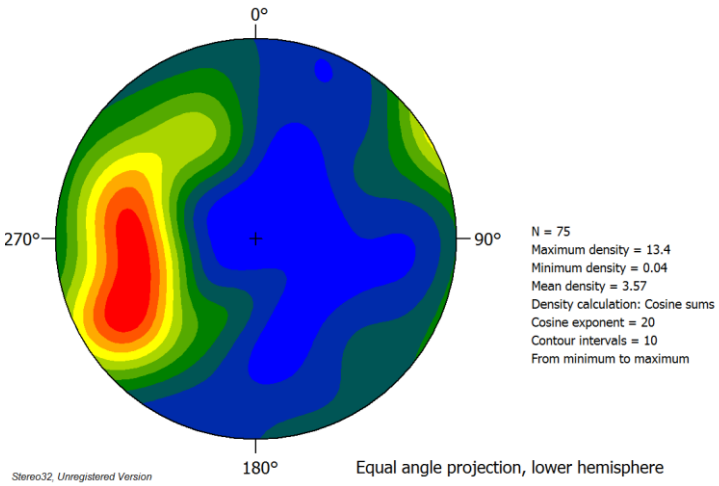

Figure 23 - Stereogram of the lineations in Domain V. Note that the main direction of the lines ranges from the N-S to the NE-SW, with a low dip angle.

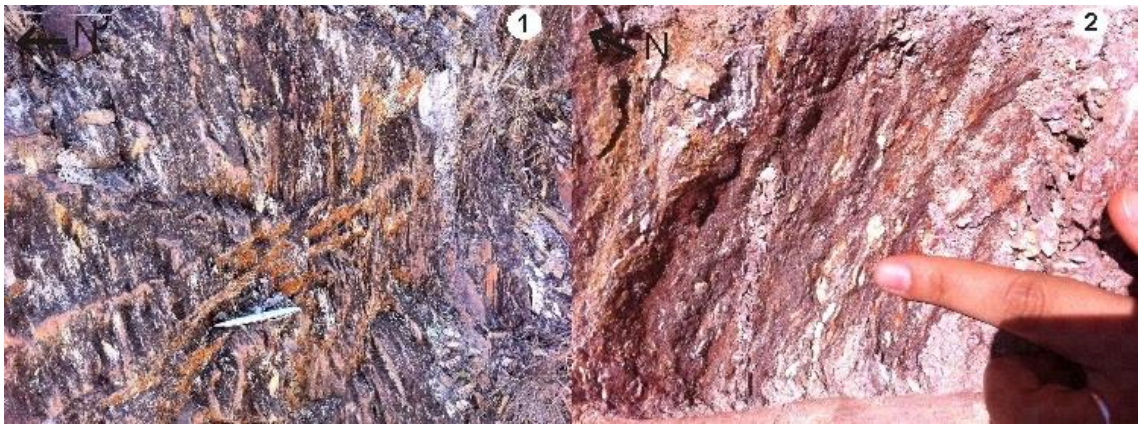

Figure 24 - Outcrops of Domain V. 1 – Purplish siltstone related to Serra do Garrote Formation, Vazante Group, with very penetrative principal foliation S2 with a N-S direction dipping to the W, related to the Paracatu shear zone; 2- Mylonitic features generated by Arrenegado Shear Zone in this region, with rotation of elements and generation of a S-C foliation.

Arrenegado Shear Zone occurs at the contact of the Vazante and Bambuí groups, is characterized by a set of N-S dextral lineaments and has rotated the previously subhorizontal foliation from the NW-SE to NE-SW. These elements suggest oblique movements that are related to high-angle shear zones in the region.

Therefore, the structural domain map can be interpreted as a result of the actuation of systems and thrust-slip in the region. Faults bound the domains, and shear zones were recognized in the detailed structural mapping performed in this work.

7.4.1. Structural Model for the Guarda Mor-MG region

A structural tectonic model was proposed for this segment of the Brasília Belt in the Guarda-Mor-MG region. The main feature that was found is a thrust fault system and transcurrent shear zones that simultaneously act in a brittle ductile environment and are associated with oblique movements that suggest tectonic mass transport from the SW to the NE, and evolved into a crustal shortening system that generated NS and NE reverse faults and shear zones. The low angle dominant tectonic (tangential) regime is understood because the overlapping tectonic rocks of the Canastra, Vazante and Bambuí Groups nappes in the system are already known and described in the region.

The area is characterized by the curving of the main NE-SW directions of the mapping units to the E-W near Guarda-Mor and continuing in the N-S direction toward Vazante. This bending can be interpreted as a large sigmoid that forms a structural tensor S, which is related to the regional tectonics and the thrust region.

Thrust fault systems put the rocks of the Canastra Group on the rocks of the Vazante Group and the Vazante Group on the Bambuí Group. The transcurrent shear zones have N-S, NE-SW-W and E-W directions, are symmetrical with each other and are controlled in large part by the orientations of the structures in the region. These shear zones have width of approximately 2 to 3 km and average lengths of 50 km but show well-marked evidence of mylonitization processes.

The lineaments, which were defined by the crests of hills, depressions and the markedly structured drainage, were analyzed using a Landsat 8 satellite image on a scale of 1:100,000 and are presented in a rosette diagram (Figure 26). Figure 25-A shows the fronts of the Serra das Araras Thrust Faults System, with a SW-NE transport that can be seen in various scales; the fronts are cut by later structures that have different directions but are always orthogonal to the main foliation, beyond the interference of the Morro Agudo Transcurrent NE-SW dextral shear zone that produced the Morro Agudo mine in that system.

Figure 25-B shows the interference of the two major fold systems: the N-S open folds that were affected by the attenuation of the deformation in the E3 phase of the D1 event, resulting in a mushroom refolding pattern type (Ramsay, 1962) and that were cut by later NW-SE to E-W brittle structures. In the southeastern portion of the structure, there is the interference of the Vazante NE-SW dextral Transcurrent Shear Zone. The structure is defined in the upper portion of the Transcurrent shear zone by its sinistral sense and E-W direction. Figure 25-C shows the NE-SW dextral Vazante Transcurrent shear zones, in addition to the Serra da Lapa and Extremo Norte Thrust Fault systems, with WSW-ENE transport, which generated several thrust fronts that often contain folded mylonite deformed prints formed by the shear zones. In

this context, there is the Vazante mine, which is in the middle of the Vazante shear zone between the two sets of thrust faults.

Therefore, because various structures overlap in this region, that were probably formed in parts at different depths in the crust, geophysical tools are needed to develop a greater understanding.

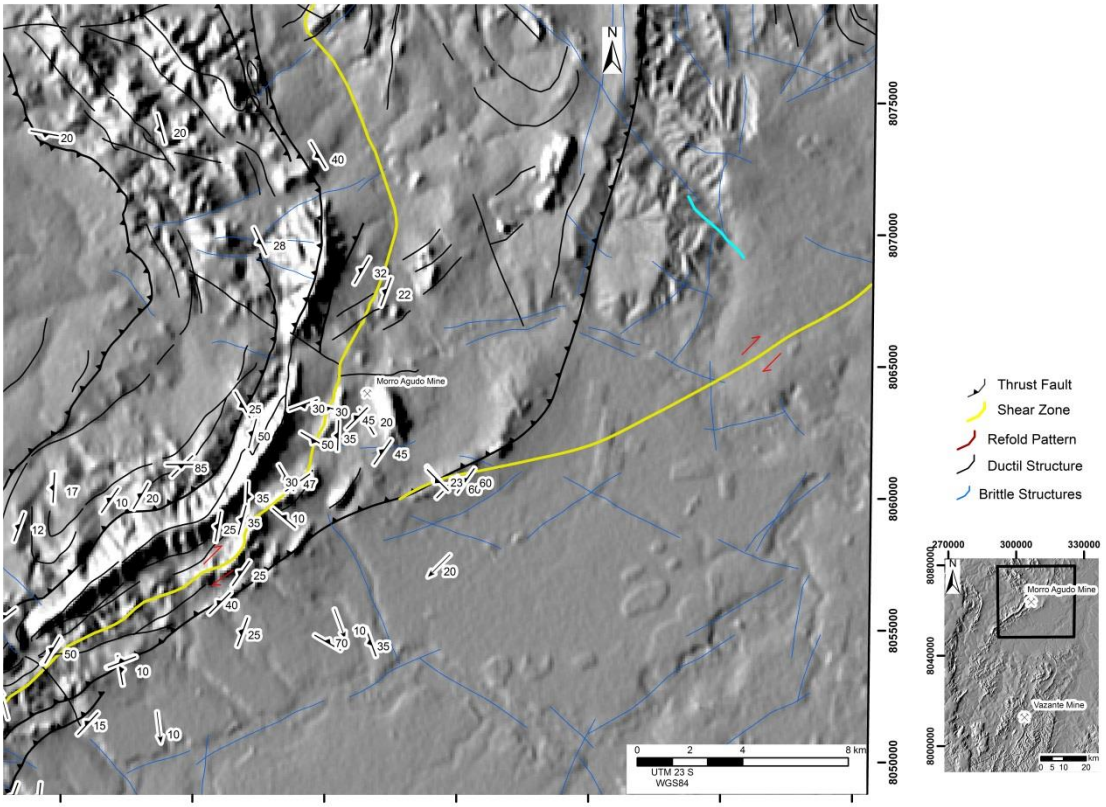

Figure 25-A - Highlight of the northern area near the Morro Agudo mine, based on field data and images from the SRTM 7 sensor, targeting the brittle and ductile structures.

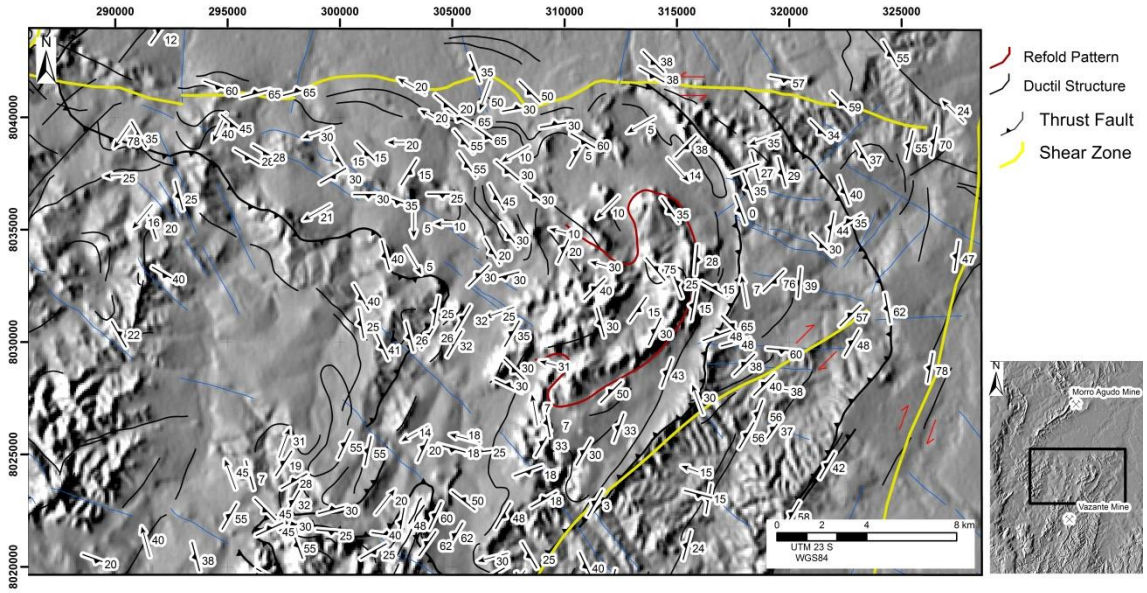

Figure 25-B - Highlight of the central area near the town of Vazamor, based on field data and images from the SRTM 7 sensor, targeting the brittle and ductile structures.

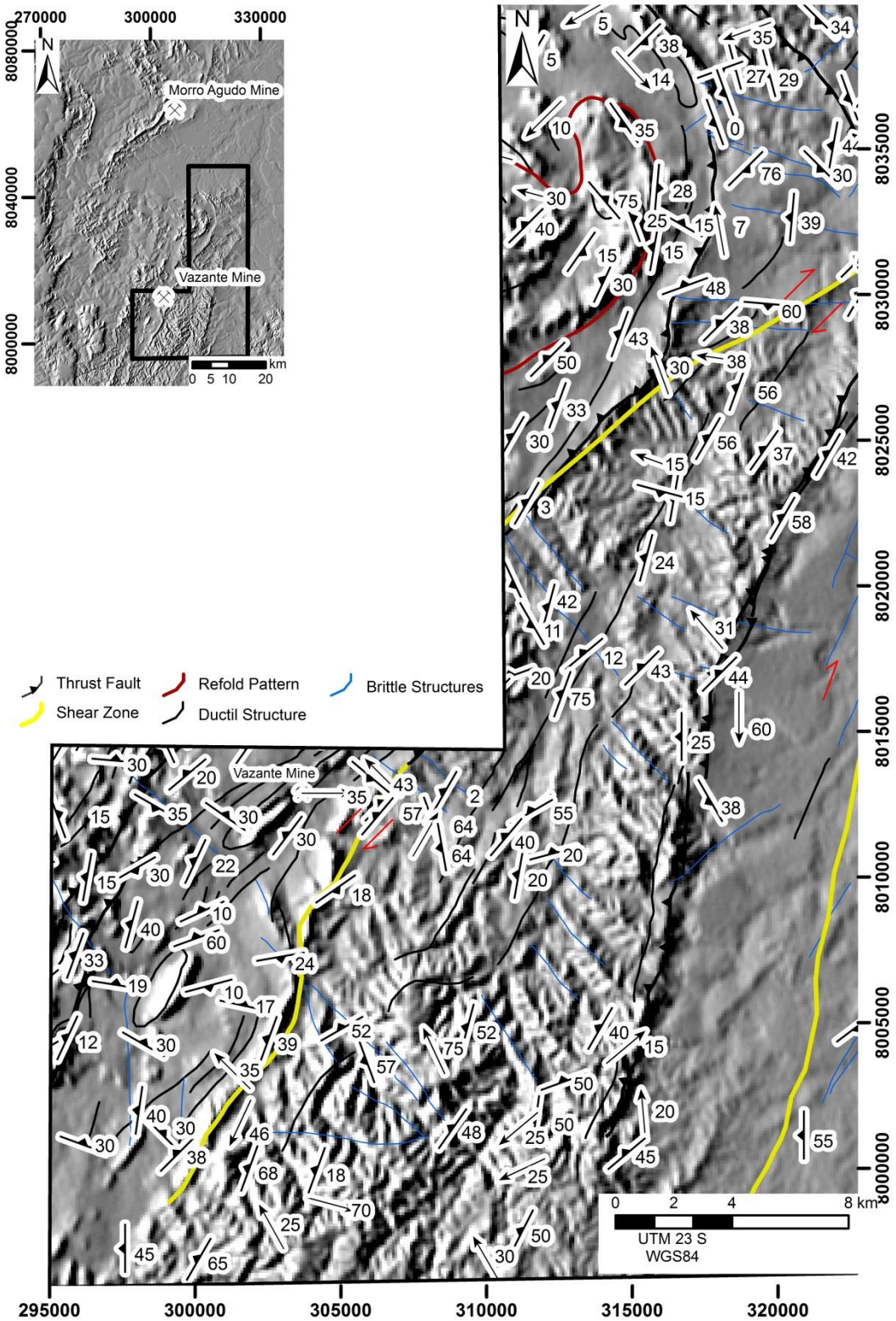

Figure 25-C - Highlight of the southern area region near the mine and town of Vazante, based on field data and images from the SRTM 7 sensor, targeting the brittle and ductile structures.

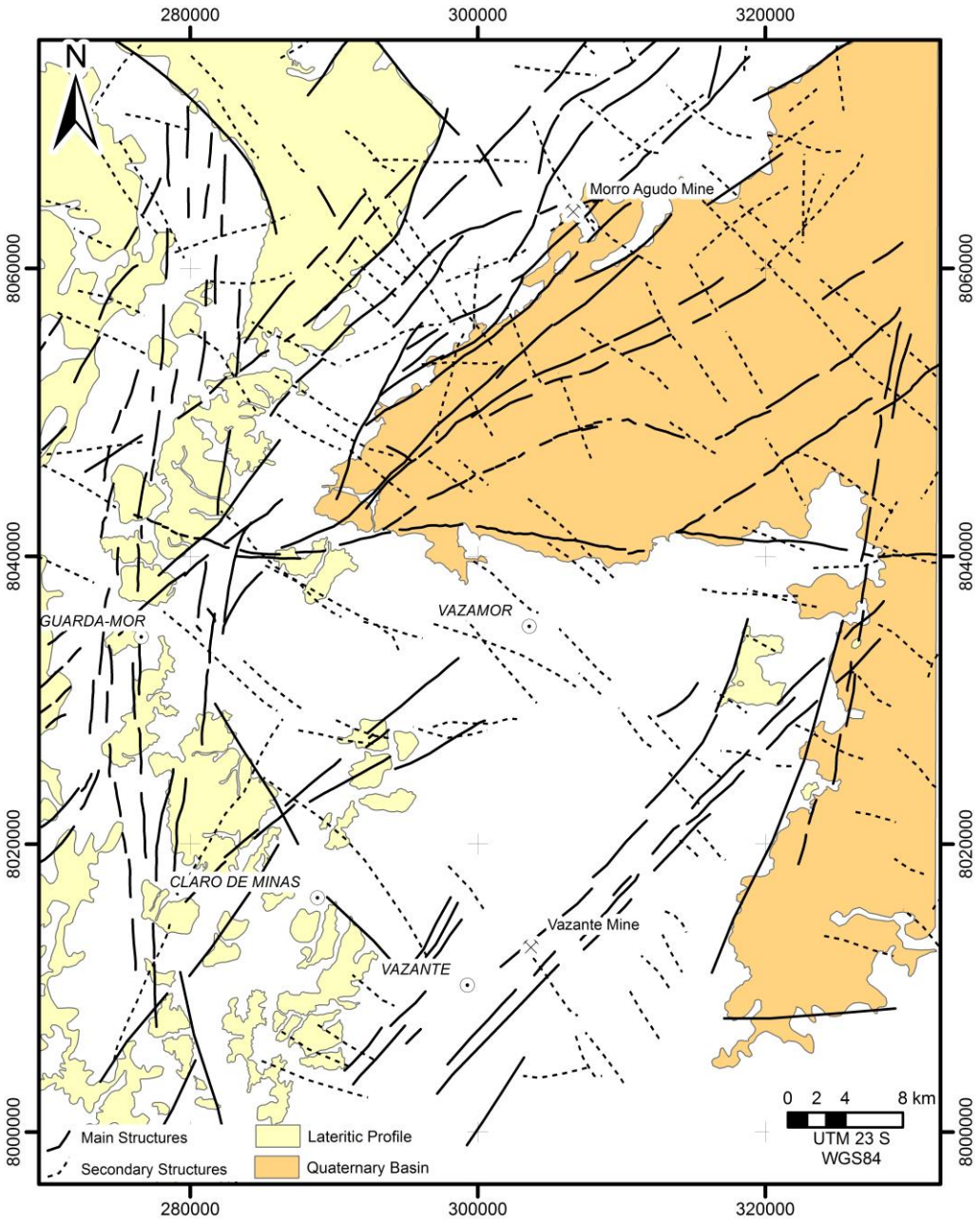

Figure 26 – Map highlighting the lateritic covers throughout the study area that shows the control of the covers by brittle structures.

The analysis of the brittle structures, whether in the field or using the satellite images and aerial photographs, showed a preferential arrangement throughout the region, with conjugate pairs that were approximately orthogonal to each other in the NE-SW and NW-SE direction and N-S and E-W directions (Figure 27). The NE-SW direction appears to be more prominent, with higher lineaments, but the NW-SE, NS and EW directions, although less frequent, also exhibit a homogeneous distribution.

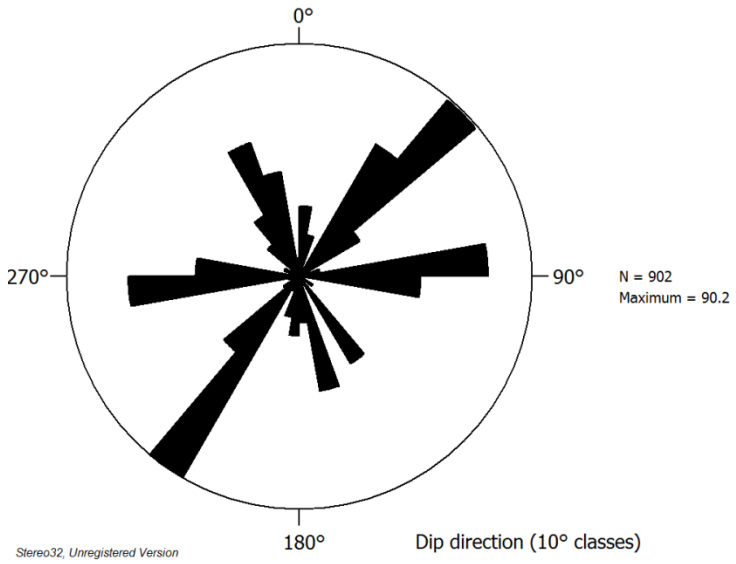

Figure 27 - Rosettes diagram that shows the brittle structures in the region.

It is believed that the fractures can be generated contemporaneously, which suggests that in the fracture formation process such conjugate pairs have been formed regionally in the entire area. Campos-Neto (1969), Freitas-Silva (1991), and Pereira (1994) also showed these brittle features as a final deformation step in the region corresponding to the regional compression relief process.

7.5.Discussion

An integration of the detailed structural geology field data and aero-magnetometric products enabled us to suggest a new tectonic interpretation of the region of the External Zone of Brasília Belt, notably the contact between Vazante, Canastra and Bambuí Groups in the Guarda-Mor region.

Aeromagnetometric data were used with structural data field at a 1:100,000 scale to characterize the tectonic framework of the Guarda-Mor region to understand the depth of the structures and their interactions with the toppings and basement. Two types of aeromagnetometric data processing were used: Euler deconvolutions and matched filter.

The contact between Canastra and Vazante groups in this region is marked by a strong discontinuity in the geophysical images, which is represented by lineaments C and D (Figures 4 and 5), that are related to the Serra das Araras and Serra das Antas thrust faults systems (Figure 14).

The Euler deconvolution showed that the tops of the magnetic sources were at depths of up to 1 km, but when the data were processed using the matched filter, supplies up to 9 km appeared, which indicated the base of the strong discontinuity. Coelho et al. (2008) and

Alvarenga et al. (2012) confirmed the existence of a strong and deep discontinuity between the two groups.

One can therefore define two distinct blocks and, consequently, different basement depths, and the deeper Canastra reference group, to preserve its main structures up to depths of 9 km (Lineaments A and B - Coromandel Thrust Fault and Serra das Araras Thrust Fault System).

It is believed that the Canastra and Vazante groups define two distinct basements with different depths, wherein a portion of the Canastra Group is deeper and part of the Vazante group is shallower. The union of the two sites would have occurred only at the end of the Neoproterozoic, in association with the generation of the thrust system.

The similarities in the 9 km deep source faults and trends in the faults and fractures observed at the surface suggest that the basement acted essentially as a tectonic screen that controlled the propagation of fractures among the sedimentary covers in the basins. According to Butler et al (2006), structures with more than 8 km deep affecting the basement are tectonic type thick-skin.

The contact between the Vazante and Bambuí Groups is defined as Lagamar thrust fault, which was initially defined by Freitas-Silva (1991) and was identified as lineament F in the geophysical interpretation (Figure 5). The estimated top depths of the magnetic source were approximately 1 km and 1.2 km, based on the Euler deconvolution and the matched filter, respectively, which indicated a shallow limit contact between the groups, which was confirmed by the studies of Coelho et al. (2008) and Alvarenga et al. (2012), who showed a thin-skin tectonic type.

Unlike the first models of the foreland basin (Dickinson, 1974), the presence of portions of thick-skin tectonic type in the midst of predominantly thin-skin portions in many fold-thrust complexes is now being considered (Butler et al., 2004; Coward et al., 1999; McDowell, 1997; Giambiagi et al, 2008).

Therefore, it is believed that the depth of the basement and of the sedimentary covers will decrease in the west-east direction, according to Figure 28.

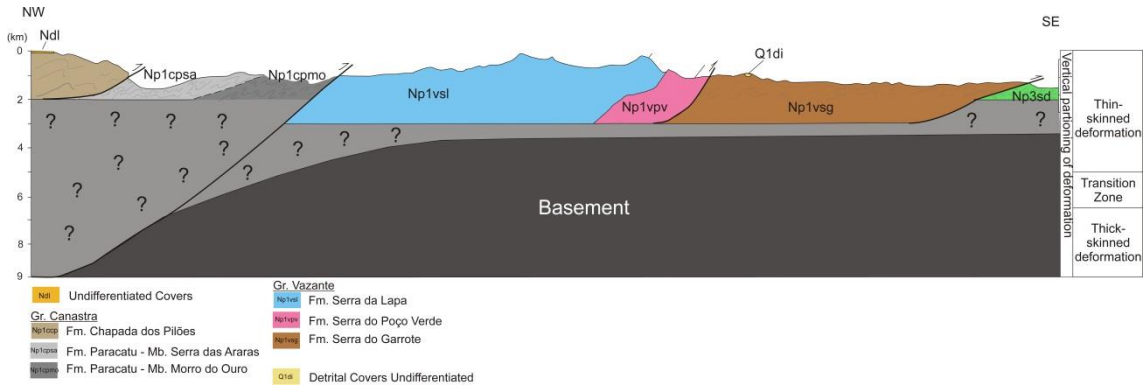

Figure 28 - Schematic profile of the study area showing the deep faults and their relationship to the basement and toppings.

Many magnetic lineaments were related to the large mapped regional structures, and their characteristics could be jointly analyzed. Thus, by integrating the data obtained in this study, it was possible to infer the depths of the sources of the magnetic anomalies and thus a better structural interpretation of the region. Table 4 shows the properties of the structures, and Figure 29 illustrates them.

Table 4 - Properties of the tectonic-geophysical structure for the region.

Geophysical Lineament	Geological Structure	Direction of Propagation	Magnetic Anomaly Source	Characteristics
A	Coromandel Thrust Fault	SW->NE	9 km	Lateral to frontal ramp
A	Paracatu Shear Zone	Dextral	1 km	Brittle to Brittle-Ductile
B	Serra das Araras Thrust Fault	SW->NE to W->E	9 km	Lateral to frontal ramp
C	Morro Agudo Shear Zone	Dextral	1,2 km	Ductile-Brittle
D	Januário Shear Zone	Sinistral	9 km	Brittle-Ductile
E	Vazante Shear Zone	Dextral	1,2 - 9 km	Brittle-Ductile
F	Arrenegado Shear Zone	Dextral	1,2 km	Brittle-Ductile
F	Extremo Norte Thrust Fault	W->E	1,2 km	Frontal ramp
-	Lagamar Thrust Fault	W->E	1 km	Frontal ramp

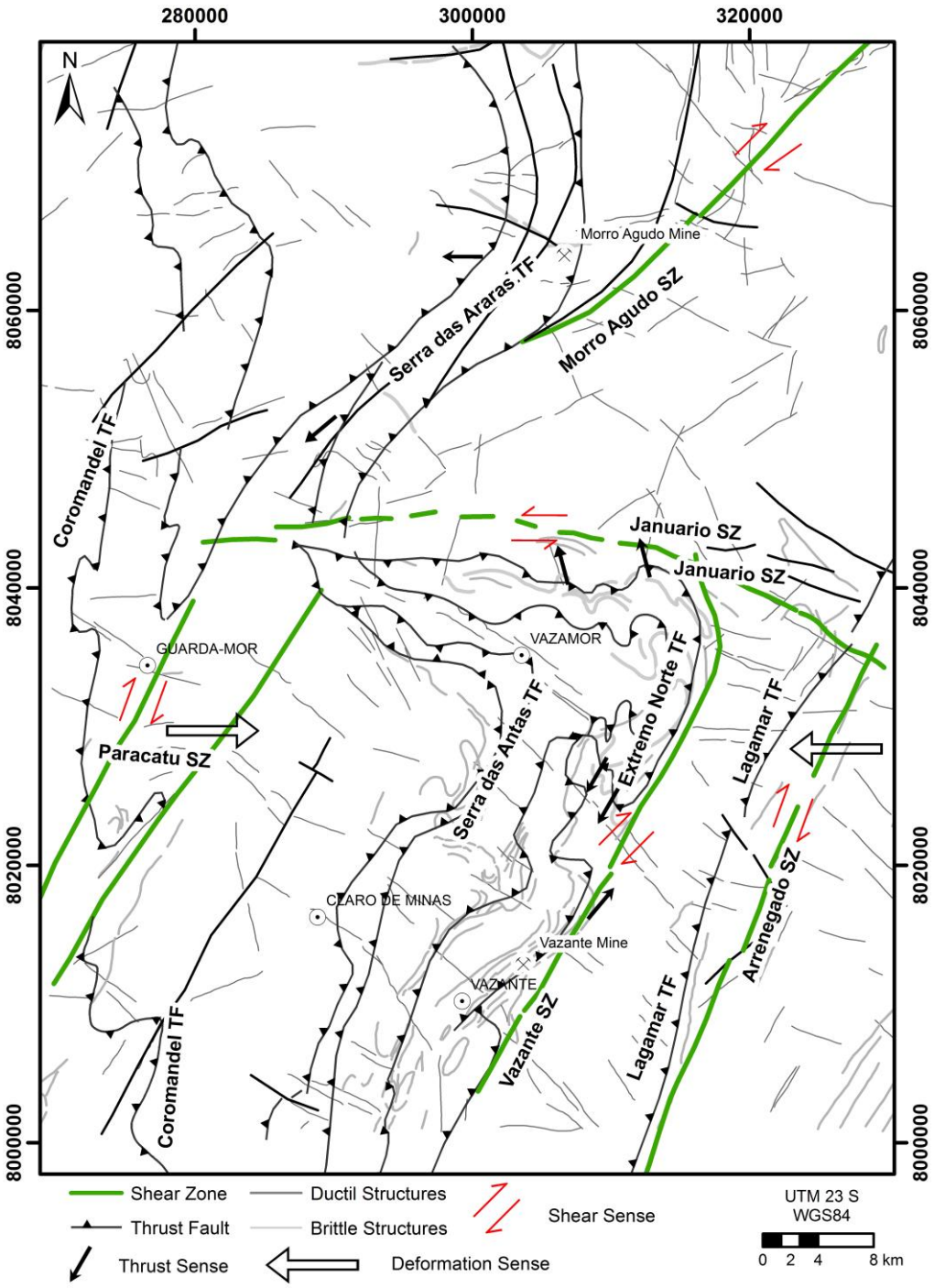

Figure 29 - Principal strain directions in the study area.

The thrust faults occur in the NE-SW and N-S directions and are truncated in the central portion of the Januário Shear Zone. The faults propagate from the southwest to the northeast and from the west to the east in some portions of the sequence. The shear zones have N-S, NE-SW-W and E direction, are symmetrical with each other, and in large part control the orientation of the lower structures in the region. These shear zones have a width of approximately 2-3 km and a length of approximately 50 km.

The Morro Agudo and Vazante shear zones, which have NE-SW directions, are defined by a magnetic relief with a low to intermediate depth of the top of the magnetic anomalies (500 m) by the Euler deconvolution and base depths of the magnetic sources of approximately 1.2 km as estimated using the matched filter. The Morro Agudo Shear Zone is characterized by a series of NE-SW dextral lineaments that dip approximately 40 ° to the west; it is considered to have a ductile-brittle character and is associated with the generation of mylonite. The Shear Vazante Zone is comprised of several small structures in the NE-SW direction, and the major flaw of Vazante (Pinho, 1990, Rostirolla, 2002), which is usually found in greenschist facies with the presence of chlorite, is considered to be brittle-ductile.

The NNE-SSW Paracatu Shear Zone, which was named after a river that runs in this region in the same direction, is defined by a series of intermediate depth NNE-SSW magnetic sources, which have top depths of up 1 km by the Euler deconvolution method and base depths of 1.2 km based on the matched filter method. Among the four shear zones, the Paracatu Shear Zone is restricted to the shallower portions of the crust, which ensures that it is the most brittle.

The NNE-SSW Arrenegado Shear Zone, which was named after a huge farm in this region, is defined by a series of intermediate depth NNE-SSW magnetic sources, which have top depths of up 1 km by the Euler deconvolution method and base depths of 1.2 km based on the matched filter method, it may forms mylonits features.

The EW Januário Shear Zone, which is near the eponymous stream, is defined by a series of small aligned sinistral lineaments, with dips of approximately 30 ° south, and it is considered to be brittle-ductile, with a moderate to high magnetic relief that cuts the entire area. Using the Euler deconvolution method, the tops of the magnetic sources were estimated to have depths up to 1 km, and the base depths of the sources were estimated to be up to 9 km using the matched filter.

The Coromandel Thrust Fault (Pereira, 1992), which is aligned roughly N-S and has an irregular design, is characterized in the study area as a frontal ramp thrust, with a ceiling block located at the Paracatu Formation and a mass transport from the SW to the NE. It is defined by a high-contrast magnetic relief from low to high in the western portion of the area, which is related to lineament A. The sources were observed up to 500 m and up to 9 km using the Euler deconvolution and the matched filter, respectively.

The Serra das Araras Thrust Fault System is located in the northern part of the area, and its approximately NE-SW direction, which indicates mass transport from the southwest to the northeast, is defined by a very low magnetic relief related to lineament B. Using the Euler deconvolution and matched filter methods, sources were observed up to 1 km and 9 km,

respectively. The system has a very strong ductile-brittle character, which is related to the generation of mylonite.

The Serra da Lapa Thrust Faults are located in the southern portion of the area; their NE-SW directions with approximately SW mass transport to the NE are defined by a very high magnetic relief that is related to lineament D. Using the Euler deconvolution and matched filter methods, the sources were observed up to 1 km up to 9 km, respectively, which is related to the generation of mylonite.

The Extremo Norte Thrust Faults are located in the southern portion of the area; their approximately NE-SW directions with west to east mass transit are defined by a region of high magnetic contrast that is related to lineament F. Using the Euler deconvolution and matched filter methods, depths of up to 500 m and up to 1.2 km, respectively, were observed.

The Lagamar Thrust Faults, which were defined initially by Freitas-Silva (1991), are comprised of a set of N-S lineaments that dip approximately 45 ° to the west. The rocks affected by this shear zone are slightly mylonite, which are considered to be brittle-ductile. In the magnetometric total gradient map, the Lagamar faults are defined as a high magnetic relief region with observed depths of up to 1 km by the Euler deconvolution method and up to 1.2 km by the matched filter method.

The thrust faults are well marked by Euler deconvolution (Figures 9a, b), generally with shallow depths of at least 500 meters for lineaments A and E, but in some parts there were deeper magnetic sources up to 1000 m in lineaments B, C, D and F. When analyzing these faults on the maps generated by the matched filter (Figures 6, 7 and 8), their expressions were observed up to 1200 m, but lineaments B and D in the Serra das Araras and Serra da Lapa Thrust Fault Systems extended up to 9 km.

The deeper structures of the Morro Agudo, Vazante and Januário Shear Zones are considered to be magnetic domain boundaries (Figures 6 and 7). The boundaries limit the depth of the lineaments, i.e., it is believed that they limit the domains that are deeper.

In the field, the structures are primarily considered to be thin-skins that are up to 8 km deep and are typically 500 m deep, based on the Euler deconvolution method (Figure 9), which agrees with results obtained by this method in other parts of the world, including the Foreland Basin of Younghae in South Korea, where the majority of the magnetic anomalies in the region were estimated to have depths of 63 m to 354 m (Abdallatif and Lee, 2001).

There are two magnetic sources, presented in the Euler deconvolution images, at greater depths (approximately 5 km in the east-central and south-central areas), which, according to the 1:100,000 geological maps of the region (Tuller et al., 2013, Signorelli et al., 2013a, Signorelli et al., 2013b, Ribeiro and Féboli, 2013, Tuller, 2014, Brito, 2014), correspond to lateritic and

alluvial cover, what suggests deep magnetic sources below the toppings. An intense system of faults and billing with NE-SW and NW-SE orientations at depths of 1.2 km based on the matched filter method and up to 1 km based on the Euler deconvolution method can be observed in the area filled by quaternary alluvium that covers the northeast portion, related to the process of reactivation of the structures that is a necessary condition for the creation of the quaternary basin (Butler and Mazzoli, 2006, Crawford et al., 2010 Sykes, 1978).

Thus, the region is marked as a foreland basin that is defined by a predominantly tectonic thin skin with the presence of imbricated thrust ramps that consist of more brittle rocks such as shales and silts and the accommodation of deformation, often given by area transcurrent shears formed by the reactivation of structures and sometimes the reactivation of basement structures, which led to the development of the shallower portions and the deeper basement (Boyce and Morris, 2002 Giambiagi et al., 2008, Brown et al., 1999 Butler et al., 1997).

From the model of Coelho et al. (2008), it was concluded that the general structures are in the first set of defined faults, with shallower depths of up to 1 km, which only deform the sedimentary cover and present a tectonic thin-skin, except of the Serra das Araras and Serra da Lapa thrust systems and the Januário Shear Zone, that, because they have a greater depth, are related to the second set of defined faults, reaching the basement, with a tectonic thick-skin of up to 9 km, that is in accordance with the seismic line studied by Coelho et al. (2008) and Alvarenga et al. (2012).

7.6.Conclusions

1. Eight macro-regional structures were identified in the region: five shear zones with NE-SW directions (the Morro Agudo and Vazante Shear Zones), N-S directions (the dextral Arrenegado and Lagamar Shear Zones) and E-W directions (the sinistral Januário Shear Zone) and four thrust faults with NS directions (the Coromandel faults), NE-SW directions (the Serra das Araras and Serra da Lapa Thrust Faults Systems and the Extremo Norte Thrust Fault), that have SW-NE main transport directions and correspond to the magnetically interpreted major lineaments in the region.

2. The deformational history of the region could be defined in four progressive stages: (i) Ductile E1 phase characterized by interfoliation slip, axial plane mylonitic foliation, where S1 // S0, there are isoclinal recumbent folds at local scale; (ii) Ductile-Brittle E2 phase characterized by low angle main foliation, thrust faults, NE-SW, N-S e E-W directional shear faults, and generalized folds, mainly symmetrical chevrons, verging to east; (iii) Brittle-Ductile E3 phase characterized by attenuation of deformation, crenulation generation in the main foliation S2, there are open folds and kink bands E-W, besides mushroom type of interference pattern; (iv)

Brittle E4 phase characterized by generation of fractures, joints and essentially brittle faults, besides small-scale drag folds.

3. The depths of the crustal block structural limits defined by the Canastra, Vazante and Bambuí Groups were determined; a 9 km deep structure limits the Canastra and Vazante Groups, and a 1 km deep structure limits the Vazante and Bambuí Groups, bringing ensemble thick and thin skin tectonics in this portion of External Zone of Brasilia Fold Belt.

4. All of structures are deeper in the west than in the east, concluding that the depth of the basement and of the sedimentary covers decrease from the west to the east in the studied area.

5. The thrust faults mapped in the region have a system of lateral ramps with mass transit SW-> NE evolving to W-> E.

6. The use of structural geology coupled to magnetometric data manipulation has proven to be indispensable for the study of the relationships between regional structures and their implications to the grounding in foreland systems.

7.7.Acknowledgements

The authors would like to thank CNPq process 550259-2011-2 that financially supported this research.

7.8.References

Abdallatif, T. F., Lee, J. M. 2001. Shallow magnetic survey of the Younghae Basin area, South Korea: Evaluation of structural setting. Geosciences Journal 5(4), pp 327-338.

Aboud, E., Salem, A., Ushijima, K. 2005. Subsurface structural mapping of Gebel El-Zeit area, Gulf of Suez, Egypt using aeromagnetic data. Earth Planets Space 57: 755-760

Airo, M.-L. & Leväniemi, H., 2012. Geophysical structures with gold potential in southern Finland. Geological Survey of Finland, Special Paper 52, 227-244.

Alvarenga, C.J.S.; Dardenne, M. A., Vieira, L. C., Martinho, C. T., Guimarães, E. M., Santos, R. V., Santana, R. O. 2012. Estratigrafia da borda ocidental da Bacia do São Francisco. Boletim de Geociências da PETROBRAS (Impresso), v. 20, p. 145-164.

Araújo Filho, J. O. - 2000 - The Pirineus Syntaxis: an example of the intersection of two Brasiliano fold-thrust belts in central brasil and its implications for the tectonic evolution of western Gondwana. Revista Brasileira de Geociências, 30(1): 144-148.

Azmy, K., Kendall, B., Creaser, R.A., Heaman, L., de Oliveira, T.F., 2008. Global Correlation of the Vazante Group, São Francisco Basin, Brazil: Re-Os and U–Pb radiometric age constraints. Precambrian Research, 164: 160–172.

Bader J. W., 2009. Structural and tectonic evolution of the Douglas Creek Arch, the Douglas Creek fault zone, and environs,northwestern Colorado and northeastern Utah; implications for petroleum accu-mulation in the Piceance and Uinta Ba-sins. Rocky Mountain Geology, 44, 121 –145.

Bellahsen, N., L. Jolivet, O. Lacombe, M. Bellanger, A. Boutoux, S. Garcia, F. Mouthereau, L. Le Pourhiet, Gumiaux, C. 2012. Mechanisms of margin inversion in the external Western Alps: Implications for crustal rheology, Tectonophysics, 560–561, 62–83, doi:10.1016/j.tecto.2012.06.022.

Bertoni, M. E., Rooney, A. D., Selby, D., Alkmim, F. F., Le Heron, D. P. 2014. Neoproterozoic Re–Os systematics of organic-rich rocks in the São Francisco Basin, Brazil and

implications for hydrocarbon exploration. Precambrian Research, v. 255, Part 1, p. 355-366.

Betts, P.G., Valenta, R.K., Finlay, J., 2003. Evolution of the Mount Woods Inlier, northern Gawler Craton, Southern Australia: an integrated structural and aeromagnetic analysis. Tectonophysics 366, 83–111

Boyce, J.I. and Morris, W.A. 2002. Basement controlled faulting of Paleozoic strata in southern Ontario, Canada: new evidence from geophysical lineament mapping. Tectonophysics, 353: 151-171.

Brito, D. C. 2014. Mapa Geológico da folha Serra da Tiririca. Ministério de Minas e Energia. Secretaria de Geologia, Mineração e Transformação Mineral. Belo Horizonte. Escala 1:100.000.

Brown, D., Alvarez-Marron, J., Perez-Estaun, A., Puchkov, V., Ayala, C. 1999. Basement influence on foreland thrust and fold belt development: an example from the southern Urals.Tectonophysics, 308, 459 – 472.

Butler, R. W. H., Lloyd, G. E., Holdsworth, R. E. 1997. The role of basement reactivation in continental deformation. Journal of the Geological Society, London, 154, 69-71.

Butler, R.W.H., Mazzoli, S., 2006. Styles of continental contraction: a review and introduction. In: Mazzoli, S., Butler, R.W.H. (Eds.), Styles of Continental Contraction: Geological Society of America: Special Paper, 414, pp. 1–10. http://dx.doi.org/ 10.1130/2006.2414(01).

Butler, R.W.H., Mazzoli, S., Corrado, S., De Donatis, M., Di Bucci, D., Gambini, R., Naso, G., Nicolai, C., Scrocca, D., Shiner, P., Zucconi, V., 2004. Applying thick-skinned tectonic models to the Apennine Thrust Belt of Italy — limitations and implications. In: McClay, K.R. (Ed.), Thrust Tectonics and Hydrocarbon Systems: AAPG Memoir, 82, pp. 647–667.

Cai, J., Lü, X. 2015. Substratum transverse faults in Kuqa Foreland Basin, northwest China and their significance in petroleum geology. Journal of Asian Earth Sciences 107, p. 72-82.

Campos Neto, M. C. 1979. Contribution à l'étude des Brasilides: Lithostratigraphie et Structure des Groupes Canastra, Paranoá et Bambuí dans l'ouest nord-ouest de l'Etat de Minas Gerais-Brésil. Dissertação de Mestrado. Université Pierre et Marie Curie, LISE / CNRS, França. 212 pp.

Campos Neto, M. C.. Geometria e fases de dobramentos brasilianos superpostos no oeste de Minas Gerais. Revista Brasileira de Geociências, São Paulo, Brasil, v. 14, n.1, p. 60-68, 1984.

Coelho, J. C. C.; Martins-Neto, M. A., Marinho, M. S. 2008. Estilos estruturais e evolução tectônica da porção mineira da bacia proterozóica do São Francisco. *Rev. bras. geociênc.* [online]. 38 (2): suppl.1, pp. 149-165. ISSN 0375-7536.

Coward, M.P., De Donatis, M., Mazzoli, S., Paltrinieri, S., Wezel, F.C., 1999. Frontal part of the northern Apennines fold and thrust belt in the Romagna–Marche (Italy): shallow and deep structural styles. Tectonics 18 (3), 559–574.

CPRM/CODEMIG. 2001. Relatório final do levantamento e processamento dos dados magnetométricos e gamaespectrométricos, área 1, Unaí-Paracatu-Vazante-Coromandel [Belo Horizonte], CPRM/CODEMIG.

Crawford, B.L., Betts, P.G., Aillères, L., 2010. An aeromagnetic approach to revealing buried basement structures and their role in the Proterozoic evolution of the Wernecke Inlier, Yukon Territory, Canada. Tectonophysics 490, 28–46, http://dx.doi.org/10.1016/j.tecto.2010.04.025.

Cunha, I. A., Coelho, C. E. S., Misi, A. 2000. Fluid Inclusion Study of the Morro Agudo Pb and Zn deposit, Minas Gerais, Brazil. Revista Brasileira de Geociências 30, 318-321.

Cunha, I. A., Misi, A., Babinski, M. 2001. Lead isotope signature of galenas from Morro Agudo Pb-Zn deposits, Minas Gerais, Brazil. In: Misi, A., Teixeira, J. B. G. (Eds.), Proterozoic Base Metal Deposits of Africa and South Africa. Proceedings of the first IGCP 450 Field Workshop. CNPq/UNESCO/IUGS, Belo Horizonte and Paracatu (MG), Brazil, pp. 45-47.

Dahlen, F.A., 1990, Critical taper model of fold-and-thrust belts and accretionary wedges: Annual Review of Earth and Planetary Sciences, v. 18, p. 55–99

Dardenne M. A., Freitas-Silva F. H., Nogueira G. M. S., Souza J. F. C. 1997. Depósitos de fosfato de Rocinha e Lagamar, Minas Gerais. In: Schobbenhaus C., Queiroz E. T., Coelho, C. E. S., Principais depósitos minerais do Brasil, DNPM/CPRM, v.IV C, p.113-122.

Dardenne, M. A. & Freitas-Silva, F. H. 1998. Modelos Genéticos dos depósitos de Pb-Zn nos Grupos Bambuí e Vazante. Workshop Depósitos Minerais Brasileiros de Metais Base, Salvados, CPGG-UFBA/ADIMB, p.86-93.

Dardenne, M. A. 2000. The Brasilia Fold Belt. *In:* Cordani, E. G., Milani, E. J. Thomaz Filho, A., Campos, D. A. Tectonic evolution of South America. Rio de Janeiro: 31° International Geology Congress. p. 231-263.

Dardenne, M.A. - 1978 - Zonação tectôncia da borda ocidental do craton do São Francisco. In: CONGR. BRAS. GEOL., 30, Recife, 1978, Anais... Recife, SBG. V. 1, p. 299-308.

Dardenne, M.A. - 1979 - Les mineralisations de plomb, zinc, fluor du Protérozoique Superieur dans le Brésil Central.Thése de Doutorat d'Etat, Université de Paris VI, 251p, (inédito).

Davis, D., Suppe, J., Dahlen, F.A., 1983. Mechanics of fold and thrust belts and accretionary wedges. J. Geophys. Res. 88, 1153–1172.

DeCelles, P. G., and Giles, K. A., 1996, Foreland basin systems: Basin Research, v. 8, no. 2, p. 105–123

Silva, L.J.H.D., Oliveira I.L., Pohren, C. B., Tanizaki, M. L. N., Carneiro, R. C., Fernandes, G. L. F., Aragão, P. E. 2011. Coeval perpendicular shortenings in the Brasìlia belt: collision of irregular plate margins leading to oroclinal bending in the Neoproterozoic of central Brazil, Journal of South American Earth Sciences, 32, p. 1 -13.

Dias, P.H.A. 2011. Estratigrafia e Tectônica da Faixa Brasília na Região de Ibiá, Minas Gerais: Estudo de Proveniência Sedimentar dos grupos Canastra e Ibiá, com base em estudos isotópicos U-Pb e Sm-Nd. Instituto de Geociências, Universidade Federal de Minas Gerais, Dissertação de Mestrado.

Dickinson, W. R. 1974. Plate Tectonics and sedimentation: Society of Economic Paleontologists and Mineralogists Special Publication 22, 304 pp.

Direen, N.G., Brock, D., Hand, M. 2005. Geophysical testing of balanced cross-sections of fold–thrust belts with potential field data: an example from the Fleurieu Arc of the Delamerian Orogen, South Australia. Journal of Structural Geology 27, 964–984

Dufréchou, G., Harris, L.B., Corriveau, L., 2014. Tectonic reactivation of transverse basement structures in theGrenville orogen of SW Quebec, Canada: Insights from gravity andaeromagnetic data. Precambrian Res. 241, 61-84.

Espurt, N., Hippolyte, J.-C., Saillard, M., Bellier, O., 2012. Geometry and kinematic evolution of a long-living foreland structure inferred from field data and cross section balancing, the Sainte-Victoire System, Provence, France. Tectonics 31, TC4021. http://dx.doi.org/10.1029/2011TC002988.

Freitas-Silva, F. H.; Dardenne, M. A. 1998. Fluid inclusions and isotopic ^{18}O and ^{13}C geochemistry of zinc ore in Vazante, Vazante/MG Fluid inclusions and isotopic ^{18}O and ^{13}C geochemistry of zinc ore in Vazante, Vazante/MG. In: 40 CONGRESSO BRASILEIRO DE GEOLOGIA, 1998, Belo Horizonte. 40 CONGRESSO BRASILEIRO DE GEOLOGIA.

Freitas-Silva F.H. 1991. Enquadramento lito-estratigráfico e estrutural do depósito de ouro de Morro do Ouro, Paracatu/MG. Dissertação de Mestrado, UnB-IG, 151p.

Freitas-Silva F.H. 1996. Metalogênese do Depósito do Morro do Ouro, Paracatu – MG. Tese de Doutorado, UnB-IG, 338 p.

Freitas-silva, F. H.; Dardenne, M. A. 1994. Proposta de subdivisão estratigráfica formal para o grupo Canastra no oeste de Minas Gerais e leste de Goiás. In: Simpósio de Geologia do Centro-Oeste, 4., 1994. Brasília. Atas... Brasília: SBG. p. 164-165.

Freitas-silva, F. H.; Dardenne, M. A., Jost, H. Evolução estrutural das formações Paracatu e Vazante na região de Paracatu-MG. In: 36 Congresso Brasileiro de Geologia, 1990, Natal. 36 Congresso Brasileiro de Geologia, 1990. p. 275-275.

Fuck, R. A. 1994. A Faixa Brasília e a Compartimentação Tectônica na Província Tocantins. In: Simpósio de Geologia do Centro-Oeste, 4., Brasília. Atas... Brasília: SBG, 1994. p. 184-187.

Geosoft. 2008. OASIS Montaj 7 GEOSOFT, Inc., Toronto

Giambiagi, L., Bechis, F., García, V., Clark, A. H. 2008. Temporal and spatial relationships of thick- and thin-skinned deformation: A case study from the Malargüe fold-and-thrust belt, southern Central Andes, Tectonophysics 459, 123–139.

Grant, F.S. 1984/1985. Aeromagnetics, geology and ore environments, I. Magnetite in igneous, sedimentary and metamorphic rocks Geoexploration, 23, pp. 303–333

Hoover, D.B. and Campbell, D.L. 1992. Geophysical models of diamond pipes, Cox and Singer model 12. in Hoover, D.B., Heran, W.D., and Hill, P.L., eds., The Geophysical Expression of Selected Mineral Deposits: United States Department of the Interior, Geological Survey, Open File Report 92-557, p.85-88, 129 p.

Jessel, M. W., Valenta, R. K., Jung, G., Cull, J. P., Gerio, A. 1993. Structural geophysics: Exploration Geophysics, 24, 599-602.

Kwon et al., 2009 S. Kwon, K. Sajeev, G. Mitra, Y. Park, S.W. Kim, I.-C. Ryu Evidence for Permo-Triassic collision in far east Asia: the Korean collisional orogeny Earth and Planetary Science Letters, 279, pp. 340–349

Macedo JM and Marshak S. 1999. Controls on the geometry of fold-thrust belt salients. Geol Soc Am Bull 111: 1808-1822.

Marcia, L. 2014. Studio Geologico Strutturale del Settore della Faixa Brasiliana compreso tra Paracatù e Vazante (Minas Gerais - Brasile). Universita' degli Studi di Cagliari. Facolta di Scienze. 93 pp. (inédita).

McDowell, R.J. 1997. Evidence for synchronous thin-skinned and basement deformation in the Cordilleran fold–thrust belt: the Tendoy Mountains, southwestern Montana. Journal of Structural Geology 19, 77–87.

Mclean, M. A., Betts, P. G. 2003. Geophysical constraints of shear zones and geometry of the Hiltaba Suite granites in the western Gawler Craton, Australia. AUSTRALIAN JOURNAL OF EARTH SCIENCES 50(4):525 – 541

Misi, A., Azmy, K., Kaufman, A. J., Oliveira, T. F., Sanches, A. L., Oliveira, G. D. 2014. Review of the geological and geochronological framework of the Vazante sequence, Minas Gerais, Brazil: Implications to metallogenic and phosphogenic models. Ore Geology Reviews v. 63, p. 76–90.

Misi, A.; Iyer, S. S S; Coelho, C. E. S; Tassinari, C. C. G; Franca-Rocha, W. J. S.; C., I. A.; Gomes, A. S. R.; Oliveira, T. F.; T., J. B. G, 2005. Sediment-Hosted Lead-Zinc Deposits of the Neoproterozoic Bambuí Group and Correlative Sequences, São Francisco Craton, Brazil: A Review and a Possible Metallogenic Evolution Model. Ore Geology Reviews, Amsterdam, v. 26, n. 3, p. 263-304.

Muzzi Magalhães P. 1989. Análise estrutural qualitativa das rochas do Grupo Bambuí, na porção sudoeste da Bacia do São Francisco. Dissertação de Mestrado, Departamento de Geologia da Escola de Minas, Universidade Federal de Ouro Preto, 100 p.

Ndougsa-Mbarga, T., Feumoe, A. N. S., Manguelle-Dicoum, E., Fairhead, J. D. 2012. Aeromagnetic Data Interpretation to Locate Buried Faults in SouthEast Cameroon. Geophysica 48(1–2), p. 49–63

Neves, L. P. 2011. Características Descritivas e Genéticas do depósito de Zn-Pb Morro agudo, Grupo Vazante. Dissertação de Mestrado – Universidade de Brasília, Brasília – DF.

Nwankwo, L. 2015. Estimation of depths to the bottom of magnetic sources and ensuing geothermal parameters from aeromagnetic data of Upper Sokoto Basin Nigeria. Geothermics 54:76–81

Oliveira, G. D. 2013. Reconstrução Paleoambiental e Quimioestratigrafia dos Carbonatos Hospedeiros do depósito de Zinco Silicatado de Vazante, MG. 79 pp. Dissertação (Mestrado) – Universidade de Brasília.

Pereira L.F. 1992. Relações tectono-estratigráficas entre as unidades Canastra e Ibiá na região de Coromandel, MG. Dissertação de Mestrado, UnB-IG, 73p.

Pereira, L.; Dardenne, M. A.; Rosière, C. A.; Pedrosa-Soares, A. C. 1994. Evolução Geológica dos Grupos Canastra e Ibiá na região entre Coromandel e Guarda-Mor, MG. Geonomos, v. 2, p. 22-32.

Pfiffner, O.A., 2006. Thick-skinned and thin-skinned styles of continental contraction. In: Mazzoli, S., Butler, R.W.H. (Eds.), Styles of Continental Contraction: Geological Society of America, Special Paper, 414, pp. 153–177. http://dx.doi.org/10.1130/ 2006.2414 (09).

Phillips, J.D. 1997. Potential-field geophysical software for the PC, version 2.2. US Geological Survey Open-File Report 97-725.

Phillips, J.D. 2001. Designing matched bandpass and azimuthal filters for the separation of potential-field anomalies by source region and source type. Australian Society of Exploration Geophysicists, 15th Geophysical Conference and Exhibition, Expanded Abstracts CD-ROM, 4p.

Pimentel, M. M. 2000. The Neoproterozoic Goiás Magmatic Arc, Central Brazil: a Review and New Sm-Nd Isotopic Data. Revista Brasileira de Geociências, 30(1):035-039.

Pinho, J. M. M. 1990. Evolução Tectônica da mineralização de zinco de Vazante, Brasília, 115p. Dissertação de Mestrado, Universidade de Brasília.

Price R. A., Mountjoy E. W. 1971. Geologic structure of the Canadian Rocky Mountains between Bow and Athabasca Rivers—A progress report. In: Wheeler J O, ed. Structure of the Southern Canadian Cordillera. Geological Association of Canada, Special Paper 6, 7–26

Ramsay, J.G., 1962. The geometry of conjugate fold systems. Geological Magazine99, 516–526.

Reid, A. B., Allsop, J.M., Granser, H., Millett, A.J., Smerton, I.W. 1990. Magnetic interpretation in three dimensions using Euler deconvolution. Geophysics, 55, 80-91.

Reid, A.B. 2003. Euler magnetic structureal index of a thin bed fault. Geophysics, 68, 1255p. doi:10.1190/1.1598117

Ribeiro, J. H., Féboli, W. L. 2013. Mapa Geológico da folha Coromandel. Ministério de Minas e Energia. Secretaria de Geologia, Mineração e Transformação Mineral. Belo Horizonte, 2013. Escala 1:100.000.

Rodrigues, J. B. 2008. Proveniência de sedimentos dos grupos Canastra, Ibiá, Vazante e Bambuí – Um estudo de zircões detríticos e Idades Modelo Sm-Nd. 128 pp. Tese (Doutorado) – Universidade de Brasília.

Ross, H.E., Blakely, R.J., Zoback, M.D. 2006. Testing the use of aeromagnetic data for the determination of Curie depth in California. Geophysics 71(5):L51–L59

Rostirolla, S. P., Mancini, F., Reis Neto, J. M., Figueira, E. G., Araújo, E. C. 2002. Análise estrutural da mina de vazante e adjacências: geometria, cinemática e implicações para a hidrogeologia. Revista Brasileira de Geociências, 32(1):59-68.

Signorelli, N, Pinho, J. M. M., Tuller, M. P.; Baptista, M. C.; Brito, D. C. 2013 b. Mapa Geológico da folha Lagamar. Ministério de Minas e Energia. Secretaria de Geologia, Mineração e Transformação Mineral. Belo Horizonte. Escala 1:100.000.

Signorelli, N; Tuller, M. P.; Pinho, J. M. M.; Baptista, M. C.; Brito, D. C. 2013 a. Mapa Geológico da folha Arrenegado. Ministério de Minas e Energia. Secretaria de Geologia, Mineração e Transformação Mineral. Belo Horizonte. Escala 1:100.000.

Stewart, J.R., Betts, P.G., Collins, A.S., Schaefer, B.F., 2009. Multi-scale analysis of Proterozoic shear zones: anintegratedstructural andgeophysical study.J. Struct. Geol. 31, 1238–1254.

Suppe, J., 1987, The active Taiwan mountain belt, in Schaer, J.P., and Rodgers, J., eds., Anatomy of mountain chains: Princeton, New Jersey, Princeton University Press, p. 277–293

Sykes, L. R. 1978. Intraplate seismicity, reactivation of preexisting zones of weakness, alkaline magmatism, and other tectonism postdating continental fragmentation. Reviews of Geophysics 16 (4) p. 621-688.

Thompson, D.T., 1982. EULDPH: A new technique for making depth estimates from magnetic data. Geophysics 47, 31-37.

Tuller, M. P. 2014. Mapa Geológico da folha Paracatu. Ministério de Minas e Energia. Secretaria de Geologia, Mineração e Transformação Mineral. Belo Horizonte. Escala 1:100.000.

Tuller, M. P.; Signorelli, N, Baptista, M. C., Brito, D. C. 2013. Mapa Geológico da folha Guarda-Mor. Ministério de Minas e Energia. Secretaria de Geologia, Mineração e Transformação Mineral. Belo Horizonte, 2013. Escala 1:100.000.

Uhlein, A., Fonseca, M. A., Seer, H. J., Dardenne, M. A., 2012. Tectônica da Faixa de Dobramentos Brasília – Setores Setentrional e Meridional. Geonomos, 20(2), 1-14.

Valeriano, C. M. A Faixa Brasília meridional com ênfase no segmento da Represa de Furnas: Estado atual do conhecimento e modelos de evolução tectônica. 1999. Tese (Livre Docência) – Universidade Estadual do Rio de Janeiro, Rio de Janeiro.

Zhang, J., Zhao, G., Shen,W., Li, S., Sun, M., Aeromagnetic study of the Hengshan-Wutai-Fuping region: Unraveling a crustal profile of the Paleoproterozoic Trans-North China Orogen, Tectonophysics (2015), doi: 10.1016/j.tecto.2015.08.025

8. Conclusões

A pesquisa realizada chegou a um conjunto de conclusões que incluem o que já foi exposto de forma detalhada nos artigos, e foram sintetizadas nos seguintes tópicos:

1- Há uma grande variação nos resultados entre as bacias do Grupo Canastra e do Grupo Vazante, que pode estar relacionado ao fato de serem de épocas e ambientes distintos e terem se unido apenas no final do Neoproterozoico, época em que as duas já estavam bem consolidadas;

2- Pelo fato de, segundo com Husson & Moretti (2002), em condições regulares nas regiões de zonas externas de cinturões orogênicos, onde porções das falhas de empurrão não são tão espessas, o campo térmico não costuma ser afetado, as baixas produções de calor correspondente às falhas de empurrão A e B, são relacionadas, de acordo com o modelo de Coelho et al. (2008) ao seu primeiro sistema de falhas, sem a contribuição do embasamento, ou seja, restritas apenas aos primeiros quilômetros da crosta;

3- Os dados da produção volumétrica de calor para a Mina de Vazante são maiores do que para a de Morro Agudo indicando que o minério silicático – willemítico, da mina de Vazante apresenta uma resposta maior de elementos radioativos que o minério de Morro Agudo, sulfídrico;

4- Constatou-se uma grande similaridade entre os resultados de fluxo de calor obtidos nesse trabalho por meio de aerogeofisica de alta resolução e os obtidos por métodos convencionais, recomendando assim uma maior utilização desta técnica em regiões do Precambriano;

5- O método aplicado para o estudo do fluxo de calor teve uma boa aplicabilidade na região, podendo servir de guia prospectivo, tendo em vista que conseguiu localizar as principais rochas hospedeiras de minério para a região, além de trazer informações sobre suas estruturas associadas.

6- Foram determinadas as profundidades das estruturas limites dos blocos crustais definidos pelos Grupos Canastra, Vazante e Bambuí, sendo 9 km a profundidade da estrutura que limita os Grupos Canastra e Vazante e 1 km a profundidade da estrutura que limita os Grupos Vazante e Bambuí;

7- Foram definidas oito estruturas macrorregionais para a região: cinco zonas de cisalhamentos, de direções NE-SW (ZC Morro Agudo, Vazante), N-S (ZC Paracatu e Arrenegado) de sentido destral e E-W (ZC Januário) de sentido sinistral; e quatro falhas de empurrão de sentido N-S (Falha de Coromandel), NE-SW (Sistema de Falhas de Empurrão Serra das Araras, Serra da Lapa e Extremo Norte), com sentido

de transporte principal de SW-NE, que correspondem aos grandes lineamentos magnéticos interpretados para a região;

8- A história deformacional da região pode ser definida em 4 fases progressivas, sendo a primeira – E1, dúctil; a segunda – E2 dúctil-rúptil; a terceira – E3 rúptil-dúctil e a quarta – E4 rúptil;

9- As falhas de empurrão cartografadas na região possuem um sistema de rampas laterais com transporte de massa de SW->NE que evolui para W->E;

10- O uso de geologia estrutural atrelado à manipulação de dados magnetométricos mostrou-se imprescindível para o estudo da relação entre estruturas regionais e sua implicação com o embasamento em sistemas *foreland*.

Desta maneira, o presente trabalho contribuiu para agregar mais conhecimento à porção central da Sequência Vazante-Paracatu, em termos de se obter uma melhor diferenciação entre as bacias sedimentares, através do estudo do fluxo de calor, bem como em uma melhor definição do arcabouço tectônico da região, com a individualização das estruturas regionais que controlam a deformação e a estimativa de suas profundidades e implicações nas profundidades do embasamento nessa região.

Fica destacado também o grande potencial das ferramentas utilizadas – estudos de fluxo de calor e o uso de filtros combinados nos dados gamaespectrométricos e magnetométricos de alta resolução – que apesar de amplamente usadas na região poderiam ser melhor usufruídas com dados de ainda melhor resolução, no caso da aeromagnetometria e dados de poços, no caso da gamaespectrometria.